Pacific Northwest
NATIONAL LABORATORY

PNNL-29052

Survival and Passage of Yearling and Subyearling Chinook Salmon and Juvenile Steelhead at Lower Granite Dam, 2018

Final Technical Report

August 2019

KD Ham
RA Harnish
AH Colotelo
KA Deters
J Martinez
PS Titzler
JR Skalski
RL Townsend
T Fu
X Li
CA Duberstein
ZD Deng
GA McMichael

U.S. DEPARTMENT OF ENERGY

Prepared for the U.S. Department of Energy
under Contract DE-AC05-76RL01830

PACIFIC NORTHWEST NATIONAL LABORATORY
operated by
BATTELLE
for the
UNITED STATES DEPARTMENT OF ENERGY
under Contract DE-AC05-76RL01830

Printed in the United States of America

**Available to DOE and DOE contractors from
the Office of Scientific and Technical
Information,
P.O. Box 62, Oak Ridge, TN 37831-0062**
www.osti.gov
**ph: (865) 576-8401
fox: (865) 576-5728
email: reports@osti.gov**

**Available to the public from the National Technical Information Service
5301 Shawnee Rd., Alexandria, VA 22312
ph: (800) 553-NTIS (6847)
or (703) 605-6000
email: info@ntis.gov
Online ordering: http://www.ntis.gov**

PNNL-29052

Survival and Passage of Yearling and Subyearling Chinook Salmon and Juvenile Steelhead at Lower Granite Dam, 2018

Final Technical Report

August 2019

KD Ham
RA Harnish
AH Colotelo
KA Deters
J Martinez
PS Titzler
JR Skalski
RL Townsend
T Fu
X Li
CA Duberstein
ZD Deng
GA McMichael

Prepared for
the U.S. Department of Energy
under Contract DE-AC05-76RL01830

Pacific Northwest National Laboratory
Richland, Washington 99354

Preface

A study of fish passage and survival at Lower Granite Dam (LGR) was conducted by Pacific Northwest National Laboratory (PNNL) and subcontractors in 2018 for the U.S. Army Corps of Engineers (USACE) Walla Walla District (CENWW). The PNNL project manager was Kenneth D. Ham. The USACE technical lead was Derek Fryer. The study was designed (1) to evaluate the passage and survival of yearling and subyearling Chinook salmon and juvenile steelhead at LGR, as stipulated by the 2008 Biological Opinion and Fish Accords and (2) to assess performance measures including route-specific fish passage proportions, travel times, and survival based on a virtual/paired-release (VIPRE) model and a virtual release with dead fish correction (ViRDCt) model.

This report should be cited as follows:

> Ham, KD, RA Harnish, AH Colotelo, KA Deters, J Martinez, PS Titzler, JR Skalski, RL Townsend, T Fu, X Li, CA Duberstein, ZD Deng, and GM McMichael. 2019. *Survival and Passage of Yearling and Subyearling Chinook Salmon and Steelhead at Lower Granite Dam, 2018: Technical Report.* PNNL-29052. Final report submitted by the Pacific Northwest National Laboratory to the U.S. Army Corps of Engineers, Walla Walla, Washington.

Executive Summary

The purpose of this passage and survival study was to estimate fish performance metrics associated with passage through Lower Granite Dam (LGR) for migrating yearling (CH1), subyearling (CH0) Chinook salmon (*Oncorhynchus tshawytscha*), and steelhead smolts (*O. mykiss*, STH) in 2018. Researchers at the Pacific Northwest National Laboratory (PNNL) collaborated with the U.S. Army Corps of Engineers (USACE) Walla Walla District (CENWW), the University of Washington, and Mainstem Fish Research to conduct a 2018 study to estimate dam passage survival and other performance metrics for CH1, CH0, and STH at LGR.

A recent court ruling ordered 2018 spring spill at federal dams on the lower Snake and Columbia rivers to increase to the maximum level within state water quality criteria waivers (≤120% in the tailrace and ≤115% at the forebay of the downstream dam). This study also included a comparison of the virtual/paired-release (VIPRE) study design, used in previous Biological Opinion (BiOp) performance standards evaluations, and the more recently developed virtual release/dead fish correction (ViRDCt) designs. Both designs relied on tagged fish released upriver from LGR at Blyton Landing, Washington, that contributed to the formation of a virtual release group at the face of the dam. A total of 1063 CH1, 1681 STH, and 2773 CH0 were implanted with tags and released for this study. The 2018 LGR study marked the first large evaluation of fish passage and survival to employ the Juvenile Salmon Acoustic Telemetry System (JSATS) injectable tag, which is smaller and requires less handling of fish for implantation. This report is a comprehensive summary of 2018 results. Study results are summarized in tables ES.1 through ES.4 below.

The removable spillway weir (RSW) proved to be the most effective passage route for all fish stocks, especially during the daytime, with fewer individuals passing the powerhouse and unmodified spill bays relative to the proportion of flow through those routes. During hours of darkness, fish routing was more similar to flow proportions among routes, with the RSW retaining some of its effectiveness advantage over other route types. This diel difference in fish behavior suggests that spill operations could be tailored differently to achieve the desired fish passage outcomes for day and night periods.

Survival estimates for CH1 and STH exceeded the BiOp requirement of 0.96 survival for spring stocks, while also meeting the precision requirements (standard error (SE) ≤ 0.025) using both the VIPRE and ViRDCt models. The VIPRE estimate of survival for the summer stock, CH0, exceeded the 0.93 requirement for survival, whereas the ViRDCt estimate was slightly below the BiOp requirement at 0.9242 (SE = 0.0098). Unexpectedly poor survival of CH0 passing over unmodified spill bays, after 15 June, and before summer spill operations began, reduced the seasonal survival estimate. Rates of survival were relatively low for fish passing during low total flow periods when spill exceeded half of the total flow. Other studies have found eddies in modeled tailrace conditions during conditions of high spill and low powerhouse flows that might increase tailrace residence times and exposure to hazards such as predation. Lower daytime survival rates for these fish suggest that sight feeding predators, including piscivorous birds, may be a factor.

The ViRDCt study designs demonstrated improved precision despite requiring the release of fewer live fish at fewer locations. We recommend this model for future studies to minimize impacts on fish and to reduce costs.

Fish that passed through the newly renovated juvenile bypass system (JBS) survived at high rates. Monitoring these fish to the downstream-most forebay arrays (Bonneville Dam forebay [458 km] in spring or Lower Monumental Dam forebay [103 km] in summer) found no evidence that JBS passage was causing additional mortality downstream.

Table ES.1. Summary of Methods and Conditions at LGR During 2018

Year: 2018			
Study Site(s): Lower Granite Dam			
Objective(s) of study: Estimate dam passage survival and other performance measures for yearling Chinook salmon, steelhead, and subyearling Chinook salmon.			
Hypothesis (if applicable): Not applicable.			
Fish: Species-race: yearling Chinook salmon (CH1), steelhead (STH), subyearling Chinook salmon (CH0) Source: Lower Granite Dam Smolt Monitoring Facility		Implant Procedure: Surgical: Yes Injected: No	
Size (median): CH1 / STH / CH0 Weight (g): 23.3 / 89.2 / 13.6 Length (mm): 138 / 222 / 110		Sample Size: CH1 / STH / CH0 # Release Sites: 3 / 3 / 3 Total # Released: 1063 / 1681 / 2773	
Tag Type: Advanced Telemetry Systems (ATS)-156dB Model: SS400; Weight (in air): 0.221 g	Analytical Models: VIPRE and ViRDCt	Characteristics of Estimate: Effects Reflected (direct, total, etc.): Direct Absolute or Relative: Absolute	

Spring Environmental/Operating Conditions (daily from 17 April 2018 through 26 May 2018):

Statistic	Mean	Min	Max
River Discharge (kcfs):	123.2	88.1	174.9
Spill Discharge (kcfs):	40.6	31.1	73.4
Percent Spill (24 h/d):	33.9	23.2	50.1
Temperature (°C):	10.9	8.9	12.8
Total Dissolved Gas %	117.1	114.1	127.9

Treatment(s): None
Unique Study Characteristics: Court-ordered spill to the gas cap

Summer Environmental/Operating Conditions (daily from 31 May 2018 through 9 July 2018):

Statistic	Mean	Min	Max
River Discharge (kcfs):	71.1	30.4	153.6
Spill Discharge (kcfs):	27.7	17.4	45.4
Percent Spill (24 h/d):	42.5	24.2	75.5
Temperature (°C):	16.3	13.2	18.5
Total Dissolved Gas %	115.4	111.6	119.2

Treatment(s): None
Unique Study Characteristics: Court-ordered spill to the gas cap through 20 June

Table ES.2. Summary of Performance Metrics at LGR, 2018, with Standard Errors in Parentheses and Travel Times Presented in Hours

Metric		CH1	STH	CH0
Dam passage survival (SE)				
	VIPRE	0.9726 (0.0159)	0.9959 (0.0099)	0.9422 (0.0217)
	ViRDCt	0.9877 (0.0062)	0.9936 (0.0037)	0.9242 (0.0098)
Forebay-to-tailrace survival (SE)				
	VIPRE	0.9728 (0.0159)	0.9961 (0.0099)	0.8837 (0.0211)
	ViRDCt	0.9877 (0.0062)	0.9936 (0.0037)	0.9097 (0.0106)
Forebay residence time (median; mean (SE))		4.92; 10.13 (0.62)	4.07; 13.42 (1.34)	8.96; 62.10 (4.03)
Tailrace egress time (median; mean (SE))		0.27; 2.00 (0.86)	0.27; 2.93 (2.27)	0.62; 2.15 (0.29)
Spill passage efficiency (SE)		0.6212 (0.0226)	0.5735 (0.0190)	0.7969 (0.0135)
Fish passage efficiency (SE)		0.9286 (0.0120)	0.9662 (0.0069)	0.9125 (0.0095)

Table ES.3. Route-Specific Dam Passage Survival Estimates

Species and Route	N (at V_1)	VIPRE (SE)	ViRDCt (SE)
Yearling Chinook Salmon			
Unmodified Spill Bay	117	0.9521 (0.0244)	0.9898 (0.0102)
Removable Spillway Weir	168	0.9855 (0.0172)	1.0016 (0.0360)
Juvenile Bypass System	138	0.9961 (0.0158)	1.0001 (0.0264)
Turbine	32	0.8779 (0.0599)	0.8697 (0.0604)
Steelhead			
Unmodified Spill Bay	173	1.0003 (0.0119)	1.0002 (0.0153)
Removable Spillway Weir	217	0.9843 (0.0141)	0.9937 (0.0063)
Juvenile Bypass System	262	1.0111 (0.0087)	1.0000 (0.0124)
Turbine	23	0.8804 (0.0715)	0.9076 (0.0626)
Subyearling Chinook Salmon			
Unmodified Spill Bay	219	0.8456 (0.0321)	0.8450 (0.0323)
Removable Spillway Weir	490	0.9655 (0.0230)	0.9654 (0.0234)
Juvenile Bypass System	95	1.0023 (0.0277)	1.0022 (0.0280)
Turbine	77	0.9949 (0.0306)	0.9949 (0.0309)

Table ES.4. Summary of Juvenile Salmonid Passage Route Distributions

Fish Stock	n	Unmodified Spill Bay	RSW	JBS	Turbine
CH1	462	0.2554 (0.0203)	0.3658 (0.0224)	0.3074 (0.0215)	0.0714 (0.0120)
STH	680	0.2544 (0.0167)	0.3191 (0.0179)	0.3926 (0.0187)	0.0338 (0.0069)
CH0	891	0.2469 (0.0144)	0.5499 (0.0167)	0.1156 (0.0107)	0.0875 (0.0095)

Acknowledgments

This study was the result of hard work by dedicated scientists and engineers from the Pacific Northwest National Laboratory (PNNL), Mainstem Fish Research (MFR), the U.S. Army Corps of Engineers (USACE) Walla Walla District (CENWW), and the University of Washington (UW). Their teamwork and attention to detail, schedule, and budget were essential for the study to succeed in providing high-quality, timely results to decision makers.

- MFR: Ryan Flaherty.
- PNNL: Brian Bellgraph, Jarod Cable, Dustin Clelland, Bernardo Do Vale Beirão, Joanne Duncan, Kristin Engbrecht, Nikki Fuller, Lysel Garavelli, Christopher Grant, Kris Hand, Josh Hubbard, Jill Janak, Kyle Larson, Huidong Li, Xinming Lin, Tim Linley, Jun Lu, Jayson Martinez, Erin McCann, Bob Mueller, Megan Nims, Brett Pflugrath, Briana Rhode, Aljon Salalila, John Stephenson, Scott Titzler, Yong Yuan, Shon Zimmerman.
- USACE: Brad Eppard, Derek Fryer, Stephen Hampton, Elizabeth Holdren, Chris Pinney, Tim Wik.

Acronyms and Abbreviations

3D	three dimensional
AR	autonomous receivers
ASW	adjustable spillway weir
AT	acoustic telemetry
ATS	Advanced Telemetry Systems
BGS	Behavioral Guidance Structure
BiOp	biological opinion
BRZ	boat-restricted zone(s)
ºC	degree(s) Celsius
CENWW	Walla Walla District
cfs	cubic feet per second
CH0	subyearling Chinook salmon
CH1	yearling Chinook salmon
dB	decibel(s)
FCRPS	Federal Columbia River Power System
FGE	fish guidance efficiency
FPE	fish passage efficiency
ft	foot (feet)
g	gram(s)
h	hours(s)
in.	inch(es)
JBS	juvenile bypass system
JFF	Juvenile Fish Facility
JSATS	Juvenile Salmon Acoustic Telemetry System
kcfs	thousand cubic feet per second
km	kilometer(s)
kW	kilowatt
L	liter(s)
LGR	Lower Granite Dam
LGS	Little Goose Dam
m	meter(s)
MFR	Mainstem Fish Research
mg	milligram(s)
mi	mile(s)
MLE	maximum likelihood estimation
mm	millimeter(s)

Acronyms and Abbreviations, continued

MS-222	tricaine methanesulfonate
n	number
NA	not applicable
NOAA	National Oceanic and Atmospheric Administration
PIT	passive integrated transponder
PNNL	Pacific Northwest National Laboratory
PRI	pulse repetition interval
psi	pounds per square inch
rkm	river kilometer(s)
RME	research, monitoring, and evaluation
ROR	run-of-river
RPA	reasonable and prudent alternative
RSW	removable spillway weir
s	second(s)
SE	standard error
SMP	Smolt Monitoring Program
SPE	spill passage efficiency
SPL	unmodified spill bays
STH	steelhead
STS	submersible traveling screens
TDG	total dissolved gas
TUR	turbines
USACE	U.S. Army Corps of Engineers
UW	University of Washington
VBS	vertical barrier screen(s)
VIPRE	virtual/paired-release
ViRDCt	virtual release with dead fish correction

Contents

Contents, continued

Figures

Figures, continued

Tables

Tables, continued

1.0 Introduction

The U.S. Army Corps of Engineers (USACE) Walla Walla District (CENWW) has funded numerous evaluations of fish passage and survival through various structural configurations and operations at dams within the Federal Columbia River Power System (FCRPS), with the goal of improving passage conditions for various populations, some of which are listed as threatened or endangered under the Endangered Species Act. This has been especially true at Lower Granite Dam (LGR), which has played an important role as a testbed for innovative fish passage structures at both powerhouse and spillway routes.

This report describes research conducted during 2018 using acoustic telemetry (AT) to evaluate juvenile salmonid passage and survival at LGR (Figure 1.1). Researchers at the Pacific Northwest National Laboratory (PNNL) in collaboration with CENWW, the University of Washington (UW), and Mainstem Fish Research (MFR) conducted this juvenile fish passage and survival study. This report provides additional detail on methods and results as a follow up to the brief, metrics-focused Biological Opinion (BiOp) report already delivered (Skalski et al. 2018).

Figure 1.1. Lower Granite Dam on the Snake River

The purpose of this study was to estimate dam passage survival at LGR as stipulated by the 2008 FCRPS BiOp (NOAA 2008) and to provide additional performance measures at the dam as stipulated in the Fish Accords (3 Treaty Tribes-Action Agencies 2008) for yearling Chinook salmon (CH1), subyearling Chinook salmon (CH0), and juvenile steelhead (STH). The spring migrant passage and survival study period extended from 17 April through 29 May 2018 followed by the summer migrant study period from 1 June through 9 July 2018. These study periods include the days when acoustically tagged fish were passing LGR, which means that upstream releases may have occurred earlier and downstream releases may have occurred later. Data collection ended on 27 August 2018. This report includes a comprehensive description of the study's methods and additional measures, including (1) route-specific survival and passage metrics for the entire season and for day and night periods, (2) horizontal and vertical approach and passage distributions, and (3) reach survival rates upstream and downstream of the dam.

1.1 Study Objectives

This 2018 study estimated performance measures for CH1, CH0, and STH as outlined in the FCRPS BiOp and Fish Accords. Additional results are provided, such as survival rates and passage distributions of juvenile salmonids passing through various routes including the turbines (TUR), juvenile bypass system (JBS), unmodified spill bays (SPL), and removable spillway weir (RSW) routes at LGR. This information can help inform the operation or configuration of the dam to achieve desired performance.

The acoustic-tag evaluation of fish passage and survival at LGR focused on the following objectives:

1. Estimate dam passage survival probability (with a standard error (SE) ≤ 0.025)
    a. Validate survival results through testing of survival model assumptions
2. Estimate survival for the following zones of inference:
    a. Project passage survival (upstream hydraulic influence to downstream hydraulic influence)
    b. Passage route survival (all available routes)
    c. Forebay survival (upstream hydraulic influence to dam passage)
3. Estimate passage distribution and standard passage efficiency metrics
    a. Spill passage efficiency (spill passage/total passage)
    b. Fish guidance efficiency (proportion of powerhouse passage guided into JBS)
    c. Fish passage efficiency (proportion of fish passing non-turbine routes)
4. Estimate passage timing
    a. Forebay residence (upstream hydraulic influence of the dam to time of dam passage)
    b. Tailrace egress (dam passage to downstream hydraulic influence in the tailrace)
    c. Project passage (upstream hydraulic influence to downstream hydraulic influence)
5. Evaluate travel time and survival as part of a JBS post-construction evaluation.

1.2 Report Contents and Organization

This report contains six chapters and five appendices, including Chapter 1.0, Introduction; Chapter 2.0, Study Background and Area; Chapter 3.0, Methods; Chapter 4.0, Results; Chapter 5.0, Discussion; and Chapter 6.0, References. The appendices contain additional information on the Assessment of Survival Model Assumptions (Appendix A); Fish Tagging and Release (Appendix B); Hydrophone and Autonomous Node Deployment Information (Appendix C); Capture Histories Used in Survival Analyses (Appendix D); and Comparison of 2018 Results with Older Studies of LGR Passage and Survival (Appendix E)

2.0 Study Background and Area

LGR is the fourth dam on the Snake River upstream of the confluence with the Columbia River. It is located at Snake River mile 107.5 (river kilometer [rkm] 173). The original dam project was authorized in 1945 by Section 2 of the Rivers and Harbors Act (59 Stat.10 1945) and approved the same year. Construction of the dam began in July 1965; the lake was filled and power generation began in 1975. Installation of the sixth turbine unit was completed in 1978. Lower Granite Lake is the reservoir upstream of the dam, and it extends 63 km (39 mi) to Lewiston, Idaho. Because LGR is the first collector dam for juveniles migrating downstream, it plays an important role in the USACE Juvenile Fish Transportation Program. It has also been a fertile site for testing concepts designed to alter fish routing through dams, to improve the effectiveness of fish collection, and to improve passage conditions and survival rates. Some of the concepts tested include the Simulated Wells Intake, Behavioral Guidance Structure (BGS), Surface Bypass and Collector, and the RSW, which is now a routine part of juvenile fish passage operations. During this 2018 study, LGR was operated with the RSW but without the other structural features, as it has been since 2007. The redesigned JBS was also operated for the first time during the 2018 fish passage season.

The dam structure at LGR is 3200 ft long and has an effective height of 100 ft. The powerhouse is 656 ft long and contains six 135,000-kW turbine units. All turbines are six-blade Kaplan units that operate at 90 rpm. The spillway is a concrete, gravity-type spillway. It is 512 ft long, and the ogee crest is at an elevation of 681 ft above mean sea level. It contains eight radial (Tainter-style) gates, each 50 ft wide by 60 ft high. The spillway has a peak flood discharge of 850,000 cfs. The RSW, a surface passage structure, is installed in Spillbay 1. This structure is intended to increase the number of migrating juvenile salmon and steelhead passing the spillway by providing surface attraction flow and favorable passage conditions. The navigation lock is a single-lift lock that is 674 ft long by 86 ft wide, with a 15-ft minimum depth and a 105-ft maximum vertical lift. Although a small proportion of juvenile migrants may pass through the lock, its operation is not managed for juvenile fish passage. The dam also has fish ladders for upstream passage of returning adult fish and an earthen-fill section.

Fish guidance screens divert a portion of the juvenile migrating salmon entering the turbine intakes away from the turbine passage and into the juvenile fish bypass and transportation systems. LGR was the first mainstem Snake River dam to have submersible traveling screens (STSs) included in its original design. In the original system, fish diverted by guidance screens entered a gatewell that included vertical barrier screens (VBSs) to allow for partial dewatering, 8-in-diameter orifices that led to a collection gallery and additional dewatering structures, and a pressurized pipe at the south end of the powerhouse. The pipe led down the tailrace into the fish and water separator, holding ponds, evaluation and monitoring facility, transport loading dock, and outfall. Fish entering the facility could either be returned to the river through the outfall or loaded into barges for transportation downstream. In 1996, the STSs were replaced with new extended-length submersible bar screens, and new VBSs were installed in the gatewells. Gatewell orifices have also been modified and enlarged. The juvenile bypass system has undergone several updates since original construction, including a significant redesign completed just prior to the 2018 juvenile fish passage season.

2.1 Performance Standards and Definitions

The FCRPS 2008 BiOp contains a reasonable and prudent alternative (RPA) that includes actions calling for juvenile salmonid survival measurements (RPAs 52.1 and 58.1). These RPAs are being addressed as part of the federal research, monitoring, and evaluation (RME) effort for the FCRPS BiOp. Most importantly, the FCRPS BiOp includes performance standards, such as that included below, for juvenile salmonid survival in the FCRPS against which the Action Agencies (Bonneville Power Administration, Bureau of Reclamation, and USACE) must compare their estimates (after the RME Strategy 2 of the RPA):

> Juvenile Dam Passage Performance Standards – The Action Agencies juvenile performance standards are an average across Snake River and lower Columbia River dams of 96% dam passage survival for spring Chinook and steelhead and 93% average across all dams for Snake River subyearling Chinook. Dam passage survival is defined as survival from the upstream face of the dam to a standardized reference point in the tailrace.

The Memorandum of Agreement between the three lower river tribes and the Action Agencies (known informally as the Fish Accords) contains three additional requirements relevant to the 2018 survival studies (after Attachment A to the Memorandum of Agreement):

> Dam Survival Performance Standard – Meet the 96% dam passage survival standard for yearling Chinook and steelhead and the 93% standard for subyearling Chinook. Achievement of the standard is based on 2 years of empirical survival data....
>
> Spill Passage Efficiency and Delay Metrics – Spill passage efficiency (SPE) and delay metrics under current spill conditions... are not expected to be degraded (“no backsliding”) with the installation of new fish passage facilities at the dams....
>
> Future RME – The Action Agencies’ dam survival studies for purposes of determining juvenile dam passage performance will also collect information about SPE, BRZ-to-BRZ (boat-restricted zone) survival and delay, as well as other distribution and survival information. SPE and delay metrics will be considered in the performance check-ins or with Configuration and Operations Plan updates, but not as principal or priority metrics over dam survival performance standards. Once a dam meets the survival performance standard, SPE and delay metrics may be monitored coincidentally with dam survival testing.

This report summarizes the results of the 2018 AT studies of CH1, STH, and CH0 at LGR to assess the Action Agencies’ compliance with the performance criteria of the BiOp and Fish Accords (Table 2.1).

Table 2.1. Definitions of Performance Measures

Measure	Definition
BiOp	
Dam passage survival	Survival from the upstream face of the dam to a standardized reference point in the tailrace.
Fish Accords	
Forebay-to-tailrace survival	Survival from a forebay array 2 km upstream of the dam to a tailrace array 2 km downstream from the dam. This metric is also known as the BRZ-to-BRZ survival estimate.
Forebay residence time	Average time smolts take to travel from the first detection on the forebay entrance array 2 km upstream of LGR to the time of the last detection on the dam-face array.
Tailrace egress time	Average time smolts take to travel from the time of the last detection on the dam-face array to the time of the last detection on the downstream tailrace array.
Spill passage efficiency	The proportion of fish passing through the dam via the spillway.
Fish passage efficiency	The proportion of fish passing through the dam via non-turbine routes (i.e., the spillway and the JBS).
Other Metrics	
Fish guidance efficiency	The proportion of fish passing through the powerhouse via the JBS.

In 2018, the LGR study area for the AT evaluation of survival and passage covered approximately 125 km of the Snake River from the primary release location at Blyton Landing, Washington (rkm 193), to the hydrophone array in the forebay of Lower Monumental Dam, Washington (rkm 68) (Figure 2.1). LGR (rkm 173) is located 20 rkm downstream from the fish release transect at Blyton Landing. Study locations, descriptions of each location, and distances upstream from the mouth of the Snake River are provided in Table 2.2.

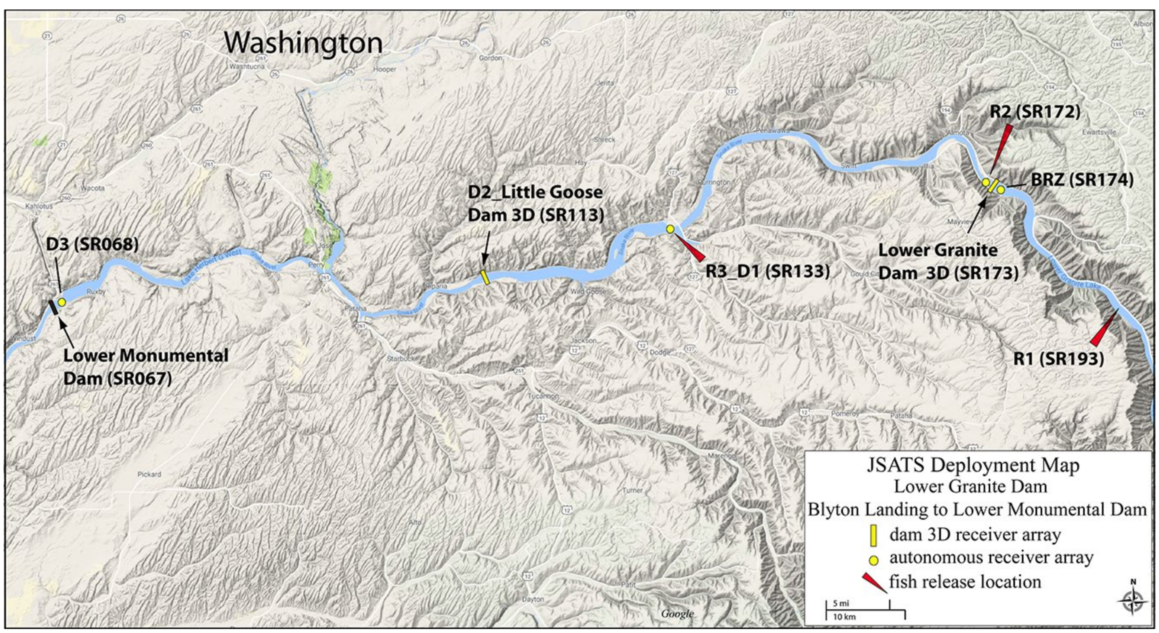

Figure 2.1. LGR Study Area Map

Table 2.2. Study Locations, Description, and Snake River Kilometers for the LGR Passage and Survival Study, 2018

Location	Description	Snake River Kilometer
Blyton Landing	Release 1 (R_1)	193
LGR Upstream BRZ	Forebay virtual release (V_1 for forebay metrics)	174
LGR Dam	Dam face virtual release (V_1 for dam passage)	173
LGR Tailrace	Tailrace reference release (R_2) and tailrace egress array	171
Willow Landing	Summer tailwater reference release (R_3) and primary survival array	140
Central Ferry	Spring tailwater reference release (R_3) and primary survival array	133
Little Goose Dam	Secondary survival array	113
Lower Monumental Dam Forebay	Tertiary survival array	068

3.0 Methods

Study methods include the release-recapture experimental design; tag specifications; fish collection, handling, tagging, and release procedures; acoustic tag detection; acoustic signal processing; and the statistical approach to data analyses.

3.1 Release-Recapture Designs for Estimating Dam Passage Survival and Sample Size Estimates

This 2018 study represents the first opportunity to compare the utility of a newer survival study design (virtual release with dead fish correction (ViRDCt)) with the virtual/paired release-recapture (VIPRE) study design, which has been used in previous BiOp performance standards evaluations. Sample sizes for the study were computed to meet the precision specified in the objectives for the VIPRE model, with an expectation that the ViRDCt model would estimate survival more precisely if assumptions were met. A more complete treatment of the survival calculations will follow in Section 3.5.1.

3.1.1 VIPRE Survival Model

The VIPRE model (Skalski et al. 2010) consists of a virtual release (V_1) of fish at the face of the dam and a paired release below the dam (Figure 3.1). The V_1 was formed from fish that arrived successfully at the face of the dam and were detected at a dam-face hydrophone array from an upstream release (R_1). By releasing fish far enough upstream, the fish should have arrived at the dam in a spatial pattern typical of run-of-river (ROR) fish. This V_1 was used to estimate survival through the dam and part of the way through the next reservoir (Figure 3.1). To account and adjust for this extra reach mortality, a paired release below LGR (i.e., R_2 and R_3 Figure 3.1) was used to estimate survival in that segment of the reservoir below the dam. Dam passage survival was then estimated as the quotient of the survival estimates from the virtual release to that of the paired release.

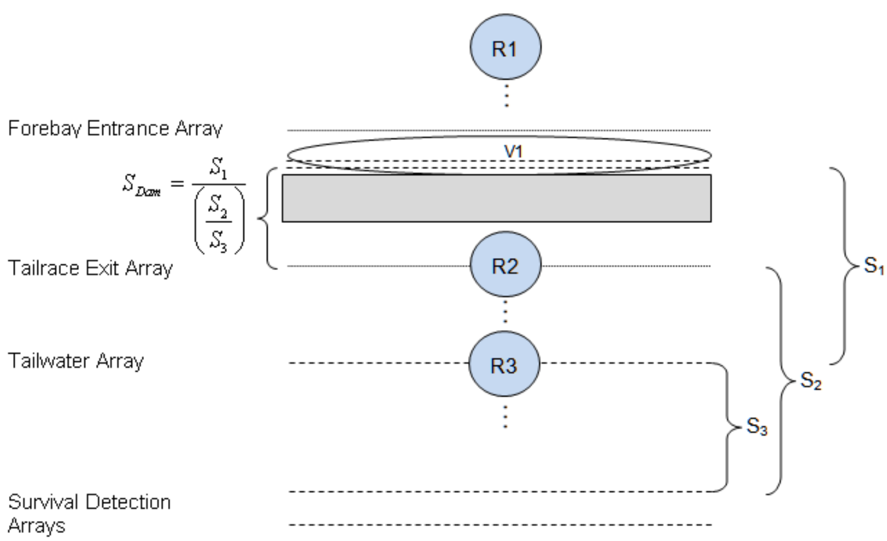

Figure 3.1. VIPRE Design to Estimate Dam Passage Survival at LGR in 2018. Release groups R_1, R_2, and R_3 are denoted along with the virtual release V_1 created at the face of the dam and the associated hydrophone detection arrays and survival parameters S_1, S_2, and S_3.

The same release-recapture design was used to estimate forebay-to-tailrace survival, except that the virtual release group was constructed of fish known to have arrived at the forebay array. The same below-dam paired release was used to adjust for the extra mortality below the dam as used to estimate dam passage survival.

3.1.2 ViRDCt Survival Model

The ViRDCt model provides an alternative design for estimating dam passage survival (Harnish et al. 2017). The R_1 release from the VIPRE model was used to form a virtual release at the dam face. However, in this design, the V_1 release was used to estimate the joint probability of fish alive or dead being detected at a tailrace array (Figure 3.2). This detection rate was then adjusted using the probability of a dead fish being carried downriver to and being detected at the tailrace array. Dead fish releases (D_1) were used to estimate the probability of fish that died during dam passage drifting downriver and being detected at the tailrace array. When no dead fish are detected at the tailwater, it is possible to use a reduced model for increased precision. One advantage of the ViRDCt model over the VIPRE model is that live fish releases are required only at R_1, which reduces the number of live fish required by more than half in some cases (Table 3.1). The number of dead fish released for the ViRDCt model is greater than for VIPRE because of the increased importance of quantifying the rate of dead fish detection at the tailrace array for each passage route type.

a. Full model

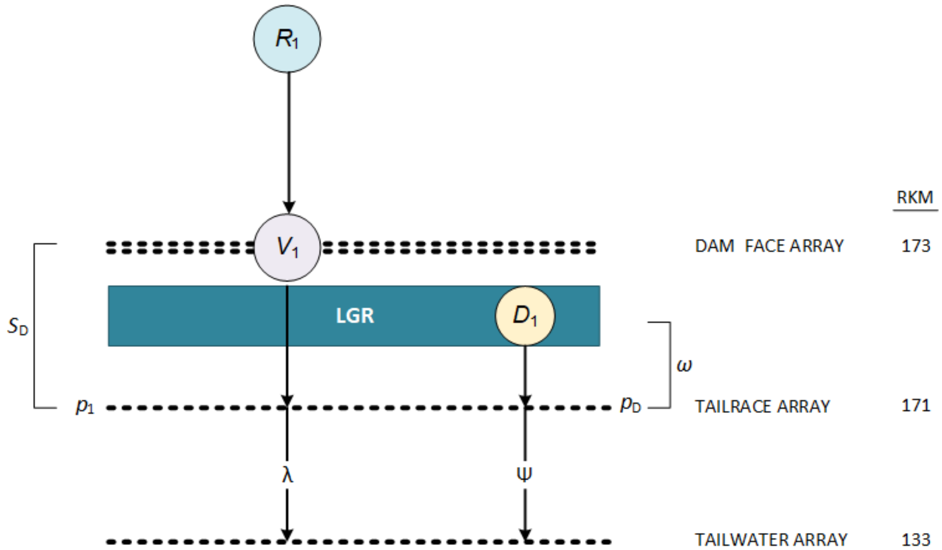

b. Reduced model

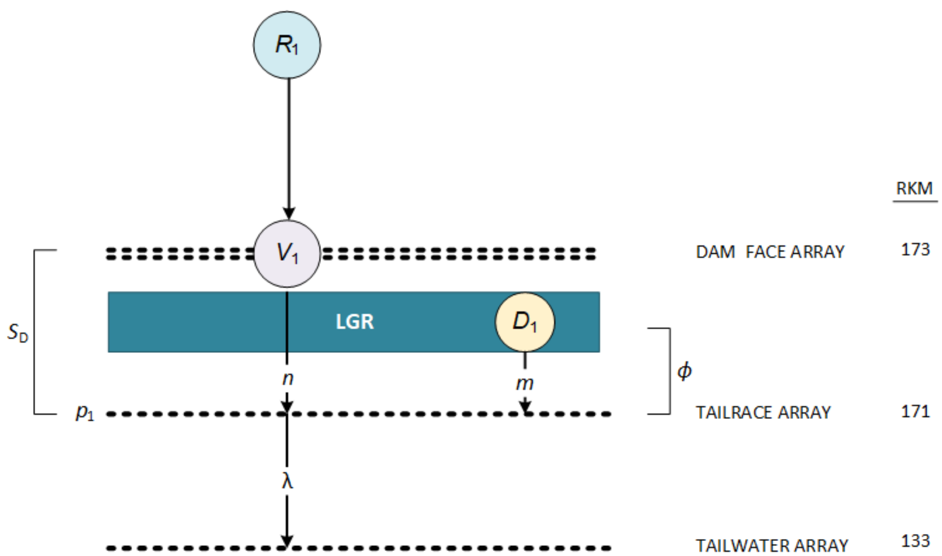

Figure 3.2. Schematic of the ViRDCt Release-Recapture Model to Estimate Dam Passage Survival at LGR in 2018. Alive (R_1), virtual (V_1), and dead fish (D_1) releases are denoted, along with hydrophone detection arrays. Schematic (a) allows dead fish detection at both the tailrace and tailwater arrays, and (b) permits dead fish detection at the tailrace only. S_D = dam passage survival; p_1 = probability of an alive V_1 fish being detected at the tailrace array; λ = joint probability of survival between tailrace and tailwater arrays and being detected as it passed the tailwater array; ω = joint probability of a dead fish from D_1 arriving at the tailrace array; p_D = probability of detecting a dead fish at the tailrace array; Ψ = joint probability that a dead fish is washed down to the tailwater array from the tailrace array and is detected at the tailwater array; ϕ = joint probability of a dead released fish (D_1) arriving at the tailrace array and being detected at that array; n = number of V_1 fish detected at the tailrace array; and m = number of D_1 fish detected at the tailrace array.

3.1.3 Sample Size Estimation

Sample sizes of R_1, R_2, and R_3 release groups were determined using survival and detection probability data from past AT studies as inputs to the SampleSize program (http://www.cbr.washington.edu/analysis/apps/samplesize). Sample sizes were adjusted until LGR VIPRE dam passage survival probability could be estimated with a precision of SE ≤ 0.025. Dead tagged fish release sample sizes were selected to obtain a season- and dam-wide (i.e., all routes combined) dead tagged fish detection rate estimate with a precision of SE < 0.030.

Table 3.1. Numbers of Fish per Stock for Release Groups R_1, R_2, R_3 (Figure 3.1), and D_1 (Figure 3.2), Along with Tag-Life Study Tags. Tags for R_1 not detected at the dam face were excluded from the virtual release V_1.

Fish stock	Release size				
	R_1	R_2	R_3	D_1	Tag life
Yearling Chinook salmon	466	299	298	212	97
Steelhead	680	501	500	183	97
Subyearling Chinook salmon	1393	690	690	289	125

3.2 Handling, Tagging, and Release Procedures

Fish obtained from the LGR Juvenile Fish Facility (JFF) via the JBS were surgically implanted with both AT and passive integrated transponder (PIT) tags and then transported to three different release points, as described in the following sections. Hatchery-reared fish were also surgically implanted with tags and euthanized prior to release into specific dam passage routes.

3.2.1 Transmitters

The AT tags used in the spring 2018 study were injectable acoustic transmitters (model ss400) manufactured by Advanced Telemetry Systems (ATS). Median dimensions of the AT tags were 15.06 mm length and 3.2 mm diameter with a weight of 218 mg in air and a volume of 121 mm^3. The tags transmitted a pulse every 3 seconds. Each pulse from an AT tag contained a complex phase-encoded signal that uniquely identified the transmitting tag. Each tag was acoustically activated approximately one day prior to being implanted in fish. Nominal tag life was 48 days.

Fish were also implanted with PIT tags equivalent to the Destron Fearing model TX1411ST, measuring 12.5 mm long and 2 mm wide and weighing 100 mg in air (60 mg in water; 0.04 mm^3 volume).

3.2.2 Fish Source

The CH1, CH0, and STH used in the study were all obtained from the LGR JFF via the JBS. USACE staff diverted fish from the JBS into an examination trough, and Smolt Monitoring Program (SMP) staff examined these fish as described by McMichael et al. (2011). PNNL staff then evaluated the candidate fish sent from SMP to determine if they met the criteria for inclusion in the study. During the routine sampling by SMP staff and examination by PNNL, fish were anesthetized using tricaine methanesulfonate (MS-222; 30-65 mg/L). A total of 2332 CH1, 3590 CH0, and 2865 STH were handled by PNNL as part of this study (Table 3.2). Fish that met acceptance criteria for the study were held for approximately 18 to 30 h in holding tanks prior to tagging. Non-sorted or excluded fish were immediately returned to the river below the dam or diverted into a recovery raceway per USACE guidelines.

Table 3.2. Total Number of CH1, STH, and CH0 Handled by PNNL During the 2018 Season and Counts of Fish in Several Handling Categories. More fish than required were made available for tagging to ensure sample size targets were met each day.

Handling Category	CH1	STH	CH0
Total handled	**2332**	**2865**	**3590**
Previously tagged	73	74	54
Fork length (FL) less than 95mm	15	0	450
FL more than 175mm (CH) or 300mm (STH)	4	8	0
Total not available for tagging	92	82	504
% Not available for tagging	**3.9%**	**2.9%**	**14.0%**
Met all acceptance criteria	2240	2783	3086
Excluded for condition	44	192	38
% Excluded	**2.0%**	**6.9%**	**1.2%**
Number tagged for live release	1069	1684	2783
Post-tagging mortality	5	3	10
% Mortality	**0.5%**	**0.2%**	**0.4%**
Pre-release tag failure	0	3	1
Pre-release PIT tag loss	3	0	1
% Pre-release tag issues	**0.3%**	**0.07%**	**0.2%**

All fish used in this study were evaluated based on a set of predetermined criteria outlined by the USACE Surgical Protocols Committee (USACE 2011). Overall, 2.0% of the CH1, 1.2% of the CH0, and 6.9% of the STH that met all the acceptance criteria for these studies were excluded based on their physical condition (Table 3.3). The primary reasons for exclusion of CH1, CH0, and STH were descaling over 20% of one side of the body, significant physical injuries, or injuries with active bleeding.

Table 3.3. Total Number of CH1, STH, and CH0 Excluded for Tagging by PNNL Based on Condition During the 2018 Season. Percentages are based on the total number of fish that met all acceptance criteria.

Reason for Exclusion	CH1		STH		CH0	
Descaling >20%	18	0.8%	142	5.1%	13	0.4%
Physical Injuries	13	0.6%	33	1.2%	18	0.6%
Disease and Infection	11	0.5%	13	0.5%	7	0.2%
Skeletal Deformities	1	0.0%	2	0.1%	0	0.0%
Moribund	1	0.0%	2	0.1%	0	0.0%
Total	44	2.0%	192	6.9%	38	1.2%

3.2.3 Tagging Procedure

The morning after collection, a team of four to six people (one data person, one anesthetist, and two to four surgeons) participated in the tagging process to minimize the negative influence of fish handling time from pre-surgery netting to post-surgery recovery. Each day, fish were tagged within a 2 to 4 h period and a new set of sterile blades were used. Throughout the day, blades were disinfected between each fish by placing them under ultraviolet light for 5 minutes (Walker et al. 2013). A synthetic water conditioner (Poly-Aqua) was used liberally on the surgical pad and other surfaces the fish would contact (measuring board, weigh boat, etc.) to counteract the disruption to mucous membranes during handling and surgical procedures.

The procedure began with an anesthetist netting a batch of fish (~15 to 25 individuals) from the post-collection holding tank and placing fish into an ~18.9 L bucket filled with aerated river water. The fish were anesthetized one at a time by placing them in a container with a 10 L solution of river water and MS-222 (80–100 mg/L) buffered with sodium bicarbonate (80–100 mg/L). In this “knockdown” solution, fish reached Stage 4 anesthesia within 2 to 3 minutes. Anesthesia solutions were changed repeatedly throughout the procedure to maintain the temperature within ± 2°C of ambient river temperatures.

Sedated fish were transferred individually to the data station in small plastic containers with approximately 0.25 L of knockdown solution (Figure 3.3). While at the data station, each fish was assigned a PIT tag and AT tag, weighed (nearest 0.1 g), and measured (fork length to the nearest 1 mm). The assigned PIT tag was scanned and recorded using a Biomark HPR Plus PIT reader. The assigned AT tag was scanned and recorded using an ATS pinger dish and the Sonic Tag Integrator interface. Doing so allowed the data person to verify that the tags were working properly at the time of implantation. Data for each fish was input electronically into a P4 software (ptagis.org) tagging session using a CalComp digitizer board and Ohaus scale. Additional data collected for each fish included species, run, adipose fin status (intact or clipped), and noteworthy abnormalities (e.g., minor descaling, fin erosion, predation marks, etc.). The fish was assigned to a surgeon and a recovery/release bucket, and data was saved using labeled buttons on the digitizer board. The fish were then placed back into their transfer container and delivered with the assigned PIT and AT tags to the assigned surgeon. A preset surgeon order was used throughout the day to satisfy a goal that each surgeon contribute at least one fish to each recovery/release bucket. In the event a surgeon effect was found during analysis, these efforts should spread the effect evenly across release locations and buckets.

During surgery, each fish was placed ventral side up in a foam pad with a carved-out, elongated, v-shaped groove. A gravity-fed river water supply line was placed into or near the fish’s mouth for the duration of the surgery to allow water to run over its gills. Fresh river water was supplied rather than a “maintenance” dose of anesthesia (40 mg/L) because tag implantation only took approximately 30 to 40 s per fish; therefore, additional anesthesia was not necessary for keeping fish sedated throughout the procedure. A surgical scalpel blade was used to make a 3 to 5 mm incision to one side of the linea alba (ventral mid-line), ending 3 to 5 mm anterior of the pelvic girdle. A PIT tag was inserted into the coelom, followed by an AT tag (battery end inserted toward the head). Both tags were inserted slightly toward the anterior end of the fish and parallel to the incision. Due to its small size, the incision was allowed to heal naturally during recovery without the use of sutures.

After tag implantation, the fish was placed in a dark 18.9 L recovery/release bucket filled with flow-through river water. After three to six fish were placed into a bucket, the bucket was transported to and submerged in a post-surgery holding trough filled with flow-through river water (Figure 3.4). Bucket lids were secured with a bungee cord to ensure fish could not escape into the holding tank. Also, small holes drilled into the recovery/release buckets allowed fresh river water to flow through (holes were small enough to keep fish from escaping). Fish were held in recovery for 12 to 30 h prior to being transported for release into the river.

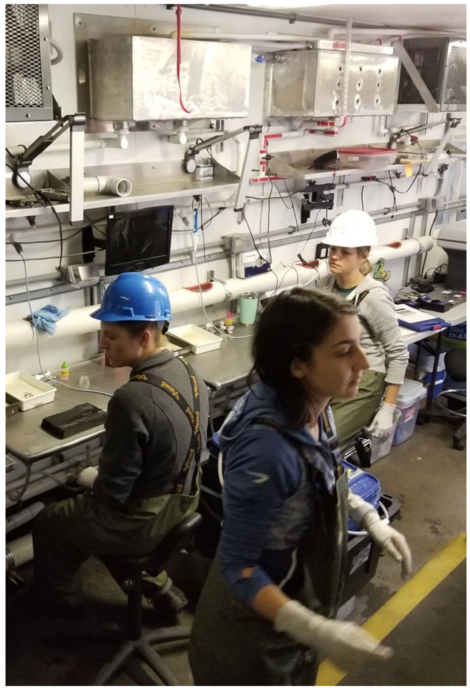

Figure 3.3. Surgery Stations in the Tagging Trailer

Figure 3.4. Post-Surgery Holding Tank with Recovery Buckets Containing Tagged Fish

3.2.4 Fish Transport and Release Procedures

All fish were transported by truck from LGR to one of three release locations within the Snake River (R_1, R_2, R_3). Prior to transport, buckets with tagged fish were placed in an insulated Bonar tote lined with acoustic absorbing material, where two Juvenile Salmon Acoustic Telemetry System (JSATS) hydrophones were mounted to record the codes of all tags in the bucket. Each bucket was uniquely identified with an alphanumeric code, and each lid had an attached PIT tag associated with the code. Each bucket was assigned a release site and location. After the presence of all tagged fish designated for each specific bucket was verified, the buckets were loaded into the transport vehicle.

To transport tagged fish, ¾-ton trucks were outfitted with two 681-L insulated Bonar totes filled half to three-quarters full with fresh river water prior to each release (Figure 3.5). Transport buckets were removed from the post-surgery holding tanks and placed in the totes, which can hold up to nine fish buckets per layer and up to two layers of buckets. A network of valves and plastic tubing was attached to an oxygen tank for delivering oxygen to the totes from a 2200-psi oxygen tank during transport. A YSI meter was used to monitor dissolved oxygen concentration and water temperature in the totes before and during transport to ensure that water quality parameters remained within the acceptable limits of 80 to 120% saturation and water temperature that varied no more than ±2°C. When measures approached unacceptable limits, staff adjusted the flow of oxygen to the tanks or added river-water ice to the river water in the tanks to maintain the desired water temperature.

Figure 3.5. Fish Release Transport Truck and Totes

Transportation routes were adjusted to provide equal travel times to R_2 and R_3 from LGR. Upon arriving at a release site, fish buckets were transferred to a boat for transport to the in-river release locations. At each release location, the fish were released at five predefined locations on a transect across the breadth of the river channel (Figure 3.6). The purpose of this release strategy was to evenly distribute fish across the channel.

Just before fish were released in the river, fish bucket lid PIT tags were scanned using a handheld PIT reader that also recorded the time and GPS location, and buckets were opened to check for dead or moribund fish. If dead or moribund fish were observed, they were removed and scanned with a Biomark portable transceiver PIT scanner to identify the implanted PIT code. The associated AT tag code was identified later from tagging data that recorded all pairs of PIT and AT tags implanted in fish from the tagging day. Moribund fish were euthanized immediately. Dead or euthanized fish were returned to the tagging facility and the tags were removed and the mortality recorded. Prior to the release of live fish, the buckets were also scanned for any dropped tags. Recovered tags were returned to the tagging facility and recorded.

Releases occurred day and night for 40–41 consecutive days for spring (17 April to 26 May) and summer (31 May to 10 July), and the timing of the releases at successive downstream locations was staggered to facilitate downstream mixing in the common tailwater. Spring releases were timed to accommodate an approximately 43-h travel time between R_1 and R_3 and 23-h travel time between R_1 and R_2. Summer releases were timed to accommodate a 64-h travel time between R_1 and R_3 and a 33-h travel time between R_1 and R_2 (Table 3.4).

Table 3.4. Typical Cycle of Releases for a 4-Day Study Block

Release Location	Release Times		
	***R*₁ (rkm 193)**	***R*₂ (rkm 171)**	***R*₃ (rkm 133)**
Spring			
Day 1	1200h		
Day 2	0600h	1100h	
Day 3		0400h	0700h
Day 4			0200h
Summer			
Day 1	0630h		
Day 2	1730h	1500h	
Day 3			2200h
Day 4		0130h	
Day 5	0630h (next block begins)		1000h

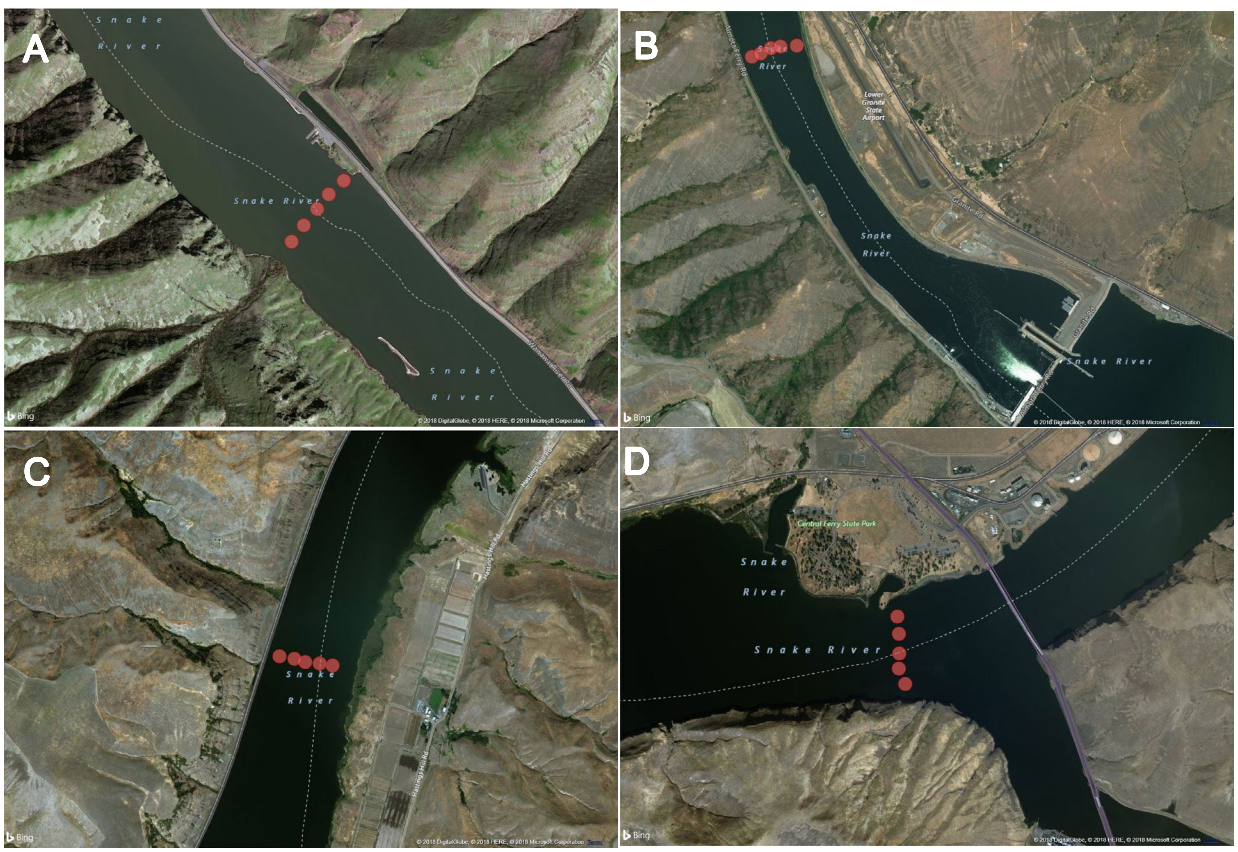

Figure 3.6. Snake River Release Locations for LGR Survival Study in 2018 (red dots in images). Images are arranged from upstream (A) to downstream (D). Water flow direction within each image is indicated by white arrows. Image A: upstream fish release location R_1 at rkm 193 near Blyton Landing, Washington; Image B: LGR tailrace release location R_2 at rkm 171; Image C: Willow Landing release location at rkm 140 used as R_3 for CH0; Image D: Central Ferry release location R_3 at rkm 133 for CH1 and STH.

3.2.5 Dead Tagged Fish Releases

For the VIPRE model, it was assumed that the detection array at the R_3 release was sufficiently far downstream to avoid detections of fish with still-active tags that died during dam passage. The dead tagged fish releases performed at LGR were used to test this assumption. A total of 212 CH1, 183 STH, and 289 CH0 were released at LGR over the course of the study (dead fish releases were more numerous than many previous VIPRE evaluations because the higher numbers were needed to support the ViRDCt evaluation, as described in the following section). Dead fish were released throughout the study to cover the range of flows during the season. To limit the number of fish taken from the LGR sampling facility, hatchery CH1 raised at PNNL's Aquatic Research Laboratory in Richland, Washington, were used for dead fish releases. STH-sized hatchery CH1 were used to represent STH in the dead tagged fish releases, and CH0-sized hatchery CH1 were used to represent CH0.

3.3 Detection of Tagged Fish

Detections of tagged fish were obtained via arrays of JSATS receivers at multiple locations in the Snake River, and each array had specific functions for the study at LGR. The JSATS arrays included cabled and star arrays associated with dam structures and autonomous node arrays anchored at several river cross-sections including the LGR forebay, tailrace, and the downstream survival detection arrays.

3.3.1 Autonomous Receiver Arrays

Autonomous receivers (AR) were deployed in transects across the Snake River at five strategically located sites (Figure 3.7). Groups of ARs are herein termed "arrays" because they operate in conjunction with each other to detect fish moving past a cross section of the river.

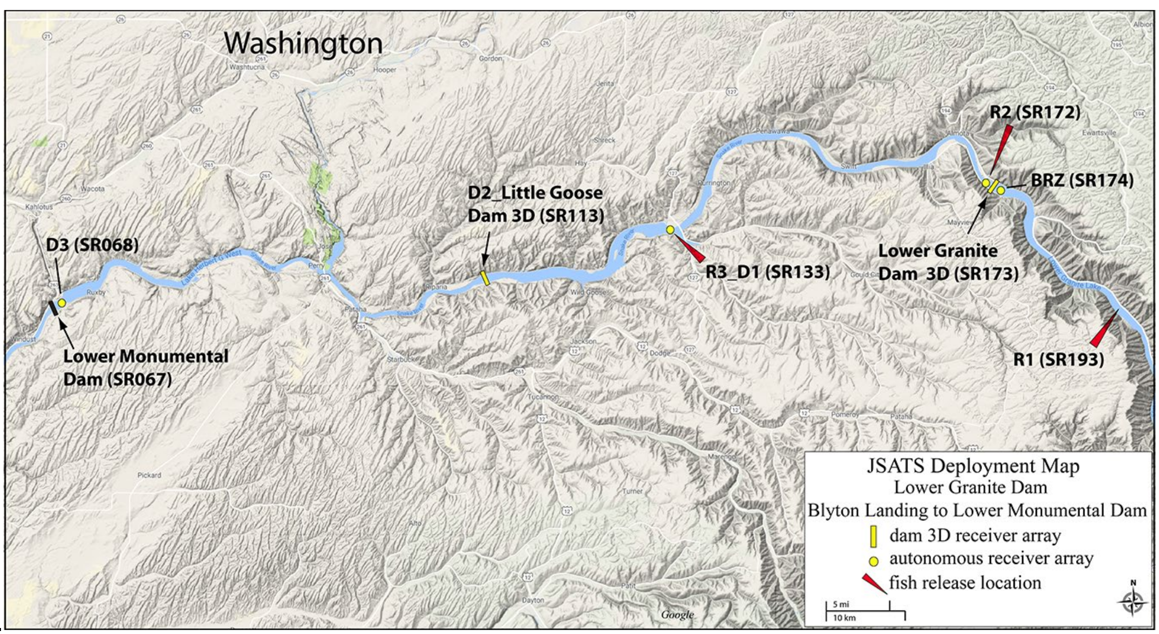

Figure 3.7. Map of Acoustic Receiver Array and Fish Release Locations

Receivers were deployed from a research vessel to form arrays that met the objectives of the LGR passage and survival study. Locations (waypoints) for each receiver were determined prior to deployment. Before each AR was deployed, researchers verified that all equipment and parts were present, operational, labeled, and documented properly. Once the research vessel was positioned as close as possible to the predetermined waypoint, two people deployed an AR assembly (anchor, acoustic release, short buoy line section, and the receiver; Figure 3.8) as described by Titzler et al. (2010). To mark the location of each AR deployed, an additional waypoint was created when the anchor landed on the river bottom. The information recorded for each deployed AR includes waypoint name, position (longitude/latitude), date, time, depth (from vessel sonar), receiver serial number, and acoustic release code. The waypoint name included array river kilometer_AR position in the array_AR serial number (e.g., SR173_01_7033).

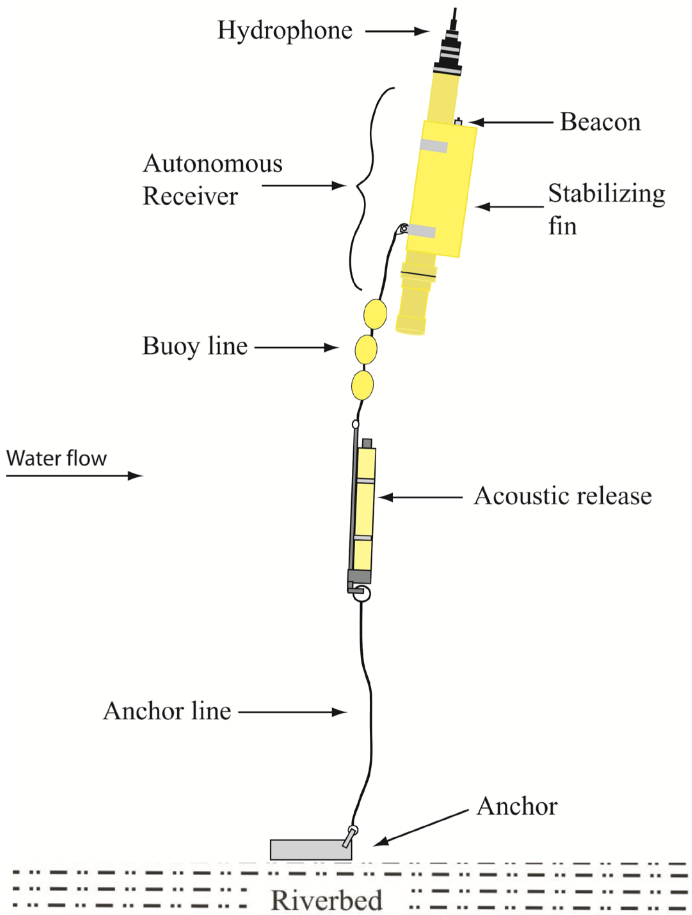

Figure 3.8. Autonomous Acoustic Receiver and Mooring Configuration Used for this Study

3.3.2 Cabled Receiver Arrays

JSATS cabled array systems were deployed for studies in the Snake River in 2012–2013 at Little Goose Dam (LGS) and Lower Monumental Dam (Skalski et al. 2013a, b, 2014). These systems demonstrated high detection efficiency and 3D tracking of tagged fish movements in the immediate forebay and for passage route assignments. A similar deployment design was implemented for the passage and survival study at LGR. Two star arrays and 14 hydrophone pairs on trolleys were used to position hydrophones at locations and to water depths required to meet 3D tracking objectives. The trolley system consisted of two trolleys separated vertically by a 4.76-mm-diameter wire rope that was measured and cut to a length that would place each trolley at a specific depth within a trolley pipe. One hydrophone and cable were secured to each of the two trolleys and were deployed in a single trolley pipe at seven pier noses across the spillway and at each wide pier nose (unit junction) across the powerhouse, leaving a total of 28 trolley-mounted hydrophones (Figure 3.9). At each location, one hydrophone was positioned at a shallow-water depth and one hydrophone was positioned deeper in the water column. The target elevations for each hydrophone are shown in Figure 3.10. For 3D coverage at the RSW, two star arrays were set on the river bottom approximately 50 m upstream of the RSW; each star array held four hydrophones (Figure 3.10). Also, battery-powered beacon transmitters were attached to the trolleys (Figure 3.9), alternating between a shallow and deep hydrophone location, with three locations at the powerhouse and two at the spillway. In addition, four beacons were attached to each of the two RSW star arrays. The beacons transmitted a 156-dB signal at either 15-s or 60-s intervals. These signals were used to verify array geometry and ensure hydrophones were properly decoding acquired acoustic signals. This deployment scheme provided a systematic and comprehensive detection grid in which tagged juvenile salmonids could be accurately tracked in 3D. JSATS hardware and software specifications are described in greater detail in the LGR Implementation Plan (McMichael et al. 2011).

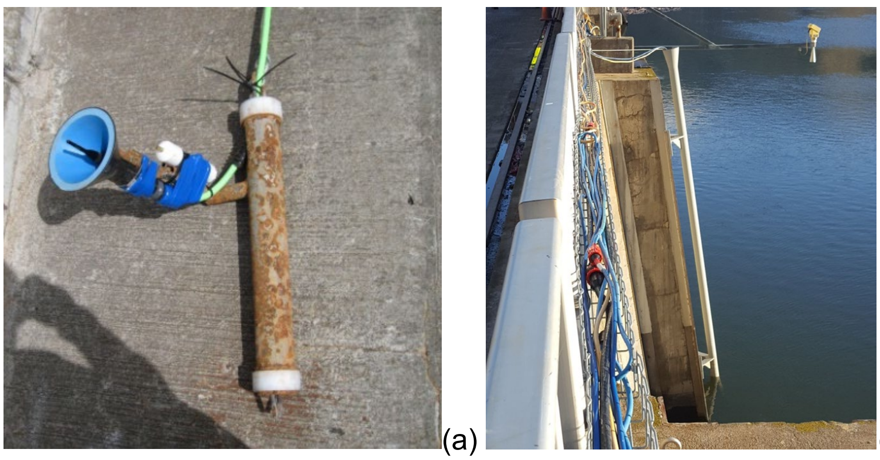
(a) (b)

Figure 3.9. Hydrophone Installation. (a) A 4-in.-diameter trolley with a hydrophone and a white beacon attached. (b) LGR powerhouse hydrophone cabling and trolley pipe.

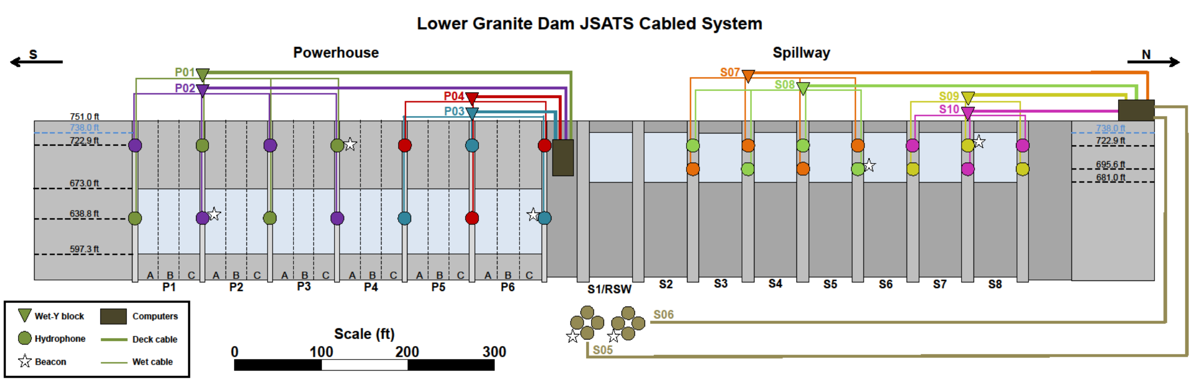

Figure 3.10. Forebay View of Lower Granite Dam Showing Hydrophone Deployment Locations at the Powerhouse, Spillway, and RSW

Two locations were used to house the electronic components used to operate the cabled receivers (i.e., computers, detectors, and receivers). The north end of the powerhouse fishway service gallery housed the electronic components used to operate the powerhouse hydrophones and a trailer placed at the north end of the spillway housed the electronic components used to operate the spillway and RSW hydrophones.

At LGS, a partial cabled array was deployed to meet 3D tracking and route assignment objectives related to a different study of adult and juvenile passage (Figure 3.11). For the LGR study, this array functioned as one of the downstream detection arrays, but LGS route information was not needed to address LGR objectives. This array consisted of 18 trolley-mounted hydrophones deployed in nine trolley pipes (four on the powerhouse and five on the spillway). At each location, hydrophones were deployed at two different depths: a shallow hydrophone that was about 4.57 m under the water surface and a deeper hydrophone that was 12.80 m (spillway) to 30.18 m (powerhouse) under the water surface. In addition, one hydrophone was deployed in a trolley pipe located on the wall just north of the adult fish ladder exit to detect any juveniles that may have passed downstream through the ladder. Battery-powered beacon tags that transmitted a 156-dB signal at either a 15 or 60-s interval were deployed on trolleys at seven locations, alternating between shallow and deep hydrophone locations. Beacon signals were used to perform in-season detection efficiency checks of individual hydrophones. This deployment scheme provided a sufficient detection grid in which acoustic-tagged fish could be accurately tracked in 3D to their route of passage.

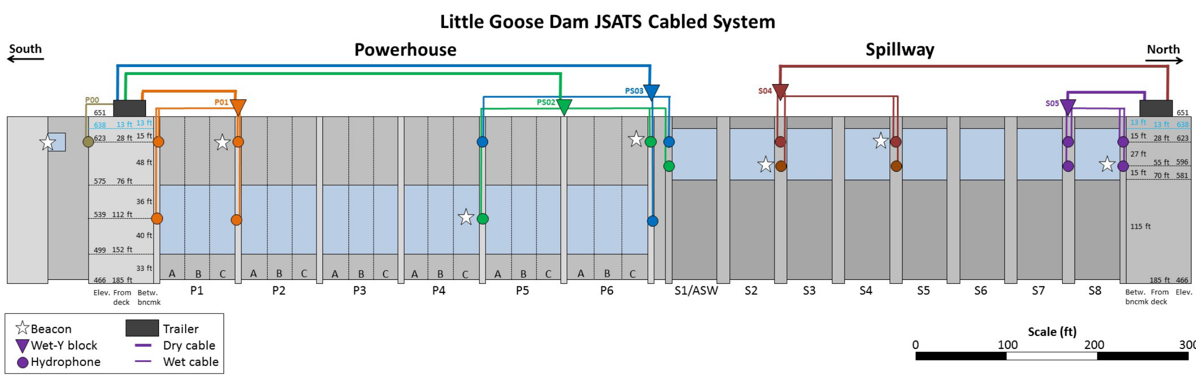

Figure 3.11. Forebay View of Little Goose Dam Showing Hydrophone Deployment Locations at the Powerhouse, Spillway, and Adjustable Spillway Weir (ASW)

3.3.2.1 Deployment Configuration

The hydrophone deployments described above can be sampled as two independent arrays to allow estimation of detection probabilities using route of passage. Figure 3.12 shows an example for hydrophones deployed on the pier noses between three adjacent turbines. The same concept can be used for hydrophones deployed at the spillway.

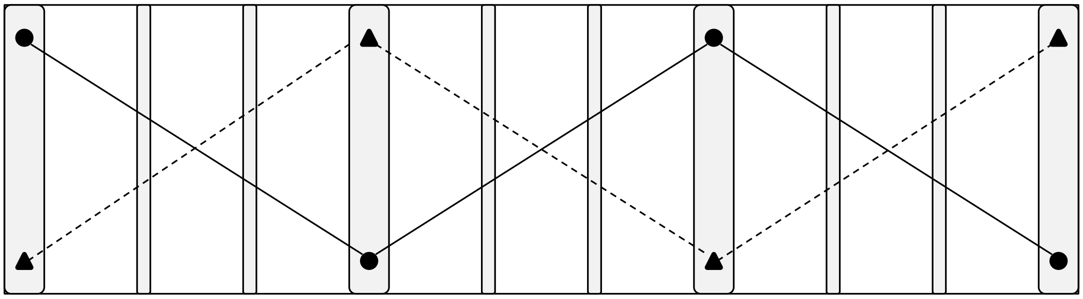

Figure 3.12. Frontal View of Hydrophone Deployments at Three Turbines Showing a Saw-Tooth Sampling Pattern to Independently Assign the Location of the Last Detection. The circles denote the hydrophones of array 1 and the triangles denote the hydrophones of array 2.

The use of two independent arrays provides estimates of the following:

- detection probability at the 1st $\hat{p}_1 = m/n_2$ array
- detection probability at the 2nd $\hat{p}_2 = m/n_1$ array
- detection probability for the $\hat{P} = 1-(1-\hat{p}_1)(1-\hat{p}_2)$ combined array

where the detection history codes:

m = number of individuals detected on both arrays
n_1= number of individuals detected on the 1st array
n_2= number of individuals detected on the 2nd array

Detection probability for each independent array is calculated by processing the detection data for each of the two arrays separately. This individual detection probability is then compared to detections calculated as if both arrays were combined. Some tags detected on the combined array may not be detected on the independent arrays. Detection histories can then be separated by passage route and described in a table (Table 3.5).

Table 3.5. LGR Detection Histories by Route of Passage for Independent Cabled Dam-Face Arrays and Detection Probability for the Combined Array

	Detection History Code			
Location	m	n_1	n_2	Detection Probability
Powerhouse	1245	1260	1249	99.996
Surface-flow outlet	1087	1102	1097	99.988
Spillway	1009	1065	1017	99.959

3.3.3 Three-Dimensional Tracking

The cabled dam-face array and star arrays deployed at LGR allowed fish behavior and route of passage through the dam to be assessed via 3D tracking of fish implanted with AT tags. Assigning spatial locations using acoustic tracking is a common technique in bioacoustics based on time-of-arrival differences among different hydrophones (Watkins and Schevill 1972). At a minimum, the process requires detections on a four-hydrophone array (see Deng et al. 2011 for details of the 3D tracking methodology).

3.4 Acoustic Signal Processing for Fish Detection

Transmissions of JSATS tag codes received on cabled and autonomous hydrophones were recorded in raw data files. These files were downloaded periodically and transported to PNNL offices in Richland, Washington, for processing. Receptions of tag codes within raw data files were processed to produce a data set of accepted tag detection events. For cabled arrays, detections from all hydrophones at a dam were combined for processing.

The following three filters were used for data from cabled arrays:

- Multipath filter: For data from each individual cabled hydrophone, all tag code receptions that occurred within 0.3 s after an initial identical tag code reception were deleted under the assumption that closely lagging signals were multipath. The first signal received is assumed to have traveled via a direct path from the transmitter to receiver, while closely spaced identical signals are assumed to have traveled along a longer path that included reflection from the water surface, bottom, or one of many structural surfaces of a dam.
- Multi-detection filter: Receptions were retained only if the same tag code was received at another hydrophone in the same array within 0.3 s, because receptions on separate hydrophones within 0.3 s (range of about 450 m) were likely from a single tag transmission.
- Pulse repetition interval (PRI) filter: Only those series of tag code receptions (or "messages") that were consistent with the pattern of transmissions from a properly functioning JSATS acoustic tag were retained. Filtering rules were evaluated for each tag code individually, and it was assumed that only a single tag would be transmitting that code at any given time. For the cabled system, the PRI filter operated on a message that included all receptions of the same transmission on multiple hydrophones within 0.3 s. Message time was defined as the earliest reception time across all hydrophones for that message. Detection required that at least six messages were received with 12 pulse intervals between the leading edges of successive messages.

Like the cabled-array data, receptions of JSATS tag codes within raw autonomous node data files are processed to produce a data set of accepted tag detection events. A single file is processed at a time, and no information on receptions at other nodes is used. The following two filters are used during processing of autonomous node data:

- Multipath filter: Same as for the cabled-array data.
- PRI filter: Only those series of tag code receptions (or "hits") that were consistent with the pattern of transmissions from a properly functioning JSATS acoustic tag were retained. Each tag code was processed individually, and it was assumed that only a single tag would be transmitting that code at any given time. Each autonomous receiver in an array was processed separately, meaning that receptions at other nodes in the same array were not considered when evaluating events for a given node.

The output of the filtering processes for both cabled and autonomous hydrophones was a data set of events that summarized accepted tag detections for all times and locations where hydrophones were operating. Each unique event record included a basic set of fields that indicated the unique identification number of the fish, the first and last detection time for the event, the location of detection, and how many messages were detected within the event. This list was combined with accepted tag detections from PIT-tag detection locations for additional quality assurance/quality control analysis prior to survival analysis.

Additional fields captured specialized information, where available. An example of such information was the route of passage, which was assigned a value for those events that immediately precede passage at a dam based on spatial tracking of tagged fish movements to the location of the last detection. Tagged fish in the immediate forebay of LGR were tracked in three dimensions to determine routes of passage.

One of the most important quality control steps was to examine the detection chronology of every tagged fish on all arrays above and below the dam-face array to identify any detection sequences that deviated from the expected upstream to downstream progression through arrays in the river. Except for possible detections on forebay entrance arrays after detection on a nearby dam-face array 1 to 3 km downstream, apparent upstream movements of tagged fish between arrays that were greater than 5 km apart or separated by one or more dams were very rare and are assumed to represent false-positive detections on the upstream array or an event involving predation. False-positive detections usually will have close to the minimum number of messages and were censored from the event data set before survival analysis.

3.5 Statistical Methods

This section describes the statistical methods used to test assumptions and estimate passage survival, tag life, forebay-to-tailrace survival, travel times, SPE, fish passage efficiency (FPE), and fish guidance efficiency (FGE).

3.5.1 Estimation of Dam Passage Survival

The VIPRE and ViRDCt models were used to estimate survival in the 2018 study of passage and survival at LGR. The VIPRE model has been used in previous evaluations of survival performance at dams in the Snake and Columbia rivers. The ViRDCt model is a more recently developed approach that has the potential to produce more precise estimates using fewer tagged fish. Comparing the performance of these models will help inform designs for future survival evaluations.

3.5.1.1 VIPRE Model

Maximum likelihood estimation was used to estimate dam passage survival at LGR based on the VIPRE design. The capture histories from all the replicate releases, both day and night, were pooled to produce estimates of dam passage survival. A joint likelihood model was constructed as a product multinomial with separate multinomial distributions describing the capture histories of the separate release groups (i.e., V_1, R_2, and R_3;Table 3.1).

The joint likelihood used to model the three release groups was initially fully parameterized. Each of the three releases was allowed to have unique survival and detection parameters. If precision was adequate (i.e., $SE \leq 0.015$) with the fully parameterized model, no further modeling was performed. If initial precision was inadequate, then likelihood ratio tests were used to assess the homogeneity of parameters across release groups to identify the best parsimonious model to describe the capture history data. This approach was used to help preserve both the precision and robustness of the survival results (Skalski et al. 2013a). All calculations were performed using Program ATLAS.[1]

Dam passage survival was estimated by the following function:

$$\hat{S}_{\text{Dam}} = \frac{\hat{S}_1}{\left(\frac{\hat{S}_2}{\hat{S}_3}\right)} = \frac{\hat{S}_1 \cdot \hat{S}_3}{\hat{S}_2} \quad (3.1)$$

where $\hat{S}_i$ is the tag-life-corrected survival estimate for the i^{th} release group (i = 1,…,3). The variance of $\hat{S}_{\text{Dam}}$ was estimated in a two-step process that incorporated the uncertainty in both the tag-life corrections and the release-recapture processes.

During the spring passage period of 2018 (through 20 June), a court order required the spill at LGR to be increased to the amount that allows total dissolved gas to remain within water quality waivers of 120% (aka "gas cap"). Spill was maintained at or above the gas cap level throughout the spring passage period. At times when the total river discharge exceeded the required spill plus the powerhouse capacity, it was necessary to spill any discharge more than those amounts, resulting in "involuntary spill."

3.5.1.2 ViRDCt Model

Maximum likelihood estimation (MLE) was used to estimate dam passage survival using the ViRDCt model (Harnish et al. 2017). Ideally, the tailwater array would be located sufficiently downstream such that none of the dead fish released (D_1) were detected by that array. An alternative model allowing detection of dead tagged fish at both the tailrace and tailwater arrays was also formulated. However, precision would be greater under the simplified model, if valid.

For the full model with possible dead fish detections at both downriver arrays (Table 3.2a), the likelihood can be written as follows:

$$\begin{aligned} L = \binom{V_1}{\vec{n}} & (S_D p_1 \lambda + (1-S_D)\omega p_D \Psi)^{n_{11}} \\ & \cdot (S_D(1-p_1)\lambda + (1-S_D)\omega(1-p_D)\Psi)^{n_{01}} \\ & \cdot \left(S_D p_1(1-\lambda) + (1-S_D)\omega p_D(1-\Psi)\right)^{n_{10}} \\ & \cdot \left[S_D(1-p_1)(1-\lambda) + (1-S_D)\left((1-\omega) + \omega(1-p_D)(1-\Psi)\right)\right]^{V_1-n.} \\ & \cdot \binom{D}{\vec{d}} (\omega p_D \Psi)^{d_{11}} (\omega(1-p_D)\Psi)^{d_{01}} \\ & \cdot \left(\omega p_D(1-\Psi)\right)^{d_{10}} \left((1-\omega) + \omega(1-p_D)(1-\Psi)\right)^{D-d.} \end{aligned} \quad (3.2)$$

where

- n_{ij} = number of V_1 release fish with capture history ij (i = 0 or 1 for detection at tailrace, j = 0 or 1 for detection at tailwater array);
- S_D = dam passage survival;
- p_1 = probability of an alive V_1 fish being detected at the tailrace array;

[1] Available at http://www.cbr.washington.edu/paramest/atlas/.

λ = joint probability of survival between tailrace and tailwater arrays and of the fish being detected at the tailwater array;
ω = joint probability of a dead fish from D_1 arriving at the tailrace array;
p_D = probability of detecting a dead fish at the tailrace array;
Ψ = joint probability that a dead fish is washed down to the tailwater array from the tailrace array and is detected at the tailwater array.

Iterative procedures from Program USER (http://www.cbr.washington.edu/analysis/apps/user) were used to estimate the model parameters and associated variances. No attempt was made to adjust for tag life because travel times to the downstream array were well within minimum tag life.

For the reduced model with dead fish from D_1 only detected at the tailrace array, the joint likelihood model can be written as follows:

$$L = \binom{V_1}{n}(S_D p_1 + (1-S_D)\phi)^n \big(S_D(1-p_1) + (1-S_D)(1-\phi)\big)^{V_1-n} \cdot \binom{D_1}{m}\phi^m(1-\phi)^{D_1-m} \cdot \binom{n_{11}+n_{01}}{n_{11}} p_1^{n_{11}}(1-p_1)^{n_{01}} \tag{3.3}$$

where

ϕ = joint probability of a dead released fish (D_1) arriving at the tailrace array and being detected at that array;
n = number of V_1 fish detected at the tailrace array;
m = number of D_1 fish detected at the tailrace array.

Parameter estimates and associated standard errors were calculated based on Program USER. This model's MLE for the estimate of dam passage survival was of closed form, where

$$\hat{S}_D = \frac{\left(\frac{n}{V_1} - \frac{m}{D_1}\right)}{\left(\hat{p}_1 - \frac{m}{D_1}\right)} \tag{3.4}$$

3.5.1.3 Tag-Life Analysis

For the spring and summer releases, 97 and 125 acoustic tags, respectively, were monitored to conduct tag-life analysis. Tags were monitored from activation to tag failure in continuous time with tags soaked in ambient river water. Failure times were fit to the four-parameter Vitality model (Li and Anderson 2009; Lady et al. 2012). The vitality model tends to fit acoustic-tag failure times well because it allows for early onset of random failure due to inconsistencies in manufacturing as well as systematic battery failure later on.

The Vitality survivorship function (Lady et al. 2012) was used to estimate tag life probability and can be rewritten as

$$S(t) = 1 - \left(\Phi\left(\frac{1-rt}{\sqrt{u^2+s^2t}}\right)\right) - e^{\left(\frac{2u^2r^2}{s^4}+\frac{2r}{s^2}\right)}\Phi\left(\frac{2u^2r+rt+1}{\sqrt{u^2+s^2t}}\right)^{e^{-kt}} \tag{3.2}$$

where

Φ = cumulative normal distribution,

r = average wear rate of components,

s = standard deviation in wear rate,

k = rate of accidental failure,

u = standard deviation in quality of original components.

The random failure component, in addition to battery discharge, gives the vitality model additional latitude to fit tag-life data not found in other failure-time distributions such as the Weibull or Gompertz. Parameter estimation was based on MLE. The parameter coefficients of the Vitality Survivorship function for tag groups used in this study are shown in Table 3.6.

Table 3.6. Vitality Survivorship Function Parameter Coefficients

Vitality Model Parameter	Spring Tag Life Coefficient (SE)	Summer Tag Life Coefficient (SE)
r	0.0160 (0.0002)	0.0170 (0.0002)
s	0.0139 (0.0107)	0.0138 (0.0011)
k	0.0012 (0.0006)	0.0018 (0.0006)
u	0.0582 (0.1582)	$5.75e^{-5}$ (0.0003)

For the virtual release group (V_1) based on fish known to have arrived at the dam face, the conditional probability of transmitter activation, given that the transmitter was active at the dam-face detection array, was used in the tag-life adjustment for that release group. The conditional probability of transmitter activation at time t_1, given it was active at time t_0, was computed by the quotient

$$P(t_1|t_0) = \frac{S(t_1)}{S(t_0)} \tag{3.3}$$

where $S(t_0)$ was the average unconditional probability that the transmitter was active when detected at the dam-face detection array, and $S(t_1)$ was the average unconditional probability that the transmitter was active when detected at the first tailwater detection array.

3.5.2 Tests of Assumptions

Approaches to assumption testing are described below.

3.5.2.1 Burnham et al. (1987) Tests

Tests 2 and 3 of Burnham et al. (1987) could be used to assess whether upstream detection history has an effect on downstream survival. Such tests are most appropriate when fish are physically recaptured or segregated during capture, as in the case with PIT-tagged fish going through the JBS. However, acoustic-tag studies do not use physical recaptures to detect fish. Consequently, these tests have little relevance in AT studies. Furthermore, the very high detection probabilities present in AT studies frequently preclude calculation of these tests. For these reasons, these tests were not performed.

3.5.2.2 Tests of Mixing

Evaluation of the homogeneous arrival of release groups at downriver detection sites was based on graphs of arrival distributions. The graphs were used to identify any systematic and meaningful departures from mixing. Ideally, the arrival distributions should overlap one another with similarly timed modes.

3.5.2.3 Tagger Effects

Subtle differences in handling and tagging techniques could influence the survival of juvenile salmonids used in the estimation of dam passage survival. For this reason, tagger effects were evaluated. The single release-recapture model was used to estimate reach survivals for fish tagged by different individuals. The analysis evaluated whether any consistent pattern of reduced reach survivals exists for fish tagged by any of the tagging staff.

For k independent reach survival estimates, a test of equal survival was performed using the F-test

$$F_{k-1,\infty} = \frac{s_{\hat{S}}^2}{\left(\frac{\sum_{i=1}^{k} \widehat{\mathrm{Var}}\left(\hat{S}_i \middle| S_i\right)}{k}\right)} \tag{3.4}$$

where

$$s_{\hat{S}}^2 = \frac{\sum_{i=1}^{k}\left(\hat{S}_1 - \hat{\bar{S}}\right)^2}{k-1} \tag{3.5}$$

and

$$\hat{\bar{S}} = \frac{\sum_{i=1}^{k}\hat{S}_i}{k}. \tag{3.6}$$

The F-test was used in evaluating tagger effects as well as delayed tag effects.

3.5.2.4 Tag Lot Effects

Tag lot effects were evaluated by comparing the tag-life distributions of the tags used in the spring- and summer-run studies using likelihood ratio tests.

3.5.2.5 Representativeness of Dead Tagged Fish Releases

An additional assumption required by the ViRDCt model is that dead tagged fish are representative of fish from the V_1 group that died during dam passage. For this reason, dead tagged fish were released into each passage route (i.e., turbine, RSW, deep spill bays, JBS) in proportion to the expected distribution of fish from the V_1 group that died during dam passage, which was estimated using data from past survival studies conducted at Snake River dams. Dead tagged fish releases occurred three to four times per week during both day and night throughout the period of acoustic-tagged fish LGR passage to accurately capture the variability in the dead tagged fish detection rate associated with dam operations and environmental conditions. The representativeness of the dead tagged fish releases was tested by comparing the spatial and temporal distribution of dead tagged fish releases to the spatial (i.e., route) and temporal distribution of fish from the V_1 group that were not detected downstream of the tailrace array (SR172).

The fish used in the dead tagged fish releases were obtained from the ARL and were euthanized by a standard protocol involving exposure to a solution of 250 mg/L MS-222 for at least 10 minutes after opercular movement has ceased (per American Veterinary Medicine Association guidelines for finfish, https://www.avma.org/KB/Policies/Documents/euthanasia.pdf). Unfortunately, the exposure time was inadequate for some fish, and these fish recovered from being anesthetized after release to migrate downriver. These revived fish were identified by their rapid exit from the tailrace and, in many cases, detection at LGS and downstream. Revived fish were removed from the dead tagged fish release and subsequent analyses. Failure to remove all false-positive dead tagged fish detections would negatively bias the ViRDCt estimates of LGR passage survival.

3.6 Forebay-to-Tailrace Survival

The same VIPRE and ViRDCt models used to estimate dam passage were used to estimate forebay-to-tailrace survival (also known as BRZ-to-BRZ survival). The only distinction is that the virtual release group (V_1) was composed of fish known to have arrived alive at the forebay array (rkm 174) instead of at the dam face (Figure 2.1).

3.6.1 Estimation of Travel Times

Travel times associated with forebay residence time and tailrace egress were estimated using arithmetic averages as specified in the Fish Accords, i.e.,

$$\bar{t} = \frac{\sum_{i=1}^{n} t_i}{n}, \tag{3.7}$$

with the variance of $\bar{t}$ estimated by

$$\widehat{\mathrm{Var}}(\bar{t}) = \frac{\sum_{i=1}^{n} (t_i - \bar{t})^2}{n(n-1)}, \tag{3.8}$$

and where t_i was the travel time of the i^{th} fish $(i = 1, \cdots, n)$. Median and range in travel times were also computed and reported.

Tailrace egress time for fish arriving at LGR was calculated differently for bypassed and non-bypassed fish before their data was pooled. For bypassed fish, tailrace egress time was measured from the last detection in the fish bypass to the last detection at the tailrace array below the dam. For all other fish, tailrace egress time was measured from the last detection at the dam-face array to the last detection at the tailrace array below the dam. Both the arithmetic average and the median were calculated. Only fish known to have passed the dam alive were used in the calculations, based on fish observed to be alive downstream.

The estimated forebay residence times were based on the time from the first detection at the forebay BRZ array 1 km above the dam to the last detection at the double array on the upstream face of LGR.

3.6.2 Estimation of SPE

SPE was estimated by the fraction

$$\widehat{\mathrm{SPE}} = \frac{\hat{N}_{\mathrm{SPL}} + \hat{N}_{\mathrm{RSW}}}{\hat{N}_{\mathrm{SPL}} + \hat{N}_{\mathrm{RSW}} + \hat{N}_{\mathrm{JBS}} + \hat{N}_{\mathrm{TUR}}} \tag{3.9}$$

where $\hat{N}_i$ was the estimated abundance of tagged fish through the i^{th} route (i = spill bays (SPL), RSW, JBS, and turbines (TUR)). The double-detection array at the dam face was used to estimate absolute abundance (*N*) through a route using the single mark-recapture model (Seber 1982:p. 60) independently at each route. The variance of $\widehat{\mathrm{SPE}}$ was estimated as follows:

$$\widehat{\mathrm{Var}}\left(\widehat{\mathrm{SPE}}\right) = \frac{\widehat{\mathrm{SPE}}\left(1-\widehat{\mathrm{SPE}}\right)}{\sum_{i=1}^{4}\hat{N}_i} + \widehat{\mathrm{SPE}}^2\left(1-\widehat{\mathrm{SPE}}\right)^2 \cdot \left[\frac{\widehat{\mathrm{Var}}\left(\hat{N}_{\mathrm{SPL}}\right)+\widehat{\mathrm{Var}}\left(\hat{N}_{\mathrm{RSW}}\right)}{\left(\hat{N}_{\mathrm{SPL}}+\hat{N}_{\mathrm{RSW}}\right)^2} + \frac{\widehat{\mathrm{Var}}\left(\hat{N}_{\mathrm{TUR}}\right)+\widehat{\mathrm{Var}}\left(\hat{N}_{\mathrm{JBS}}\right)}{\left(\hat{N}_{\mathrm{TUR}}+\hat{N}_{\mathrm{JBS}}\right)^2}\right]. \tag{3.10}$$

3.6.3 Estimation of Fish Guidance Efficiency

At the powerhouse, FGE was estimated by the following fraction:

$$\widehat{\mathrm{FGE}} = \frac{\hat{N}_{JBS}}{\hat{N}_{JBS}+\hat{N}_{TUR}}, \tag{3.11}$$

The variance of $\widehat{\mathrm{FGE}}$ was estimated as:

$$\mathrm{Var}\left(\widehat{\mathrm{FGE}}\right) = \frac{\widehat{\mathrm{FGE}}\left(1-\widehat{\mathrm{FGE}}\right)}{\sum_{i=1}^{2}\hat{N}_i} + \widehat{\mathrm{FGE}}^2\left(1-\widehat{\mathrm{FGE}}\right)^2 \cdot \left[\frac{\mathrm{Var}\left(\hat{N}_{JBS}\right)}{\hat{N}_{JBS}^2} + \frac{\widehat{\mathrm{Var}}\left(\hat{N}_{TUR}\right)}{\hat{N}_{TUR}^2}\right]. \tag{3.12}$$

Because the detection probability of acoustic-tagged fish at the face of the LGR was virtually 1.0, passage calculations were reduced to binomial or multinomial proportions.

3.6.4 Estimation of FPE

FPE was estimated as the fraction of fish through non-turbine routes, where

$$\widehat{\mathrm{FPE}} = \frac{\hat{N}_{\mathrm{SPL}} + \hat{N}_{\mathrm{RSW}} + \hat{N}_{\mathrm{JBS}}}{\hat{N}_{\mathrm{SPL}} + \hat{N}_{\mathrm{RSW}} + \hat{N}_{\mathrm{JBS}} + \hat{N}_{\mathrm{TUR}}}. \tag{3.13}$$

The variance of $\widehat{\mathrm{FPE}}$ was estimated as

$$\widehat{\mathrm{Var}}\left(\widehat{\mathrm{FPE}}\right) = \frac{\widehat{\mathrm{FPE}}\left(1-\widehat{\mathrm{FPE}}\right)}{\sum_{i=1}^{4}\hat{N}_i} + \widehat{\mathrm{FPE}}^2\left(1-\widehat{\mathrm{FPE}}\right)^2 \tag{3.14}$$

$$\cdot\left[\frac{\widehat{\mathrm{Var}}\left(\widehat{N}_{\mathrm{SPL}}\right)+\widehat{\mathrm{Var}}\left(\widehat{N}_{\mathrm{RSW}}\right)+\widehat{\mathrm{Var}}\left(\widehat{N}_{\mathrm{JBS}}\right)}{\left(\widehat{N}_{\mathrm{SPL}}+\widehat{N}_{\mathrm{RSW}}+\left(\widehat{N}_{\mathrm{JBS}}\right)\right)^{2}}+\frac{\widehat{\mathrm{Var}}\left(\widehat{N}_{\mathrm{TUR}}\right)}{\widehat{N}_{\mathrm{TUR}}^{2}}\right].$$

Because the detection probability of acoustic-tagged fish at the face of the LGR was virtually 1.0, passage calculations were reduced to binomial or multinomial proportions.

4.0 Results

This section summarizes river conditions, passage routing, passage timing, vertical distributions, and survival rates for the spring and summer study periods at LGR in 2018. Results are presented separately for spring and summer study periods. Appendices (A−E) provide additional detail about the assessment of survival model assumptions (A), fish tagging and release (B), hydrophone and autonomous node locations (C), capture histories (D), and comparisons with older radiotelemetry results (E).

4.1 Results – Spring

This section describes the river conditions, approach and passage distributions, passage metrics, travel times, and survival estimates for CH1 and STH during the spring study period at LGR in 2018.

4.1.1 Spring River Conditions

River conditions such as discharge, operations, and water quality at LGR may influence passage or survival. Daily discharge, spill, temperatures, and historical data was downloaded from the UW DART website (http://www.cbr.washington.edu/dart). Dissolved gas data for the tailrace was downloaded from the USACE Northwest Division Dataquery site (http://www.nwd-wc.usace.army.mil/dd/common/dataquery/www/).

At LGR, spring spill passage operations were in effect from 3 April through 20 June, and summer spill passage operations began 21 June and continued to 31 August. It is important to differentiate between these fish passage operation periods and the “spring” and “summer” study periods used in this study, which are based on the historic migration timing of the fish runs under study. In 2018, spill during the spring passage operations period at FCRPS dams, including LGR, was directed by court order to increase spill to the 120/115% gas cap. This means that the project is to spill to the maximum level that meets, but does not exceed, the total dissolved gas (TDG) criteria waivers as allowed under state law at ≤120% in the tailrace and ≤115% in the forebay of the next dam downstream. In recent years, planned spill at LGR was 20 kcfs during the spring, well below the gas cap spill level at typical river flow levels during the spring.

In 2018, mean daily discharge and spill were consistently at or above the 10-year average (2008–2017) during the spring study period (Figure 4.1). TDG was above average throughout the spring study period, consistent with the court-ordered increase in spill (Figure 4.2). Temperatures were near average during the spring study period (Figure 4.3).

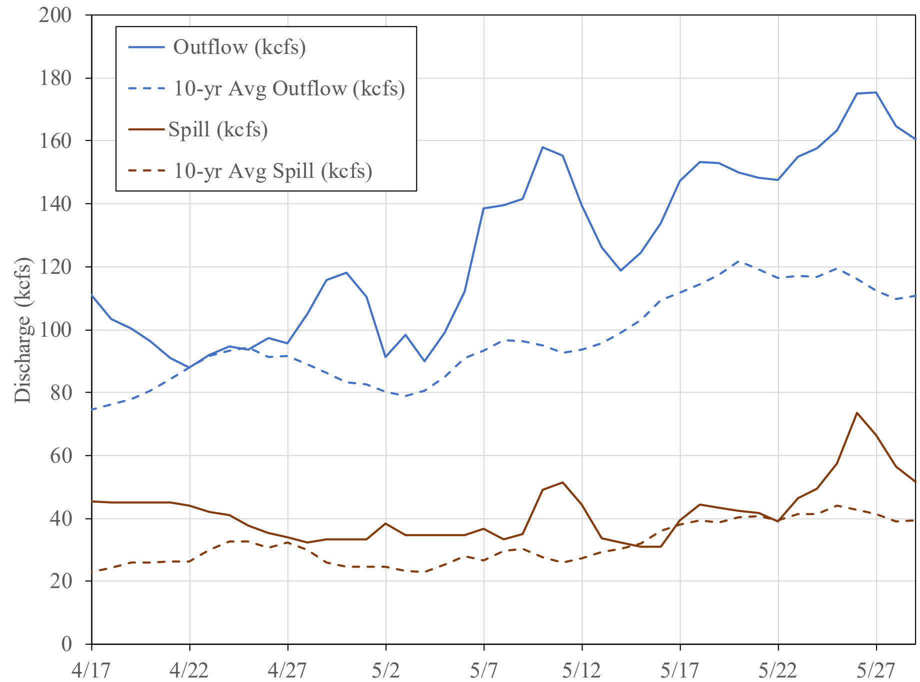

Figure 4.1. Mean Daily Water Discharge (kcfs) and Spill from LGR During the 2018 Spring Study Period and the Preceding 10-Year Average (2008−2017). Data Source: Columbia River DART (Data Access in Real Time) www.cbr.washinton.edu/dart.

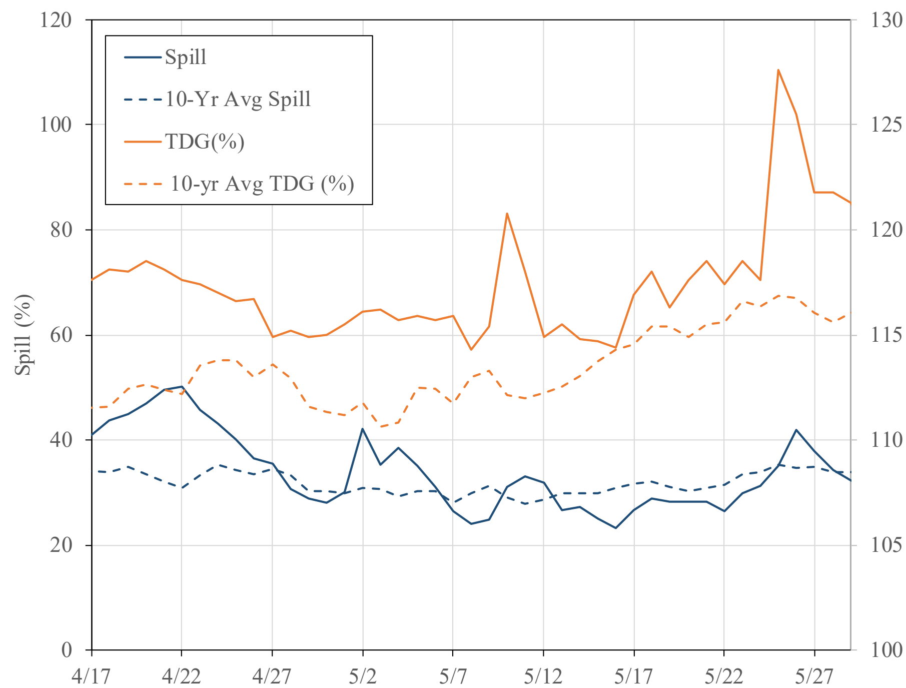

Figure 4.2. Daily Spill as a Percentage of Total Discharge and TDG as Percent of Saturation at Lower Granite Dam in 2018 and the Preceding 10-Year Average (2008−2017). Data Source: Columbia River DART (www.cbr.washington.edu/dart) and USACE Northwest Division Dataquery site (http://www.nwd-wc.usace.army.mil/dd/common/dataquery/www/).

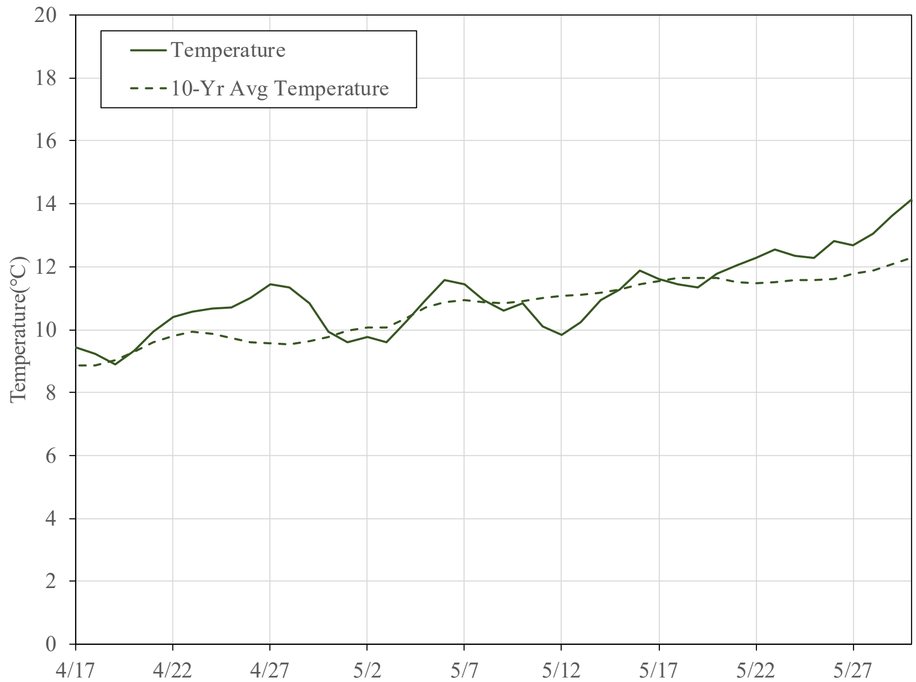

Figure 4.3. Mean Daily Water Temperature at LGR in 2018 and the Preceding 10-Year Average (2008−2017). Data Source: USACE Northwest Division Dataquery site (http://www.nwd-wc.usace.army.mil/dd/common/dataquery/www/).

4.1.2 Spring Passage Timing

For the estimates of dam passage survival to be representative of the ROR fish, releases need to occur over the majority of the respective fish runs. Timing of the tag releases was compared to the passage timing of the respective fish runs as quantified by the SMP's run time monitoring at LGR. From 17 April, when the first fish in spring were released, through the last spring release on 26 May 2018, 80.1% of the CH1 and 70.8% of the STH passed LGR (Figure 4.4). 19.3% of the CH1 and 25.8% of the STH passed the dam prior to tagged fish releases. By the time of the last fish release on 26 May 2018, 99.4% of the CH1 run and 96.6% of the STH run had passed LGR. This also means that 0.6% of the CH1 and 3.4% of the STH passed after tagged fish releases had ended.

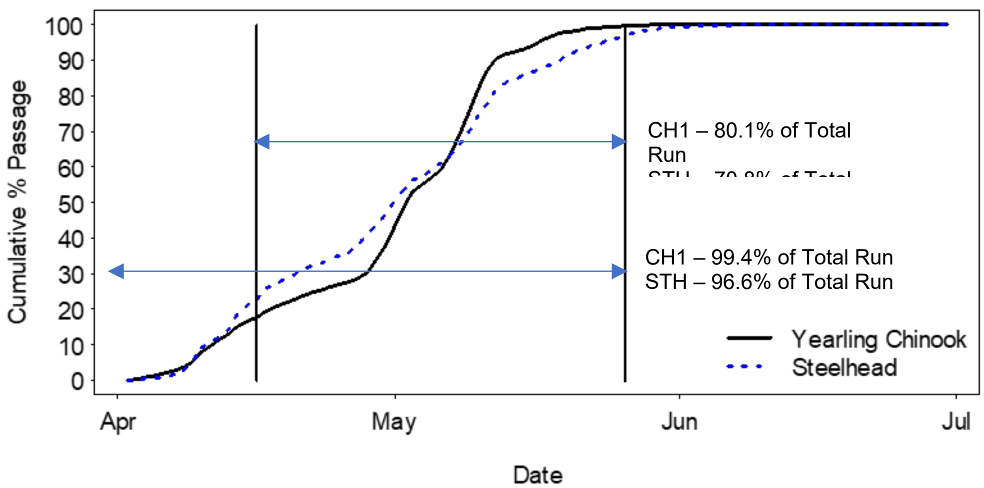

Figure 4.4. Plots of the Cumulative Percent of CH1 and STH that Had Passed LGR in 2018 Based on SMP Data and Study Begin and End Dates (vertical bars).

4.1.3 Spring Passage Distributions and Efficiency Metrics

Locations where fish pass the dam can change as operations change. Passage distributions, however, are not perfectly correlated with flow distributions, so it is important to evaluate how passage distributions responded to river conditions and dam operations in 2018.

4.1.4 Passage Distributions

Passage proportions through the various routes of LGR were calculated by examining the position and direction of 3D tracks ending near the dam face plus PIT-tag detections in the juvenile bypass. Because detection rates approached 1.0 for all routes, passage proportions were based on binomial sampling (Table 4.1). Both spring fish stocks used the unmodified spill bays similarly with about 25% passage. A larger proportion of CH1 passed the RSW compared to STH, but a smaller proportion passed the JBS. Small proportions of CH1 (7%) and STH (3%) passed the turbines.

Table 4.1. Route-Specific Passage Proportions for CH1 and STH at LGR. Standard errors are in parentheses.

Fish Stock	n	Unmodified Spill Bay	RSW	JBS	Turbine
CH1	462	0.2554 (0.0203)	0.3658 (0.0224)	0.3074 (0.0215)	0.0714 (0.0120)
STH	680	0.2544 (0.0167)	0.3191 (0.0179)	0.3926 (0.0187)	0.0338 (0.0069)

Plotting CH1 passage by individual turbine or spill bay revealed that the RSW in spill bay 1 passed a higher proportion of CH1 than any other single route (Figure 4.5). The proportion passage through a route relative to the proportion of discharge is termed its “effectiveness.” When the proportion passing a route is equal to the proportion of flow through that route, effectiveness equals 1.0. For CH1, only the RSW and spill bays 2 and 4 exhibited effectiveness exceeding 1.0. When flow and passage were broken out by day and night periods (based on civil twilight), the graphical trends suggest that effectiveness values were more similar among routes and, in most instances, closer to 1.0 (Figure 4.6). This suggests that CH1 behavior is less influential on passage routing during hours of darkness. CH1 passing at night were significantly more likely to pass through turbines compared to those that passed during the day (Fisher's exact test $P < 0.001$).

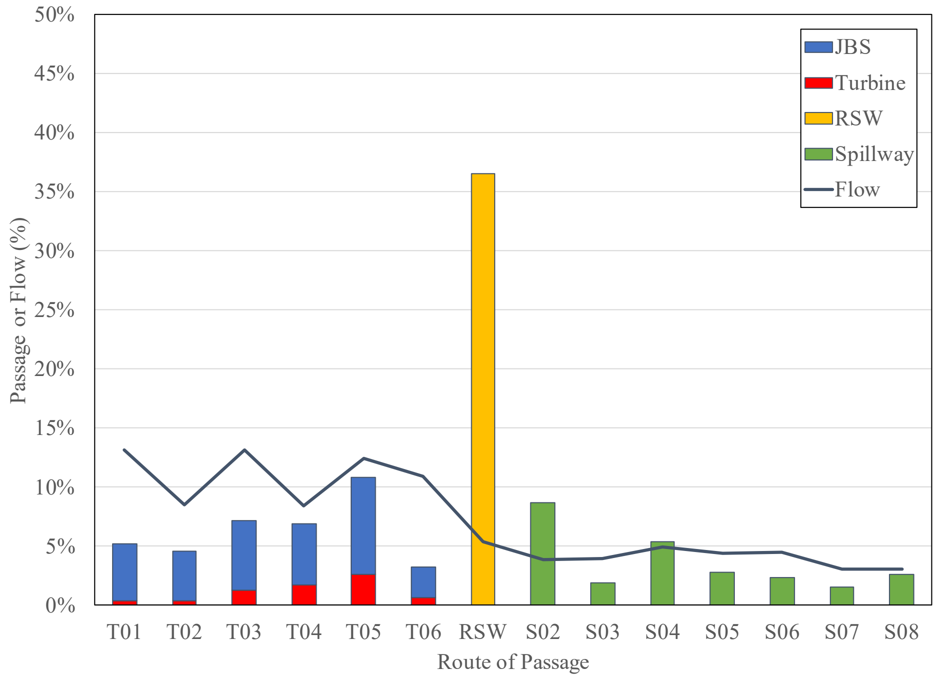

Figure 4.5. Distribution of Passage and Flow Among Routes for CH1 at LGR in 2018

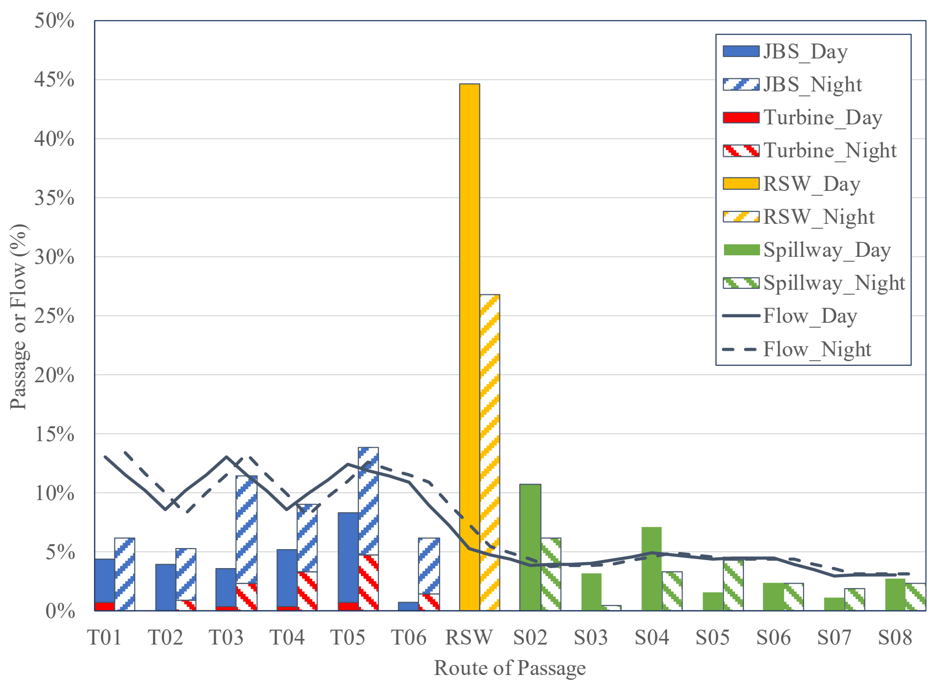

Figure 4.6. Distribution of Passage and Flow Among Routes During Day and Night for CH1 at LGR in 2018

Passage routing for STH was similar to routing for CH1, with the RSW passing a higher proportion of STH than any other single route (Figure 4.7). Only the RSW and spill bay 2 achieved effectiveness greater than 1.0. When flow and passage were broken out by day and night periods, the RSW appeared to be less effective at night, with passage moving to unmodified spill bays and JBS (Figure 4.8). STH turbine passage increased much less at night than it did for CH1 and was not significantly higher than the proportion of STH that passed through turbines during the day (Fisher's exact test $P = 0.194$).

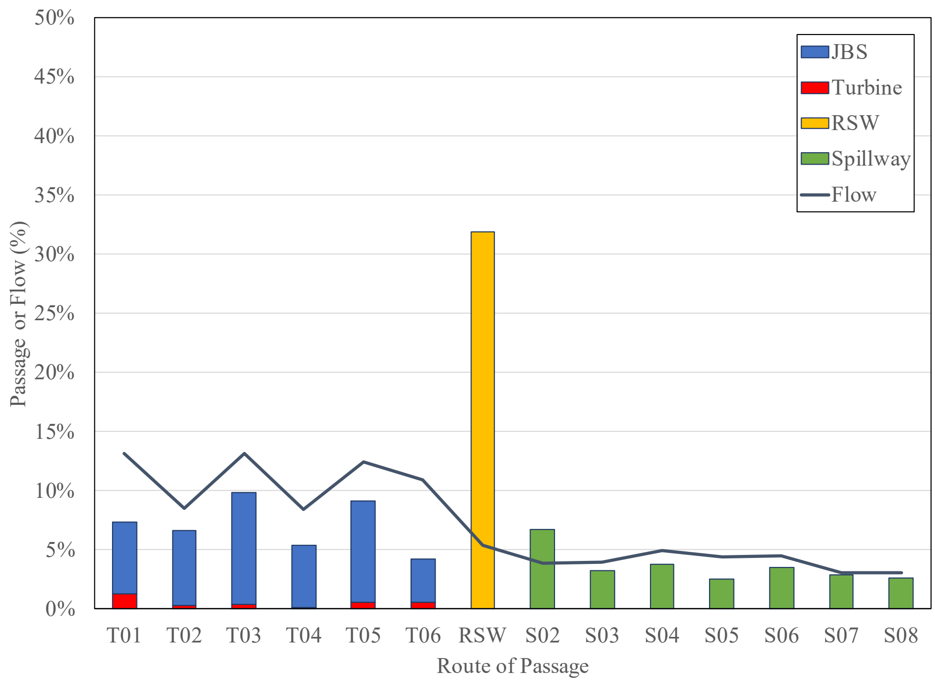

Figure 4.7. Distribution of Passage and Flow Among Routes for STH at LGR in 2018

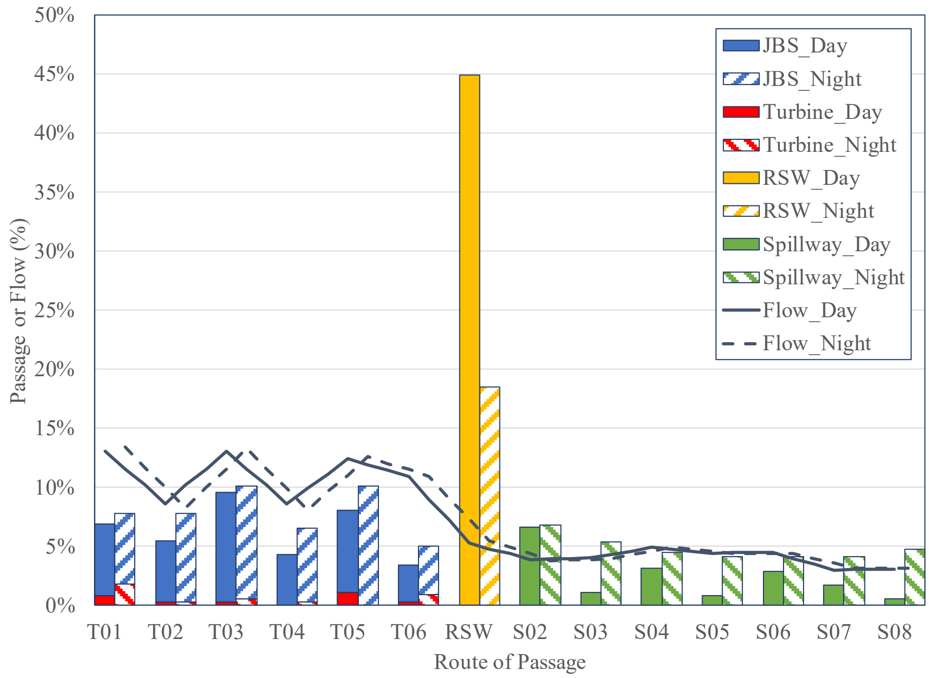

Figure 4.8. Distribution of Passage and Flow Among Routes During Day and Night for STH at LGR in 2018

4.1.4.1 Spring Passage Metrics

Passage distributions among routes can be summarized as efficiency metrics for the dam or powerhouse. SPE was approximately 60% of the total passage for both CH1 and STH (Table 4.2). FGE was 81% for CH1 and 92% for STH. FPE was 93% for CH1 and 97% for STH.

Table 4.2. Estimates of Passage Efficiency Metrics for CH1 and STH at LGR, 2018. Standard errors are in parentheses.

Fish Stock	SPE	FGE	FPE
CH1	0.6212 (0.0226)	0.8115 (0.0295)	0.9286 (0.0120)
STH	0.5735 (0.0190)	0.9207 (0.0158)	0.9662 (0.0069)

4.1.4.2 Spring Vertical Distributions

The depth at which fish approach the dam can influence the routes of passage that they encounter. At 75 m upstream of LGR, CH1 fish passing all route types were at relatively shallow depths with only subtle differences among route types (Figure 4.9). As fish moved closer to the dam, JBS- and turbine-passed fish were found progressively deeper in the water column, while deep spill- and RSW-passed fish remained at shallower depths. At 75 m upstream of LGR, STH passing any route type were also at relatively shallow depths (Figure 4.10). As STH approached the dam, fish passing all route types were found at least slightly deeper, but JBS- and turbine-passed fish were distributed at much greater depths.

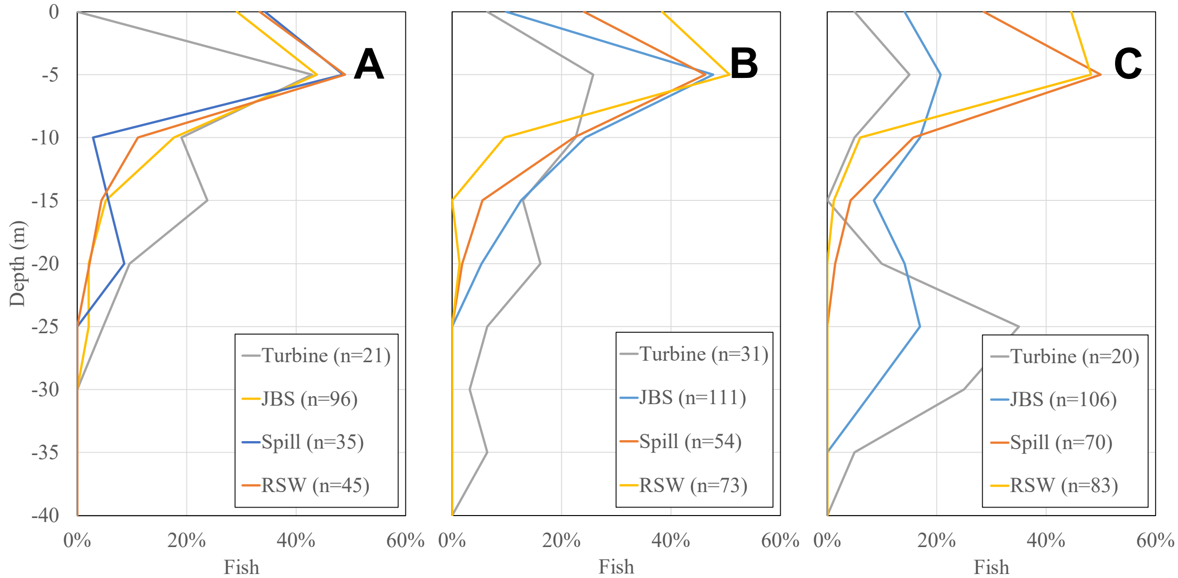

Figure 4.9. Vertical Distribution by Route of Passage for CH1 at 75 m (A), 25 m (B), and 5 m (C) Upstream of LGR. Values of n represent the number of fish detected in the zone of interest.

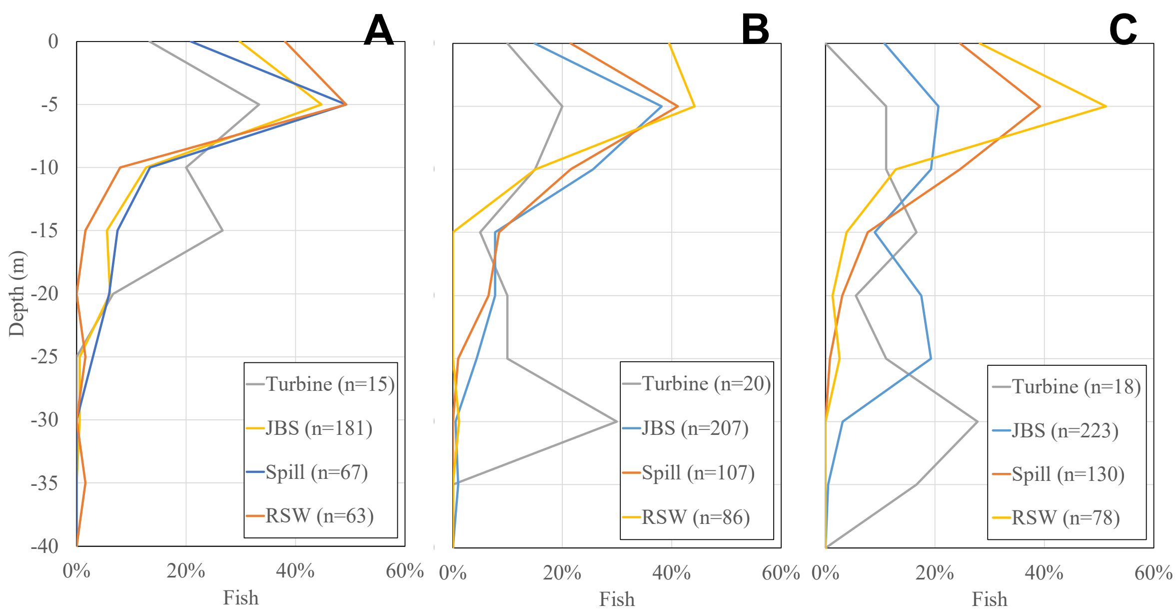

Figure 4.10. Vertical Distribution by Route of Passage for STH at 75 m (A), 25 m (B), and 5 m (C) Upstream of LGR. Values of n represent the number of fish detected in the zone of interest.

The vertical distribution plots above show that fish are diving or ascending to the depth of passage as they near the dam, but another type of plot may allow us to infer something about the state of depth acclimation of the fish. Tracks in 3D are broken into segments, where each segment represents a continuous series of detections passing filter criteria. Between those segments, fish are likely upstream of the detection zone. Two types of segments are of interest here: the first segment, when the fish first enters the forebay area, and the last segment, immediately before passing. In some cases, these were the same segment. By focusing on the first half of these segments, it is hoped that the depths will be less influenced by the fish's approach to the dam.

Depth distributions of CH1 and STH entering the forebay (Figure 4.11, plot A, and Figure 4.12, plot A) differ slightly by route, and that differentiation increases as they near their passage time (Figure 4.11, plot B, and Figure 4.12, plot B). Upon entering the forebay detection time for the first time, vertical distributions already appear to differ among routes, suggesting that the depth a fish is traveling, and perhaps depth acclimation, influences what routes the fish uses to pass the dam.

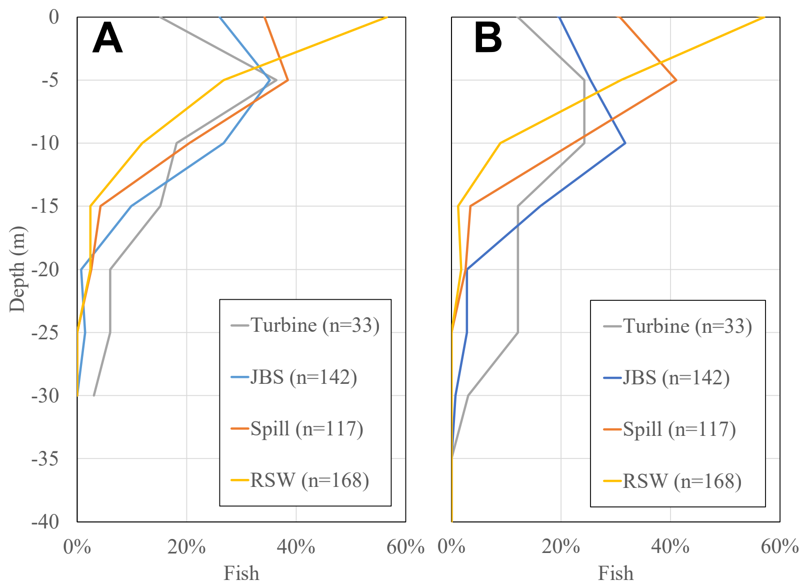

Figure 4.11. Vertical Distribution by Route of Passage for CH1 at First Half of First Track Segment (A), and First Half of Last Track Segment (B) Upstream of LGR. Values of n represent the number of fish with 3D tracks.

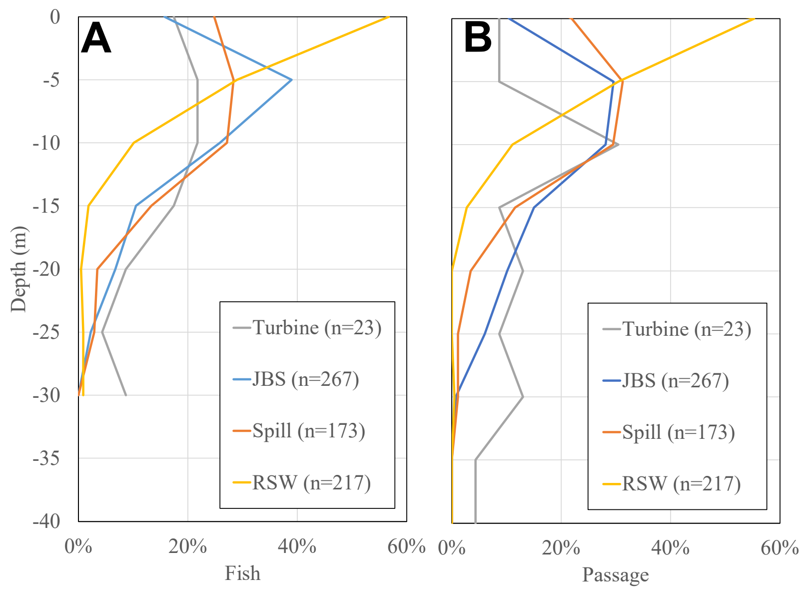

Figure 4.12. Vertical Distribution by Route of Passage for STH at First Half of First Track Segment (A), and First Half of Last Track Segment (B) Upstream of LGR. Values of n represent the number of fish with 3D tracks.

4.1.4.3 Spring Travel Times

Travel times through reaches above and below the dam can help understand whether changes in operation encourage or discourage fish to pass the dam and continue their migration downstream. Travel times may also play a role in the risk of being preyed upon.

4.1.4.4 Spring Forebay Residence Times

Using the R_1 releases, forebay residence times from the first detection at the forebay array to the last detection at the dam-face array were calculated (Table 4.3). Median forebay residence times were 4.92 h for CH1 and 4.07 h for STH. Figure 4.13 illustrates the long-tailed distribution of forebay residence times caused by a smaller number of individuals remaining in the forebay for much longer than the bulk of individuals passing in the first few hours after arriving in the forebay. These results show that the vast majority of CH0 and STH pass LGR within a few hours of arrival in the forebay.

Table 4.3. Forebay Residence Times and Tailrace Egress Times for CH1 and STH at LGR, 2018.

Reach and Metric	CH1	STH
Forebay		
Mean (SE)	10.13 (0.62)	13.42 (1.34)
Median	4.92	4.07
Range	0.53–135.25	0.60–453.43
Tailrace		
Mean (SE)	2.00 (0.86)	2.93 (2.27)
Median	0.27	0.27
Range	0.17–313.65	0.17–1519.17
Project		
Mean (SE)	12.16 (1.10)	15.84 (2.58)
Median	5.49	4.53
Range	0.80–329.42	0.85–1520.63

4.1.4.5 Spring Tailrace Egress Time

The intervening time from the last detection at the dam face or JBS to the last detection at the tailrace array were calculated for CH1 and STH (Table 4.3). Egress times were consistently short across stocks, with mean values ranging from 2.00 h ($\widehat{\mathrm{SE}}(\bar{t}) = 0.86$) to 2.93 h ($\widehat{\mathrm{SE}}(\bar{t}) = 2.27$) with medians of 0.27 h for both stocks. Figure 4.14 shows that the vast majority of fish for both stocks exited the tailrace within the first hour after passing LGR.

a. CH1

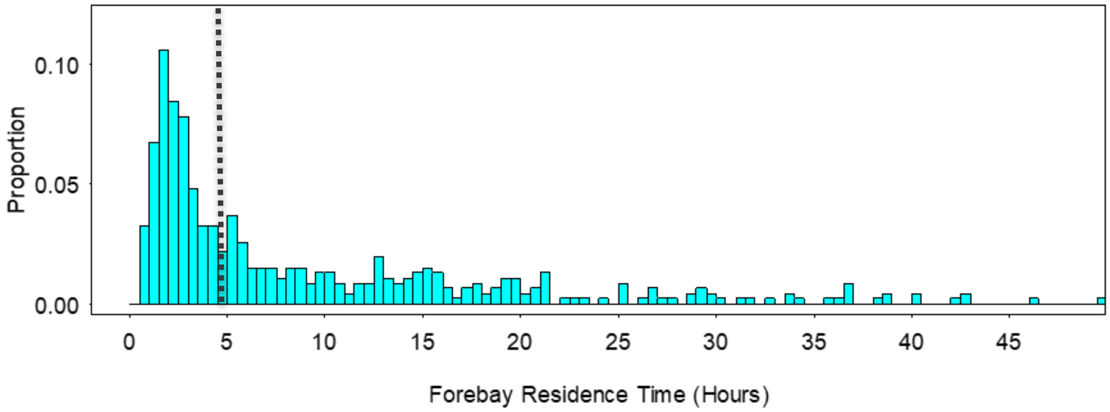

b. STH

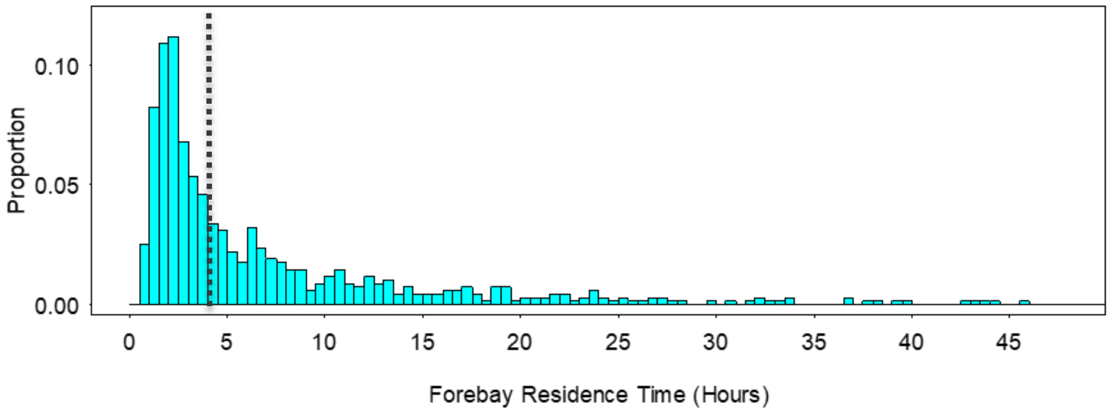

Figure 4.13. Distribution of Forebay Residence Times for (a) CH1 and (b) STH at LGR, 2018. Dashed lines indicate the median value.

4.1.4.6 Spring Project Passage Time

The intervening time from the first detection at the forebay array (1 km upstream of the dam) to the last detection at the tailrace array was calculated for CH1 and STH (Table 4.3). Again, CH1 and STH had similar mean passage times of 12.16 h ($\widehat{\mathrm{SE}}(\bar{t}) =$ 1.10) and 15.84 h ($\widehat{\mathrm{SE}}(\bar{t}) =$ 2.58), respectively. Median project passage times were similar for CH1 and STH at 5.49 h and 4.53 h, respectively. For both stocks, the majority of individuals transited the forebay, dam, and tailrace within a few hours of their arrival in the forebay.

a. CH1

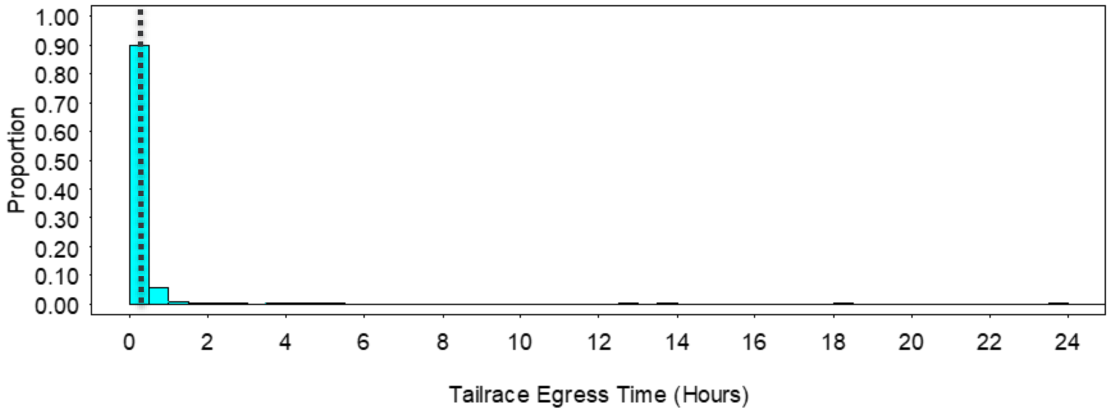

b. STH

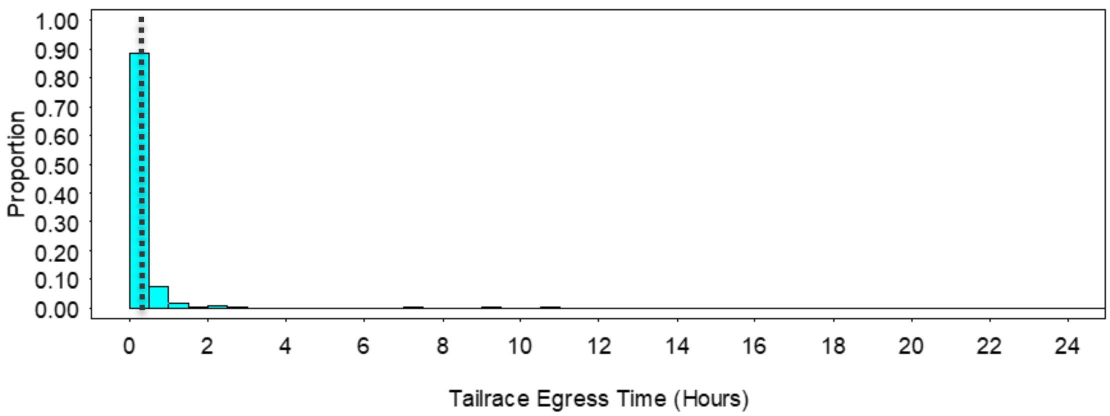

Figure 4.14. Distribution of Tailrace Egress Times for (a) CH1 and (b) STH at LGR, 2018. Dashed lines indicate the median value.

4.1.5 Spring Survival

Estimates of survival for CH1 and STH are presented in this section. Survival model assumptions were assessed to ensure that the assumptions of the survival model were met. Tests of assumptions are detailed in Appendix A.

4.1.5.1 Spring Dam Passage Survival

For each fish stock, season-wide estimates of dam passage survival were generated by the VIPRE and ViRDCt models (Table 4.4). The estimates of dam passage survival from the two alternative models were consistent within a fish stock. Weighted averages of the survival estimates were 0.9857 and 0.9939 for CH1 and STH, respectively. ViRDCt estimates were all within 1 $\widehat{\text{SE}}$ of the VIPRE estimates. For CH1, the VIPRE model estimate was lower than the ViRDCt estimate, while the opposite was true for STH. All four estimates of dam passage survival had standard error estimates < 0.025, which was the precision goal of the study. As expected, the standard errors from the ViRDCt model were lower than those from the VIPRE model. All but one of the four estimates had an SE within the BiOp requirement of ≤ 0.015, despite planning the study to achieve SE ≤ 0.025.

Table 4.4. Comparison of Estimates of Dam Passage Survival from the VIPRE and the ViRDCt Models by Fish Stock at LGR, 2018. Standard errors in parentheses.

Model	CH1	STH
VIPRE	0.9726 (0.0159)	0.9959 (0.0099)
ViRDCt	0.9877 (0.0062)	0.9936 (0.0037)
Weighted Average	0.9857 (0.0051)	0.9939 (0.0008)

Based on the beginning and end of civil twilight, fish passing the dam during the day may encounter different operations and river conditions than those passing during night and may also behave differently. If those conditions or behaviors influence survival rates, then survival during the day may differ from survival at night. In this study, survival differed little among diel periods, with CH1 surviving at a slightly higher rate during the day and STH surviving at nearly the same rate day or night (Table 4.5). Breaking the day into two diel periods makes it more difficult to achieve proper temporal mixing of V_1, R_2, and R_3 groups as assumed for the VIPRE model, so this comparison was made using the ViRDCt model which does not rely on R_2 or R_3 releases.

Table 4.5. Comparison of Day Versus Night Estimates of Dam Passage Survival by Fish Stock at LGR, 2018. Computed using ViRDCt. Standard errors in parentheses.

CH1		STH	
Day	Night	Day	Night
0.9946 (0.0054)	0.9766 (0.0136)	0.9919 (0.0057)	0.9953 (0.0048)

4.1.5.2 Spring Forebay-to-Tailrace Survival

By forming the virtual release, V_1, at the forebay hydrophone array instead of the dam face array, forebay-to-tailrace survival (also known as BRZ-to-BRZ survival because these boundaries often coincide with the BRZ upstream and downstream of the dam) were estimated using both the VIPRE and ViRDCt models (Table 4.6). For spring stocks, every fish detected at the forebay array was also detected at the dam face, and vice versa. Consequently, the estimates of forebay-to-tailrace survival are nearly identical to the estimates of dam passage survival. The slight differences are due to very small corrections in tag life.

Table 4.6. Estimates of Forebay-to-Tailrace Survival from the VIPRE and ViRDCt Models by Fish Stocks at LGR, 2018. Standard errors in parentheses.

Model	CH1	STH
VIPRE	0.9728 (0.0159)	0.9961 (0.0099)
ViRDCt	0.9877 (0.0062)	0.9936 (0.0037)
Weighted Average	0.9857 (0.0050)	0.9939 (0.0008)

4.1.5.3 Spring Route-Specific Passage Survival

Fish passing through different routes at a dam often survive at different rates. These route-specific survival rates can be estimated by treating the tagged fish going through the various passage routes as separate virtual releases. The VIPRE and ViRDCt models were used to estimate route-specific passage survival by fish stock (Table 4.7). For both fish stocks, JBS had very high survival with estimates essentially equaling 1.0. The RSW had the next highest values of route-specific survival with all estimate values exceeding 0.98. STH survival at unmodified spill bays was essentially 1.0 but ranged from 0.9521 to 0.9898 for CH1. Survivals were lowest for fish passing turbines, with estimates from 0.8779 to 0.9076.

Table 4.7. Route-Specific Survival by Species at LGR in 2018

Species and Route	N (at V_1)	VIPRE (SE)	ViRDCt (SE)
CH1			
Unmodified Spill Bay	117	0.9521 (0.0244)	0.9898 (0.0102)
Removable Spillway Weir	168	0.9855 (0.0172)	1.0016 (0.0360)
Juvenile Bypass System	138	0.9961 (0.0158)	1.0001 (0.0264)
Turbine	32	0.8779 (0.0599)	0.8697 (0.0604)
STH			
Unmodified Spill Bay	173	1.0003 (0.0119)	1.0002 (0.0153)
Removable Spillway Weir	217	0.9843 (0.0141)	0.9937 (0.0063)
Juvenile Bypass System	262	1.0111 (0.0087)	1.0000 (0.0124)
Turbine	23	0.8804 (0.0715)	0.9076 (0.0626)

These high rates of survival for CH1 and STH over the entire day leave little room for differences among daytime and nighttime periods. Due to temporal mixing of V_1, R_2, and R_3 groups, it is not possible to accurately pair V_1 fish with fish from R_2 and R_3 by diel period. Therefore, only the ViRDCt model was used to evaluate route-specific survival by diel period. Table 4.8 contrasts ViRDCt survival estimates by route between daytime and nighttime periods, with the greatest difference being that of less than 0.02 for CH1 passing unmodified spill bays. Other stocks and routes differed by less than 0.01 between daytime and nighttime periods.

Table 4.8. Route-Specific Survival by Species and Diel Period at Lower Granite Dam in 2018

	Daytime		**Nighttime**	
Species and Route	**N (at V_1)**	**ViRDCt (SE)**	**N (at V_1)**	**ViRDCt (SE)**
CH1				
Unmodified Spill Bay	73	0.9835 (0.0164)	44	1.0012 (0.0369)
Removable Spillway Weir	112	1.0011 (0.0501)	56	1.0036 (0.0986)
Juvenile Bypass System	59	1.0011 (0.0654)	79	1.0000 (0.1155)
Turbine	6	NA (NA)	26	0.8402 (0.0898)
STH				
Unmodified Spill Bay	59	1.0007 (0.0421)	114	1.0002 (0.0269)
Removable Spillway Weir	155	0.9913 (0.0087)	62	1.0000 (1.0441)
Juvenile Bypass System	119	1.0000 (0.0270)	143	1.0000 (0.0502)
Turbine	10	0.9000 (0.0949)	13	0.9060 (0.0913)

The high route-specific survivals through the LGR study area show only that turbine survivals lag behind other routes. To delve deeper into route-specific survival, we computed single-release estimates of survival through detection arrays stretching further downstream. As cumulative survival decreased with increasing distance downstream from LGR, any influence of the passage route at LGR would be reflected in cumulative survival rates. In the spring, detection arrays deployed for the System Survival Study (Harnish et al. 2018) allowed survival of these LGR passage groups to be estimated for reaches extending downstream to the forebay of Bonneville Dam, 458 km downstream of the LGR tailrace. Figure 4.15 shows the cumulative survival trends for CH1 and STH. While the lines do not remain strictly parallel, the trends are inconsistent and there is enough uncertainty around the estimates to question whether apparent trends are meaningful. With those caveats in mind, it is intriguing that cumulative survival of CH1 passing the RSW or unmodified spill bays appears relatively higher than powerhouse routes at the furthest downstream array. For STH, route survivals retain a similar grouping at all array locations, which suggests that those differences reflect the survival differences between routes at LGR; downstream survival is similar between routes.

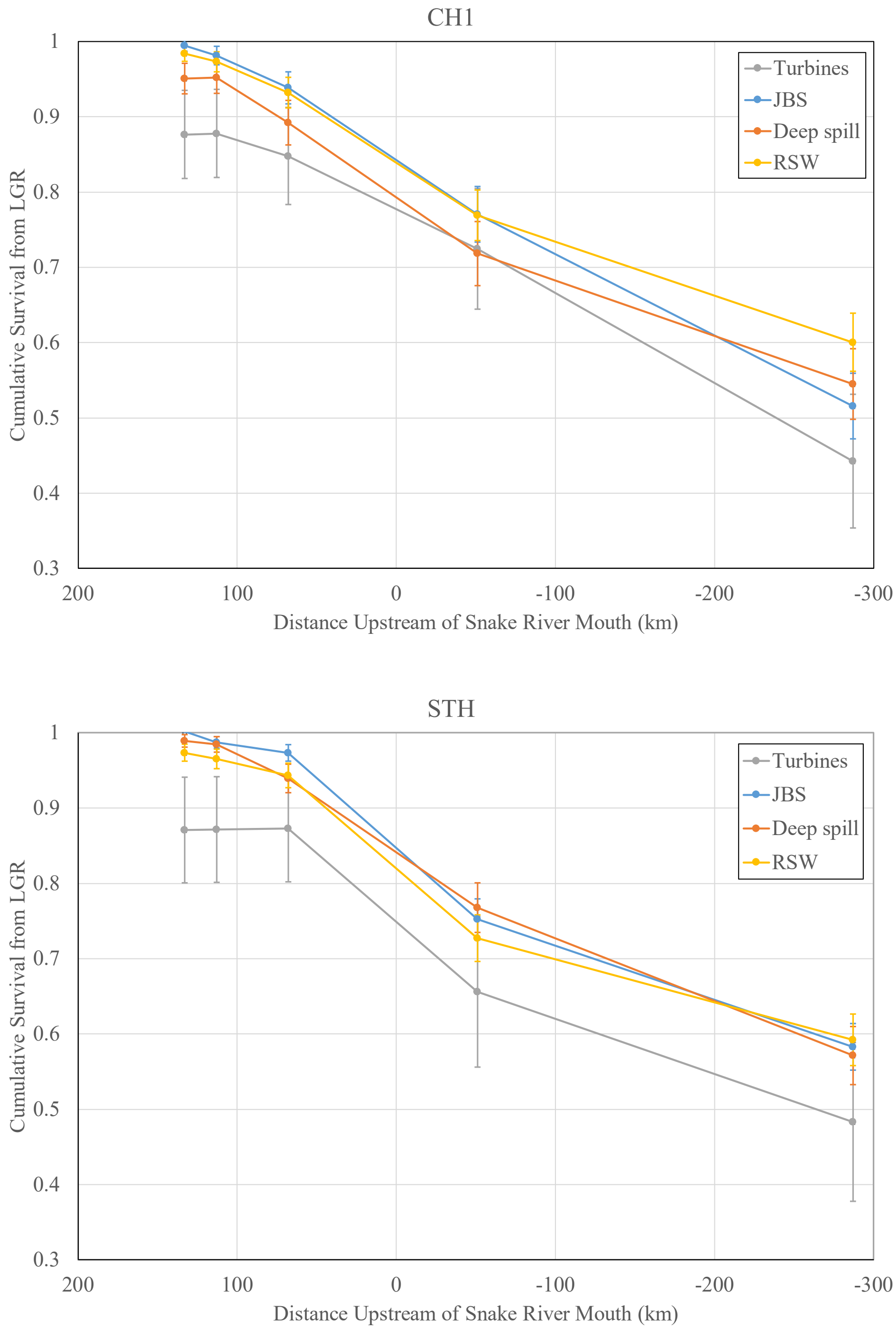

Figure 4.15. Cumulative Survival by Route from LGR for Yearling Chinook (CH1) and Steelhead (STH) to Detection Arrays Downstream. Error bars are standard errors. Negative distances indicate sites in the Columbia River downstream of the Snake River mouth.

4.2 Results – Summer

This section describes the river conditions, approach and passage distributions, passage metrics, travel times, and survival estimates for CH0 during the summer study period at LGR in 2018.

4.2.1 Summer River Conditions

Spring spill operations were in effect at LGR from 3 April through 20 June, and summer spill operations began 21 June and continued to 31 August. In 2018, spring spill at FCRPS dams, including LGR, was directed by court order to increase to 120/115% gas cap spill. This means that the project was to spill to the maximum level that meets but does not exceed the TDG criteria allowed under state law. During the summer spill operations period of 2018, planned spill at LGR remained unchanged from recent years at 18 kcfs, including discharge over the RSW.

The summer study period extended from 31 May through 9 July 2018, beginning during the spring operational period (with the court-ordered spill to the gas cap) and extending several weeks into the summer operational period, where spill was set at 18 kcfs as in recent years. Mean daily discharge in summer was initially above average but quickly transitioned to below the 10-year average (Figure 4.16). Spill was near average during the early portion of the summer study period and below average for the latter half of the summer study period. The transition from spring spill operations to summer spill operations on 21 June was obvious, as the spill transitioned from above average to below average.

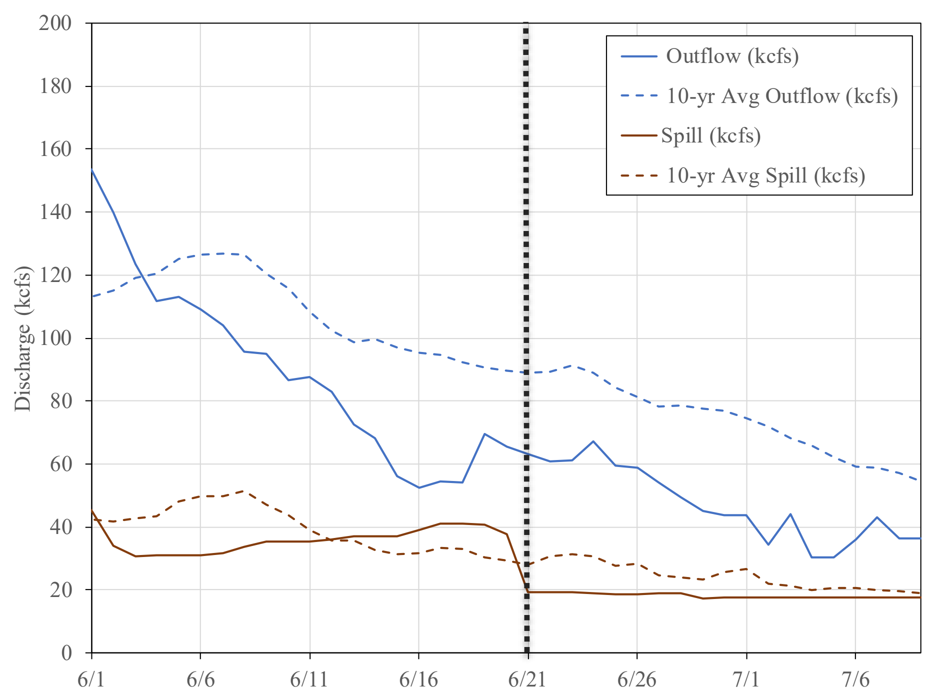

Figure 4.16. Mean Daily Water Discharge (kcfs) and Spill from LGR During the Summer Study Period and the Preceding 10-Year Average (2008−2017). Vertical dotted line indicates the transition to summer spill operations. Data Source: Columbia River DART (www.cbr.washinton.edu/dart).

The proportion of water spilled was well above average from 10 June through 20 June, as the gas cap spill was maintained while total discharge levels dropped (Figure 4.17). TDG remained at high levels until the transition to summer spill operations on 21 June. During the summer study period, temperatures remained above average (Figure 4.18).

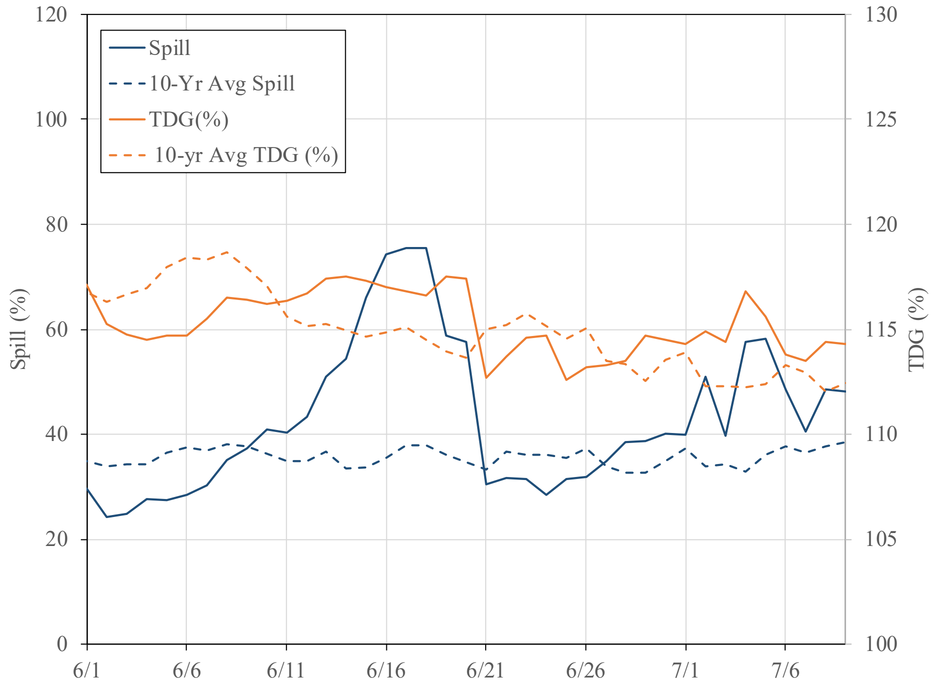

Figure 4.17. Mean Daily Water Spill Percent and TDG Saturation at LGR During the Summer Study Period and the Preceding 10-Year Average (2008−2017). Data Source: Columbia River DART (www.cbr.washington.edu/dart) and USACE Northwest Division Dataquery site (http://www.nwd-wc.usace.army.mil/dd/common/dataquery/www/).

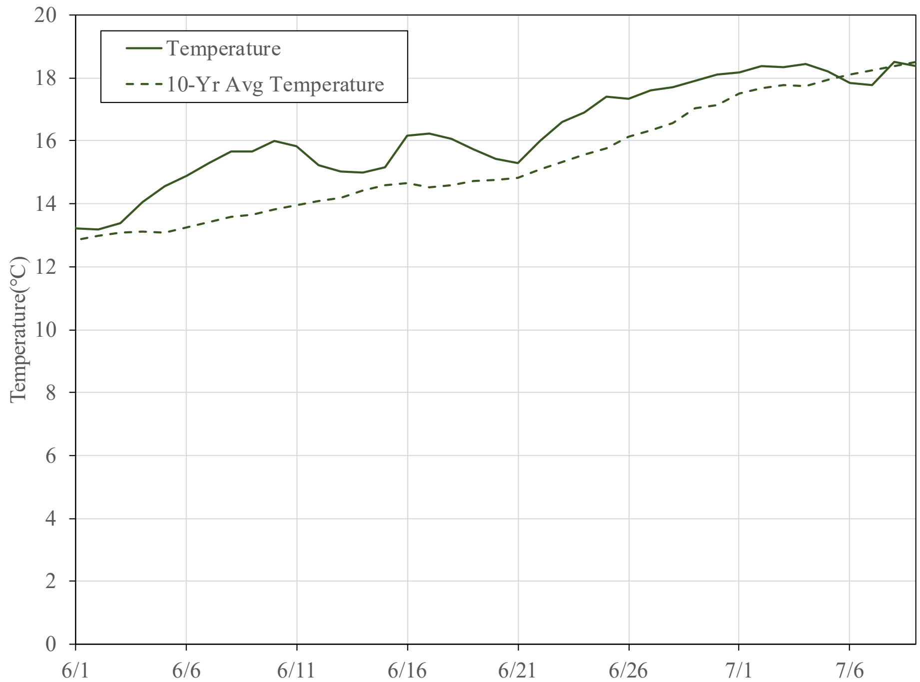

Figure 4.18. Mean Daily Water Temperature at LGR During the Summer Study Period in 2018 and the Preceding 10-Year Average (2008−2017). Data Source: USACE Northwest Division Dataquery site (http://www.nwd-wc.usace.army.mil/dd/common/dataquery/www/).

4.2.2 Passage Timing

Comparing the timing of the tag releases to the passage timing of the CH0 as sampled by the SMP at LGR shows that the releases covered only 41% of the CH0 migration (Figure 4.19). Ideally, this number would approach 80%, but this stock posed a couple of challenges. First, the migration initially ramps up rapidly. Although those first arrivals were collected, releasing them approximately 2 days later (per the protocol for collecting, tagging, and holding fish prior to release) gives the impression that around half of the run was missed. This apparent discrepancy is an artifact of the cycle of collection, tagging, and release of fish. Second, CH0 migration tails off slowly, with some fish holding over until the following spring. By the end of the study on 9 July 2018, 90.0% of the CH0 run had passed LGR, which also means that 10% had yet to pass. We would not recommend attempting to tag the latter portion of the migration due to the high temperatures (>20 ℃; not ideal for handling fish and doing surgeries for tagging) and the potential that an increasing proportion of fish would choose not to migrate.

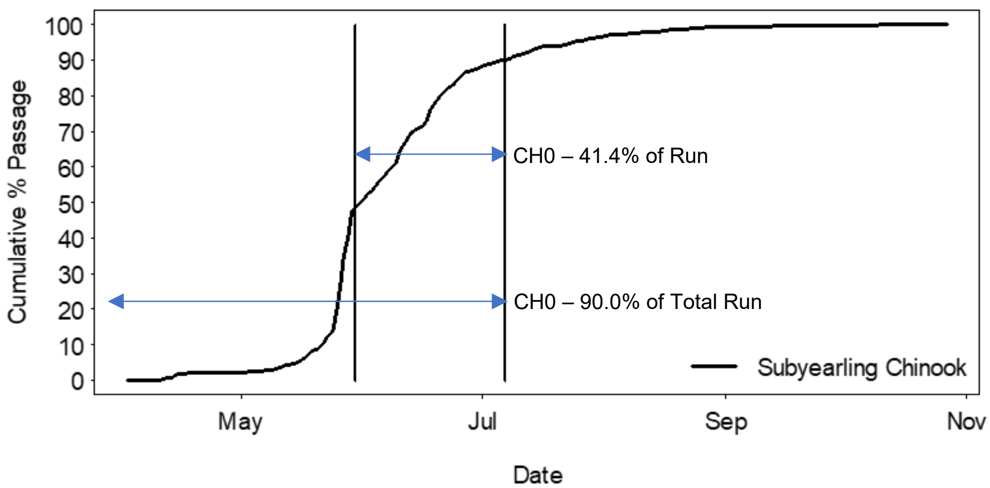

Figure 4.19. Plots of the Cumulative Percent of CH0 that had Passed LGR in 2018 Based on SMP Data and Study Begin and End Dates (vertical bars).

4.2.3 Summer Passage Distributions and Efficiency Metrics

Where fish pass the dam can change as operations change. Passage distributions, however, are not perfectly correlated with flow distributions, so it is important to evaluate how passage distributions responded to river conditions and dam operations in 2018. Court-ordered spill was expected to increase the proportion of fish passing the spillway (increased SPE), but this increased spill extended only through 20 June.

4.2.3.1 Summer Passage Distributions

Based on the upstream release R_1, passage proportions through the various routes of LGR were calculated using the last detections at the dam-face array (or PIT-tag detections in the JBS). Routes of passage delineated were the unmodified spill bays, RSW, JBS, and TUR. Because detection rates were near 1 for all routes, passage proportions were based on binomial sampling (Table 4.9). Approximately 55% of CH0 passed LGR via the RSW. An additional 25% passed via the unmodified spill bays. Few individuals passed the powerhouse, with 12% through the JBS and 9% through the TUR.

Table 4.9. Route-Specific Passage Proportions for CH0 at LGR. Standard errors are in parentheses.

n	Unmodified Spill Bay	RSW	JBS	TUR
891	0.2469 (0.0144)	0.5499 (0.0167)	0.1156 (0.0107)	0.0875 (0.0095)

Plotting flow and passage by turbine or spill bay revealed that the RSW in spill bay 1 passed a much higher proportion of CH0 than any other single route (Figure 4.20). The adjacent spill bays S02 and S03 also passed a higher proportion of fish than flow, but passage was much less than flow for powerhouse routes. Comparing passage distributions among day and night, the difference for CH0 was striking (Figure 4.21). At night, passage proportions were more similar to flow proportions. The proportion of fish passing the RSW passage was reduced, but still far exceeded the proportion of flow through that route. Powerhouse passage proportions were much higher at night than during the day despite similar flow proportions in each diel period.

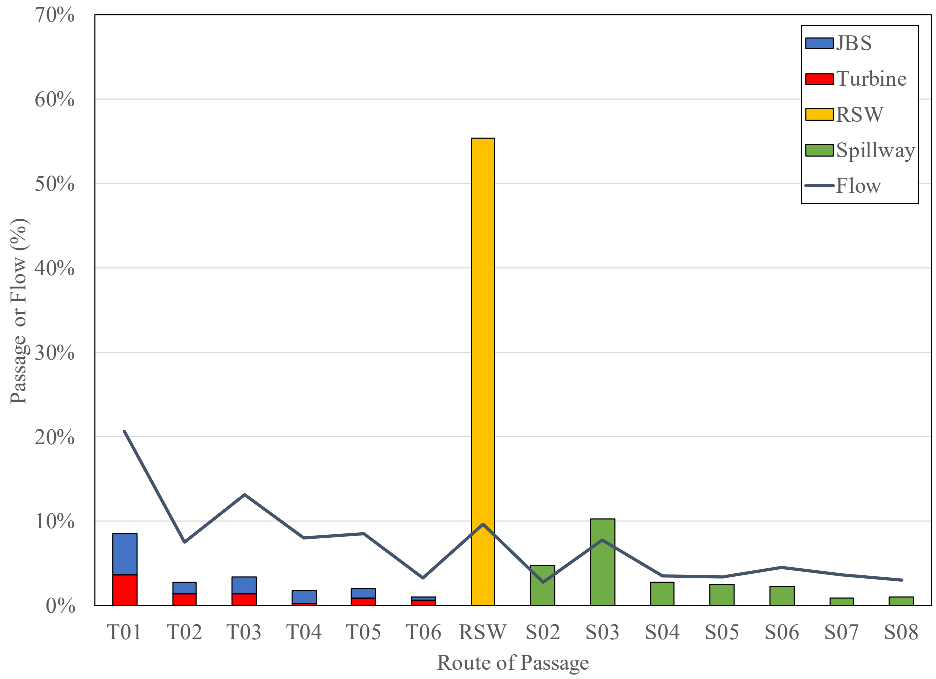

Figure 4.20. Distribution of Passage and Flow Among Routes for CH0 at LGR in 2018

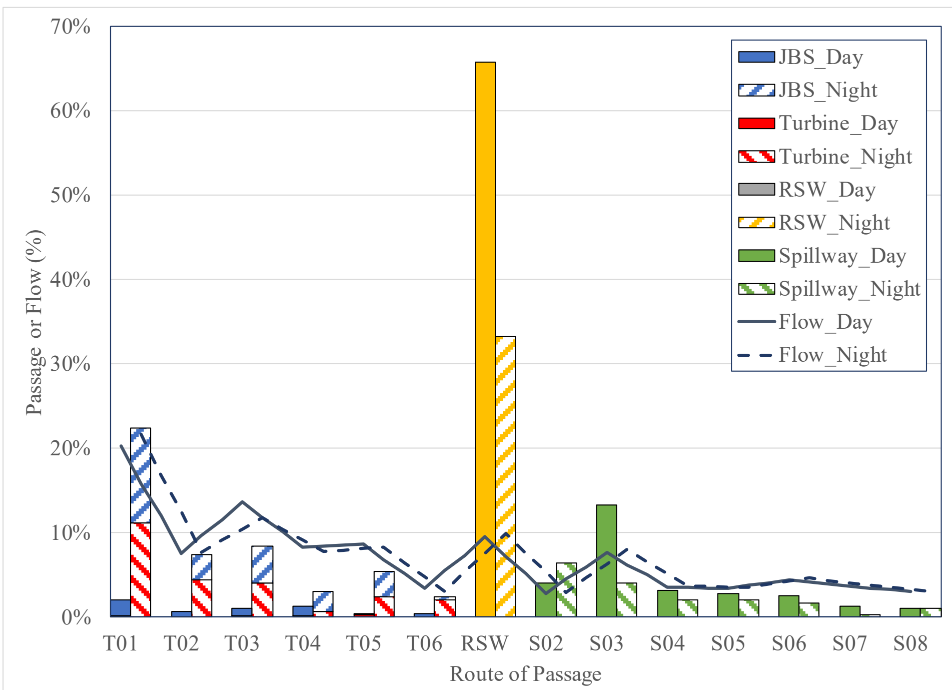

Figure 4.21. Distribution of Passage and Flow Among Routes During Day and Night for CH0 at LGR in 2018

4.2.3.2 Summer Passage Metrics

With an FGE of only 0.5692, CH0 were much less likely than CH1 (0.8115) or STH (0.9207) to be guided into the JBS, but SPE for CH0 was high (Table 4.10). As a result, FPE was still above 90%.

Table 4.10. Estimates of SPE, FPE, and FGE for CH0 at LGR, 2018. Standard errors are in parentheses.

SPE	FPE	FGE
0.7969 (0.0135)	0.9125 (0.0095)	0.5692 (0.0368)

4.2.3.3 Summer Vertical Distributions

In the summer, CH0 were distributed deeper in the water column than spring stocks even at 75 m upstream (Figure 4.22). This is consistent with the lower FGE values for CH0 relative to spring stocks. TUR- and JBS-passed fish moved deeper as they moved closer to the dam, while spill- and RSW-passed fish remained at shallow depths at all distances from the dam.

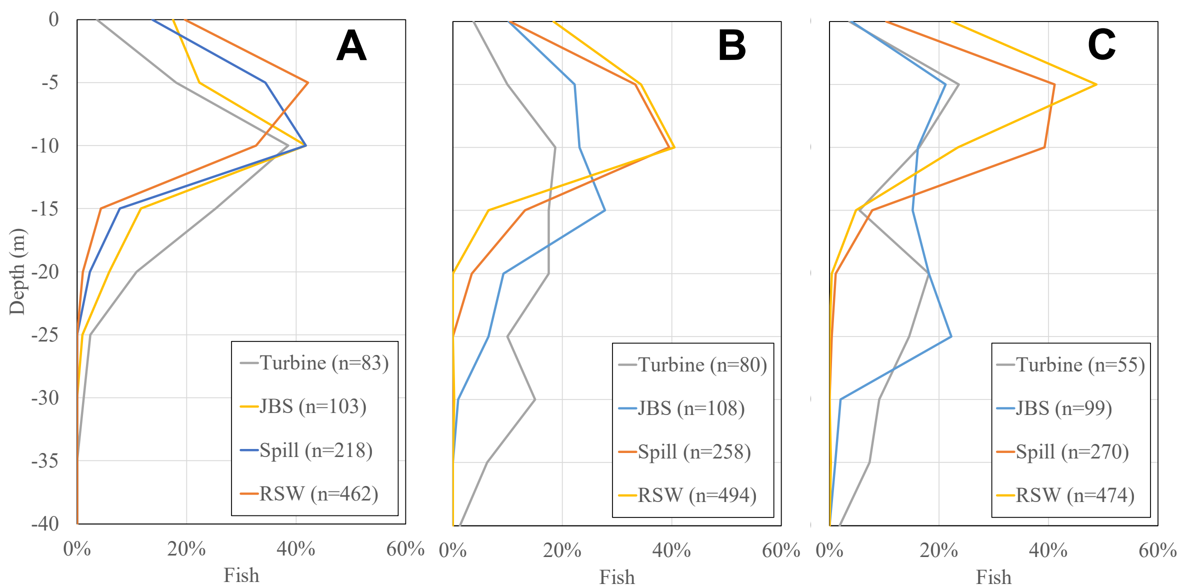

Figure 4.22. Vertical Distribution by Ultimate Route of Passage for CH0 at 75 m (A), 25 m (B), and 5 m (C) Upstream of LGR. Values of n represent the numbers of fish detected in the zones of interest.

Plotting vertical distributions of CH0 when the fish first enters the forebay area and immediately before passing (Figure 4.23, plot A) reveals that CH0 were less commonly found at shallow depths relative to CH1 (Figure 4.11, plot A) or STH (Figure 4.12, plot A). Depth distributions of CH0 differed more among routes of passage as the fish neared their time of passage (Figure 4.23, plot B). Those distributions were also typically at greater depths than CH1 (Figure 4.11, plot B) or STH (Figure 4.12, plot B) nearing their time of passage.

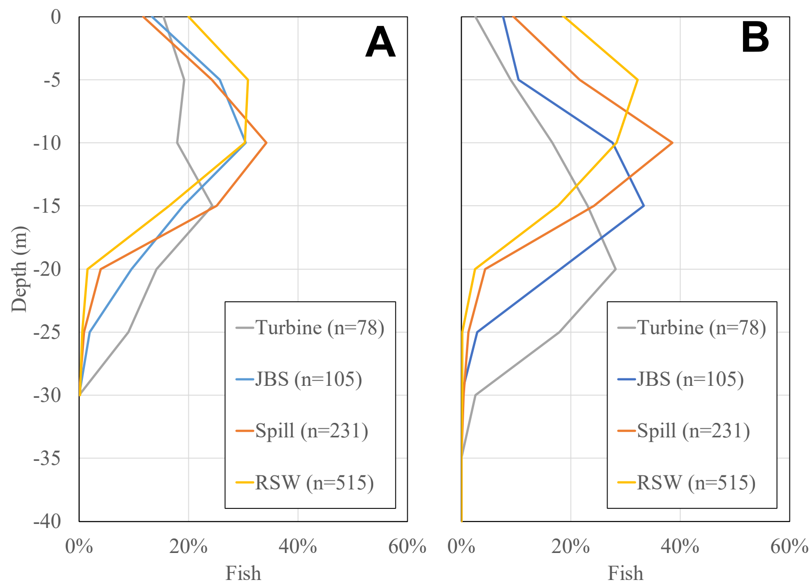

Figure 4.23. Vertical Distribution by Route of Passage for CH0 at First Half of First Track Segment (A) and First Half of Last Track Segment (B) Upstream of LGR. Values of n represent the number of fish with 3D tracks.

4.2.4 Summer Travel Times

Travel times through reaches above and below the dam can help understand whether changes in operation encourage or discourage fish to pass.

4.2.4.1 Summer Forebay Residence Times

Using the R_1 releases, forebay residence times from the first detection at the forebay array to the last detection at the dam-face array were calculated (Table 4.11). CH0 had a mean forebay residence time of 62.10 h and a median of approximately 9 h. Figure 4.24 illustrates that many CH0 spent several hours in the forebay. While these forebay residence times are longer than for spring stocks, most CH0 passed the dam within the same day as they arrived in the forebay.

Table 4.11. Forebay Residence Times and Tailrace Egress Times for CH0 at LGR, 2018.

Metric	Mean (SE)	Median	Range
Forebay Residence Time (h)	62.10 (4.03)	8.96	0.55–942.43
Tailrace Egress Time (h)	2.15 (0.29)	0.62	0.20–539.48
Project Passage time (h)	55.83 (3.84)	10.67	1.17–945.47

4.2.4.2 Summer Tailrace Egress Time

Most CH0 exited the tailrace quickly, with a mean tailrace egress time of 2.15 h, and a median of only 0.62 h (Table 4.11). Few individuals took more than a few hours to make it out of the tailrace (Figure 4.25). Tailrace egress times were considerably longer than spring stocks, but they do not suggest fish are behaving in ways that prolong their tailrace residence.

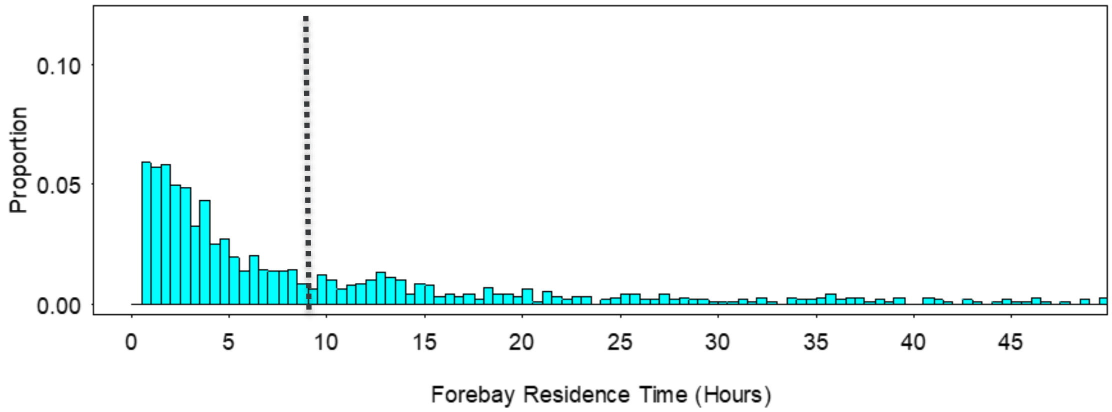

Figure 4.24. Distribution of Forebay Residence Times for CH0 at LGR, 2018. Dashed lines indicate the median value.

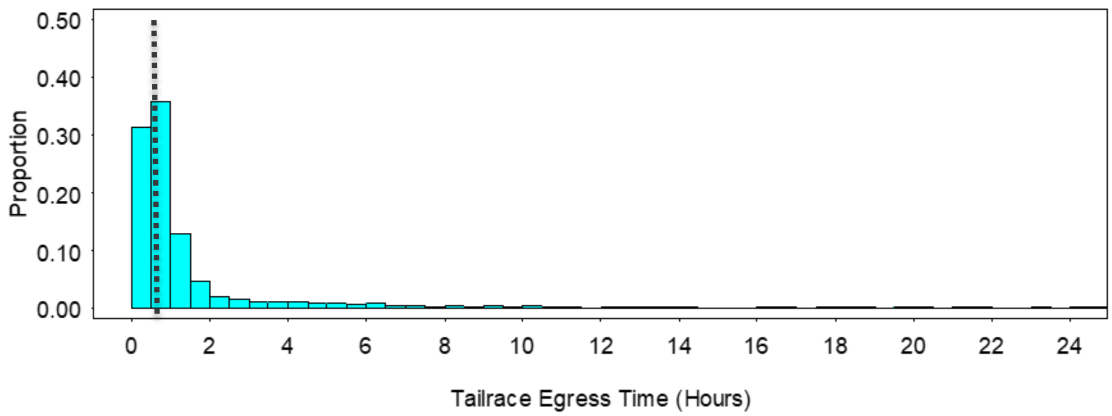

Figure 4.25. Distribution of Tailrace Egress Times for CH0 at LGR, 2018. Dashed lines indicate the median value.

4.2.4.3 Summer Project Passage Time

The intervening time from the first detection at the forebay array (1 km upstream of the dam) to the last detection at the tailrace array was calculated for CH0 (Table 4.11). On average, CH0 took almost 56 h to pass the project, but the median fish passed in just under 11 h. That high average value reflects a small number of individuals that spent multiple days transiting the LGR project.

4.2.5 Summer Survival

Estimates of survival for CH0 are presented in this section. Survival model assumptions were assessed to ensure that the assumptions of the survival model were met. Tests of assumptions are detailed in Appendix A.

4.2.5.1 Summer Dam Passage Survival

Estimates of dam passage survival for CH0 were generated by the VIPRE and ViRDCt models (Table 4.12). The estimates of dam passage survival from the two alternative models were within 2% of each other. Weighted averages of the survival estimates were 0.9272. For CH0, the VIPRE model produced a higher survival estimate, but the ViRDCt estimate was within 1 $\widehat{SE}$

of the VIPRE model. Both estimates of dam passage survival had standard error estimates that were < 0.025, the precision goal of the study. As expected, the standard errors from the ViRDCt model were lower than those from the VIPRE model. In calculating dam passage survival for CH0, fish arriving at LGR after 9 July 2018 were excluded from the V_1 group because they arrived after the last R_2 and R_3 releases.

Table 4.12. Comparison of Estimates of CH0 Dam Passage Survival from the VIPRE and ViRDCt Models at LGR, 2018. Standard errors in parentheses. Individuals detected after 9 July 2018 at the LGR face were excluded from the analysis.

Model	Dam Passage Survival
VIPRE	0.9422 (0.0217)
ViRDCt	0.9242 (0.0098)
Weighted Average	0.9272 (0.0068)

CH0 survival during daytime was about 6% less than during nighttime(Table 4.13). Route-specific survivals during daytime and nighttime are provided below in Figure 4.21. Given those survival rates among routes and diel periods, the only route with a diel change in survival and sufficient numbers of individuals passing to account for the observed drop in daytime survival is the unmodified spill route.

Table 4.13. Comparison of Day versus Night ViRDCt Estimates of CH0 Dam Passage Survival at LGR, 2018. Standard errors in parentheses.

	Day	Night
ViRDCt	0.9030 (0.0139)	0.9652 (0.0115)

4.2.5.2 Summer Forebay-to-Tailrace Survival

By forming the virtual release, V_1, at the forebay hydrophone array instead of the dam face array, forebay-to-tailrace survival can be estimated using both the VIPRE and ViRDCt models (Table 4.14). Not all CH0 entering the forebay array were detected at the dam face, so forebay-to-tailrace survival was a few percentage points lower than dam passage survival.

Table 4.14. Comparison of Forebay-to-Tailrace Survival Estimates from the VIPRE and ViRDCt Models by Fish Stock at LGR, 2018. Standard errors in parentheses. CH0 detected at forebay array after 9 July 2018 were excluded from the analysis.

Model	Forebay-to-Tailrace Survival
VIPRE	0.8837 (0.0211)
ViRDCt	0.9097 (0.0106)
Weighted Average	0.9045 (0.0104)

4.2.5.3 Summer Route-Specific Dam Passage Survival

Treating the tagged fish going through the various passage routes as separate virtual releases, the VIPRE and ViRDCt models were used to estimate route-specific passage survival (Table 4.15). The JBS had the highest passage survival of any route at LGR with survival probability values essentially equaling 1.0. Unexpectedly, turbine survival estimates also exceeded 99%. The RSW had the next highest values of route-specific survival (0.9654–0.9655). Comparing survivals of groups passing during daytime or nighttime, daytime survivals were lower for unmodified spill bays and the RSW (Table 4.16). Daytime survival was higher for the JBS and could not be computed for turbine-passed fish due to the small number of fish that passed through the turbines during daytime (N = 5).

Table 4.15. Route-Specific Survival for CH0 at LGR in 2018

Route	N (at V_1)	VIPRE (SE)	ViRDCt (SE)
Unmodified Spill Bay	219	0.8456 (0.0321)	0.8450 (0.0323)
Removable Spillway Weir	490	0.9655 (0.0230)	0.9654 (0.0234)
Juvenile Bypass System	95	1.0023 (0.0277)	1.0022 (0.0280)
Turbine	77	0.9949 (0.0306)	0.9949 (0.0309)

Table 4.16. Route-Specific Survival for CH0 during Daytime and Nighttime at LGR in 2018

	Daytime		Nighttime	
Route	N (at V_1)	ViRDCt (SE)	N (at V_1)	ViRDCt (SE)
Unmodified Spill Bay	167	0.8063 (0.0349)	52	0.9375 (0.0354)
Removable Spillway Weir	394	0.9428 (0.0134)	96	0.9479 (0.0227)
Juvenile Bypass System	29	1.007 (0.1304)	66	0.9838 (0.0288)
Turbine	5	NA (NA)	72	0.9848 (0.0151)

Route-specific survivals for CH0 were relatively high through the LGR tailrace for most route types, so single-release estimates of survival through detection arrays stretching further downstream were computed to see if these groups differentiated further after leaving the LGR tailrace. The downstream survival arrays allowed single-release survivals to be estimated for reaches extending to LGS at Columbia River km 635, and the joint probability of survival and detection to be estimated at the forebay of Lower Monumental Dam at Columbia River km 590. If route-specific mortality was being expressed after exiting the tailrace, cumulative survivals would diverge if that mortality differed by route. Figure 4.26 shows that cumulative survival lines for CH0 appear to converge, with deep spill estimates recovering much of the apparent deficit in survival through the tailrace. We again caution that the apparent trends among reaches are inconsistent and there is enough uncertainty around the estimates to question whether apparent trends are meaningful.

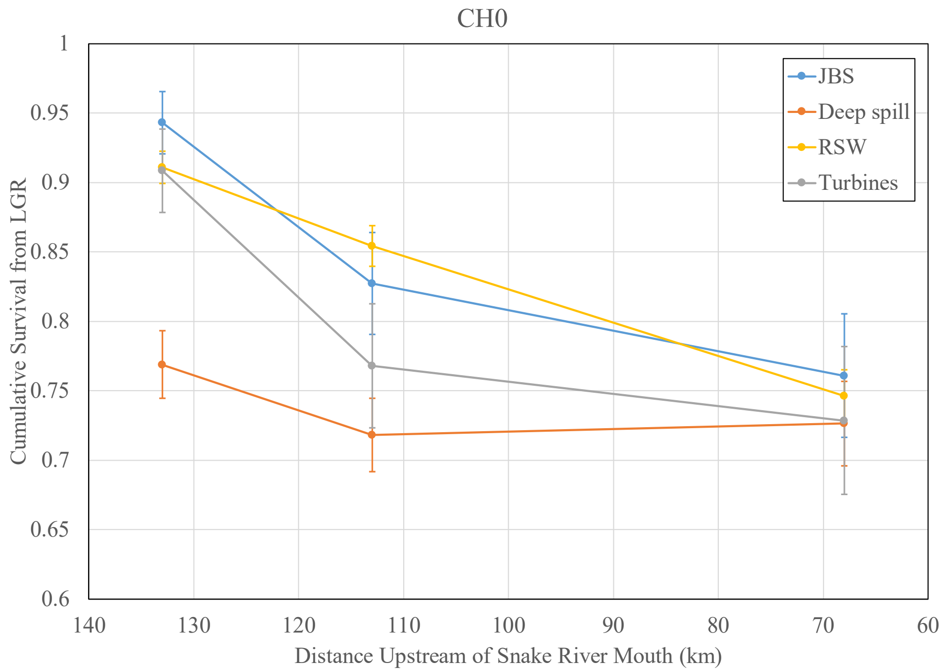

Figure 4.26. Cumulative Survival by Route from LGR for Yearling Chinook (CH1) and Steelhead (STH) to Detection Arrays Downstream. Error bars are standard errors.

5.0 Discussion

This section includes discussion of the statistical performance and survival model assumptions, tailwater mortality, historical context, RSW performance, JBS performance, and recommendations based on the comprehensive analysis of data collected in 2018.

5.1 Comparison of VIPRE vs. ViRDCt Models for Estimating Dam Passage Survival

The VIPRE survival model has been used in dozens of performance standards evaluations at FCRPS mainstem dams (Skalski et al. 2016), but the ViRDCt survival model has the potential to provide the same information while requiring fewer release points and fewer tagged fish. This 2018 study was the first opportunity for a formal side-by-side comparison of these two models for two fish stocks in the spring and one stock in the summer. The estimates of survival from the two alternative release-recapture models comported well within and across fish stocks (Table 5.1). Estimates from the two models were generally within 1 SE of each other, as estimated by the VIPRE model. No one model appeared to systematically have higher or lower survival estimates than the other. Within the limits of the field trial, it appears both models were attempting to estimate the same values of dam passage survival.

Table 5.1. Comparison of Dam Passage Survival Estimates from the VIPRE and ViRDCt Models by Fish Stock at LGR, 2018. Standard errors in parentheses.

	CH1	STH	CH0
VIPRE	0.9726 (0.0159)	0.9959 (0.0099)	0.9422 (0.0217)
ViRDCt	0.9877 (0.0062)	0.9936 (0.0037)	0.9242 (0.0098)
Weighted Average	0.9857 (0.0051)	0.9939 (0.0008)	0.9272 (0.0068)

Route-specific survivals subdivide the available numbers of fish for calculating the estimates and are a more challenging comparison among the two survival models. Table 5.2 compares route-specific survival estimates between the two models. Only one of the 12 estimates (CH1, unmodified spill bay) differs by more than one standard error in both directions, with the VIPRE estimate being lower (0.9521) than the ViRDCt estimate (0.9898). The VIPRE estimate of JBS survival for STH (1.0111) was higher but within one SE of the ViRDCt estimate, while the ViRDCt estimate (1.000) was more than one SE below the VIPRE estimate. This calculated difference is not particularly meaningful, as neither survival rate could exceed 1.000. When comparing standard errors, we see that the SEs were nearly identical for CH0. For CH1, three of the four routes had a smaller SE using the VIPRE model. For STH, two routes had a smaller SE using VIPRE and two had a smaller SE using ViRDCt. Comparing 2018 LGR estimates of route-specific survivals shows more similarity than differences between the two models.

Table 5.2. Route-Specific Survival by Species at LGR in 2018. Bold results indicate that model estimates differ by more than one standard error in both directions.

Species and Route	N (at V_1)	VIPRE (SE)	ViRDCt (SE)
CH1			
Unmodified Spill Bay	117	**0.9521 (0.0244)**	**0.9898 (0.0102)**
Removable Spillway Weir	168	0.9855 (0.0172)	1.0016 (0.0360)
Juvenile Bypass System	138	0.9961 (0.0158)	1.0001 (0.0264)
Turbine	32	0.8779 (0.0599)	0.8697 (0.0604)
STH			
Unmodified Spill Bay	173	1.0003 (0.0119)	1.0002 (0.0153)
Removable Spillway Weir	217	0.9843 (0.0141)	0.9937 (0.0063)
Juvenile Bypass System	262	1.0111 (0.0087)	1.0000 (0.0124)
Turbine	23	0.8804 (0.0715)	0.9076 (0.0626)
CH0			
Unmodified Spill Bay	219	0.8456 (0.0321)	0.8450 (0.0323)
Removable Spillway Weir	490	0.9655 (0.0230)	0.9654 (0.0234)
Juvenile Bypass System	95	1.0023 (0.0277)	1.0022 (0.0280)
Turbine	77	0.9949 (0.0306)	0.9949 (0.0309)

Although route-specific estimates were quite similar across the models, the ViRDCt model produced whole-dam survival estimates with lower SE (Table 5.1). The SEs from the ViRDCt model were less than half the size of the SEs from the VIPRE model. This improvement in precision was accomplished despite the ViRDCt model using less than half the number of acoustic tags used by the VIPRE model. These results strongly suggest that future studies to monitor dam passage survival could generate more precise estimates or generate the same precision at a lower cost using the ViRDCt approach.

5.2 Comparison of the LGR 2018 Passage and Survival Results with Radiotelemetry Studies (2002–2007) during RSW Operation

It is useful to compare the 2018 results to those of several radiotelemetry studies of juvenile salmon and steelhead passage conducted at LGR between 2002 and 2007 (Plumb et al. 2003; Plumb et al. 2004; Perry et al. 2007; Beeman et al. 2008; Puls et al. 2008). These studies included at least one treatment that is similar to the 2018 configuration with the RSW in operation and the absence of the BGS.

For CH1, 2018 FPE and SPE estimates fell in the middle of radiotelemetry estimates, but the 2018 estimate of FGE was higher than all radiotelemetry estimates. The VIPRE estimate of dam passage survival was essentially the same as the higher of two radiotelemetry estimates, while the ViRDCt estimate was 0.015 higher.

For STH, 2018 FPE and SPE estimates fell in the middle of radiotelemetry estimates, and the 2018 estimate of FGE was near the high end of radiotelemetry estimates. Both the VIPRE and ViRDCt estimates of dam passage survival were approximately 0.036 higher than the single radiotelemetry estimate.

For CH0, 2018 FPE estimates fell near the middle of radiotelemetry estimates, SPE estimates were approximately 0.035 higher than the high range of radiotelemetry estimates, and FGE was approximately 0.037 lower than the lowest radio telemetry estimate. The VIPRE estimate of dam passage survival was 0.055 higher than the single radiotelemetry estimate, while the ViRDCt estimate was 0.037 higher.

Differences in passage distributions among routes for CH1 and STH were primarily differences in FGE, with radiotelemetry estimates being lower. With relatively high flows in the spring of 2018 but near average spill, the proportion of flow through the powerhouse would have been higher. Higher powerhouse flow proportions would likely increase FGE because the attraction of the RSW for surface-oriented individuals would be less pronounced.

Estimates of FGE were higher for radiotelemetry studies and estimates of SPE were lower. For CH0 in the summer, relatively low total flows with some periods of above-average spill proportions would encourage greater spill passage. This would not only increase SPE but would also likely attract surface-oriented individuals away from the powerhouse, leading to lower FGE.

Survival estimates in 2018 for CH1 were similar to those in radiotelemetry studies, but STH and CH0 estimates were higher than radiotelemetry estimates. These comparisons are based on one or two years of radiotelemetry data, and that makes it difficult to tease apart the influence of river conditions from the influence of tag size and other technical differences. The take-home message for survival is that 2018 dam passage survival estimates were not lower than previous radiotelemetry studies.

5.3 Comparison of the LGR 2018 Survival Estimates with Prior Performance Standards Evaluations at Other Dams

The 2018 study to estimate dam passage survival at LGR was the first at that location. Consequently, there is no direct reference to compare the 2018 LGR results with earlier values using a similar approach (see Appendix E for comparison with radiotelemetry studies from 2002 through 2006). However, the 2018 LGR results can be compared to the estimates of dam passage survival reported by Skalski et al. (2016) collected during compliance studies at other FCRPS dams from 2010–2014.

Nine estimates of dam passage survival using the VIPRE model were generated for CH1 at other FCRPS projects, with a range of 0.9597 ($\widehat{\mathrm{SE}} = 0.0176$) to 0.9868 ($\widehat{\mathrm{SE}} = 0.0090$) and a mean value of 0.9678 (Skalski et al. 2016). The survival value of 0.9726 ($\widehat{\mathrm{SE}} = 0.0159$) for CH1 generated at LGR in 2018 comports well with these historical values elsewhere.

Nine estimates of dam passage survival using the VIPRE model were generated for STH at other FCRPS projects, with a range of 0.9534 ($\widehat{\mathrm{SE}} = 0.0097$) to 0.9952 ($\widehat{\mathrm{SE}} = 0.0083$) and a mean value of 0.9792 (Skalski et al. 2016). The 2018 estimate of dam passage survival for STH at LGR of 0.9959 ($\widehat{\mathrm{SE}} = 0.0099$) is on the high side of the historical range observed elsewhere.

Eleven estimates of dam passage survival using the VIPRE model were generated for CH0 at other FCRPS projects, with a range of 0.9076 ($\widehat{\mathrm{SE}} = 0.0139$) to 0.9789 ($\widehat{\mathrm{SE}} = 0.0079$) and a mean value of 0.9441 (Skalski et al. 2016). The 2018 estimate of dam passage survival for CH0 at LGR of 0.9422 ($\widehat{\mathrm{SE}} = 0.0217$) is very similar to the mean of historical values observed elsewhere.

The two estimates of dam passage survival for the spring migrants at LGR in 2018 exceed the 2008 BiOp survival standard of ≥ 0.96. Similarly, the VIPRE survival estimate for CH0 at LGR in 2018 exceeded the 2008 BiOp survival standard of ≥ 0.93 for summer migrants.

5.4 JBS Performance

Prior to the 2018 field season, the JBS underwent major upgrades including enlarged orifices, a widened collection channel, and new primary dewatering structures, transportation channels, and emergency and primary bypass outfalls. The expected effect of this facility upgrade was improved survival for emigrating salmon. A detailed evaluation of condition changes and travel times of CH1 moving through the JBS showed a significant reduction in descaling rates and an increase in travel rates (Colotelo et al. 2018). Survival for fish tagged in this study that swam downriver to LGR and were guided into the JBS survived at high rates through the tailrace, which supports the other findings that JBS conditions are favorable to fish (Table 5.3).

Table 5.3. JBS Survival by Species at LGR in 2018

Species	N (at V_1)	VIPRE (SE)	ViRDCt (SE)
CH1	138	0.9961 (0.0158)	1.0001 (0.0264)
STH	262	1.0111 (0.0087)	1.0000 (0.0124)
CH0	95	1.0023 (0.0277)	1.0022 (0.0280)

5.5 Low CH0 Survival

Survival of CH0 that passed through traditional deep spill bays at LGR in 2018 was unexpectedly low. Subyearlings migrate during a period when the temperature is relatively high and increasing, and they are also known to cease migration in higher proportions late in the season. Those factors would presumably apply to other route types as well, but survival elsewhere remained relatively high. Low CH0 survival through unmodified spill bays was first evaluated by examining survival over the course of the season. Regression tree analyses were used to split the detection history data into two mutually exclusive groups, each of which was as homogeneous as possible with regard to response (detection at Central Ferry) and predictor (day of LGR passage) values. Partitioning was done according to a splitting "cut" value for the predictor variable. Splitting was based on maximizing the LogWorth significance value, which is the negative log of the adjusted *P*-value, for each split candidate (Sall 2002). The adjusted *P*-value that resulted from a split had to be less than 0.05 to be significant.

Regression tree analyses indicated CH0 that passed LGR through traditional deep spill bays prior to 15 June 18:00 were significantly more likely to be detected at Central Ferry than those that passed deep spill bays from 15 June 18:00 through 9 July ($P < 0.001$). Of the 71 CH0 that passed prior to 15 June 18:00, 97% were detected at Central Ferry compared to 74% of the 148 CH0 that passed after that time (but prior to 10 July).

Dam passage survival was estimated for these two groups, producing similar results to those obtained from the regression tree analysis. CH0 that passed through deep spill bays during the early part of the summer season had a dam passage survival estimate of 0.9689 (SE = 0.0228) compared to 0.7760 (0.0413) for those that passed deep spill bays during the latter part of the season.

As of 15 June, the temperature had reached only about 15ºC, which should not result in significant mortality. TDG did not rise sharply at that time. Flows were dropping, and there was a notable increase in spill proportion to above 60% as a result of decreasing flows while maintaining spill to the gas cap (Figure 4.17). Mortality of individuals was relatively high during this brief period between 15 June and the start of the summer operational period, at which point spill to the gas cap was not required and the operational guidelines resulted in a reduced spill proportion and a higher proportion of discharge through the powerhouse. Mortality again increased after 28 June, as total flows continued to drop and spill proportions continued to increase, along with increasing temperatures and the possibility that individuals were ceasing migration. Tailrace egress times were only slightly elevated for fish that survived and were not available for most that did not survive, as deceased fish were less likely to exit the tailrace.

While the mechanisms of this unexpected mortality remain uncertain, one possibility is that spilling a high proportion of water could result in eddies forming in the tailrace that cause some fish (in particular fish passing through deep spill) to remain in the tailrace for a longer time, increasing their exposure to hazards such as predators. This possibility is supported by the appearance of an eddy downstream of the LGR powerhouse in computational fluid dynamics modeling results for a condition with low powerhouse discharge and high spill discharge (Faber et al. 2003).

Although it is difficult to assign causation for low CH0 survival during some operational periods in 2018, we feel it is reasonable to recommend careful consideration of unit priorities and spill patterns to be used during low-flow, high-spill conditions. Where possible, guidelines should promote tailrace conditions that are conducive to rapid egress downstream.

5.6 Conclusions and Recommendations

The newer ViRDCt model produced survival estimates that were consistent with the more established VIPRE model, and those estimates exceeded BiOp requirements for spring stocks of 0.96 survival. Although the 2018 evaluation of LGR survival was designed to meet less stringent precision requirements (SE≤0.025) based on the VIPRE design, the ViRDCt estimates easily met the BiOp precision requirements (SE≤0.015). The VIPRE estimate of survival for the summer stock, CH0, exceeded the requirement for survival > 0.93 with an SE of 0.0217, while the ViRDCt estimate was slightly below the BiOp requirement at 0.9242 with an SE of 0.0098. That low survival includes unexpectedly poor survival of CH0 passing over unmodified spill bays after 15 June. While it may only be coincidental, much of the mortality occurred for fish passing at times when spill exceeded half of the total flow. Further study will be needed to provide reliable guidance on LGR spill operations during low-flow conditions.

Notable differences between VIPRE and ViRDCt designs were the improved precision achieved by ViRDCt and its reduced requirement for fish and release locations, which allows for a more cost-effective study. We recommend that future survival evaluations apply the ViRDCt model design to achieve the desired level of precision at a reduced cost.

The 2018 LGR study was the first large-scale passage survival evaluation that employed the smaller injectable tag. No problems have been noted in fish health, tag retention, tag life, detection range, or any other biological or technological sense of how the tags performed. The precision of the survival estimates corroborates findings that the injectable tags performed as well as or better than expected. We recommend that future studies use the injectable tag to reduce fish handling and to take advantage of the longer tag life.

Fish released upstream of LGR that passed through the newly renovated JBS survived at high rates. Monitoring these passage groups with the best available downstream detections arrays in each period (Bonneville Dam forebay [458 km] in spring, Lower Monumental Dam forebay [103 km] in summer) yielded no evidence that JBS passage was causing additional mortality downstream (see Figure 4.15 and Figure 4.26 above).

The RSW proved to be the most effective passage route, especially during the daytime, when fewer individuals passed the powerhouse and unmodified spill bays for all stocks of fish tested. During the nighttime, fish routing was much more like flow proportions among routes, with the RSW retaining some of its effectiveness advantage over other route types. This diel difference in fish behavior suggests that spill operations could be tailored differently to achieve the desired fish passage outcomes for day and night periods.

6.0 References

3 Treaty Tribes-Action Agencies. 2008. Memorandum of Agreement Among the Umatilla, Warm Springs and Yakama Tribes, Bonneville Power Administration, U.S. Army Corps of Engineers, and U.S. Bureau of Reclamation. Portland, Oregon. April 4, 2008. Available online at http://www.salmonrecovery.gov/Files/BiologicalOpinions/3-tribe-AA-MOA-Final.pdf.

Beeman, JW, SD Fielding, AC Braatz, TS Wilkerson, AC Pope, CE Walker, JM Hardiman, RW Perry, and TD Counihan. 2008. *Survival and Migration Behavior of Juvenile Salmonids at Lower Granite Dam, 2006*. Final Report of Research by the U.S. Geological Survey to the U.S. Army Corps of Engineers, Walla Walla District, Contract W68SBV60378208, Walla Walla, Washington.

Burnham KP, DR Anderson, GC White, C Brownie, and KH Pollock. 1987. “Design and analysis methods for fish survival experiments based on release-recapture.” *American Fisheries Society Monograph* 5.

Colotelo AH, Rhode BM, McCann E, Harnish RA, Martinez JJ, Duncan JP, Grant C. 2018. *Post-Construction Evaluation of the Upgraded Juvenile Bypass System at Lower Granite Dam – Draft Report*. Richland, WA: Pacific Northwest National Laboratory.

Deng ZD, MA Weiland, T Fu, TA Seim, BL Lamarche, EY Choi, TJ Carlson, and MB Eppard. 2011. “A Cabled Acoustic Telemetry System for Detecting and Tracking Juvenile Salmon: Part 2. Three- Dimensional Tracking and Passage Outcomes.” *Sensors* 11(6):5661−5676. doi:10.3390/s110605661.

Faber DM, MA Weiland, TJ Carlson, KM Cash, and SA Zimmerman. 2003. The Feasibility of Using an Ultrasonic Fish Tracking System in the Tailrace of Lower Granite Dam. PNNL-14340, prepared by Pacific Northwest National Laboratory, Richland, Washington, for the U.S. Army Corps of Engineers, Portland District, Portland, Oregon, under Contract DE-AC06-76RLO1830.

Harnish RA, KD Ham, JR Skalski, RL Townsend, JM Lady, KD Deters, PS Titzler, AH Colotelo, T Fu, X Li, JJ Martinez, Z Deng, MK Nims, EL McCann, Y Yuan, CL Grant. 2018. *Yearling Chinook Salmon and Juvenile Steelhead Passage and Survival through the FCRPS, 2018 – Draft Report.* PNNL-28325. Richland, WA: Pacific Northwest National Laboratory.

Harnish RA, KD Ham, KA Deters, AH Colotelo, PS Titzler, and EE Hockersmith. 2017. *Examination of Ice Harbor Dam BiOp Performance Standard Evaluation Assumptions - Final Report*. PNNL-26207. Richland, WA: Pacific Northwest National Laboratory.

Lady JM, P Westhagen, and JR Skalski. 2012. *Program ATLAS 1.2: Active Tag Life Adjusted Survival*. Columbia Basin Research, University of Washington, Seattle.

Li T, and JJ Anderson. 2009. “The vitality model: A way to understand population survival and demographic heterogeneity.” *Theoretical Population Biology* 76:118–131.

McMichael, GA, JP Duncan, PS Titzler, EW Oldenburg, RA Harnish, KA Deters, KD Ham, BJ Bellgraph, RP Mueller, RS Brown, AC O’Toole, JR Skalski, RL Townsend, Z Deng, JJ Martinez, MA Weiland, JS Hughes, F Khan. 2011. *Implementation Plan for Using Acoustic Telemetry Methodology to Estimate Survival and Passage Metrics at Lower Granite Dam*. PNWD-4317 prepared for the U.S. Army Corps of Engineers, Walla Walla District by Battelle-Pacific Northwest Division, Richland, Washington.

NOAA (National Oceanic and Atmospheric Administration). 2008. *Biological Opinion – Consultation on Remand for Operation of the Federal Columbia River Power System, 11 Bureau of Reclamation Projects in the Columbia Basin and ESA Section 10(a)(1)(A) Permit for Juvenile Fish Transportation Program.* National Marine Fisheries Service (NOAA Fisheries) – Northwest Region, Seattle, Washington. Available at: http://www.salmonrecovery.gov/.

Perry, RW, TJ Kock, MS Novick, SD Fielding, GS Hansen, JM Sprando, TS Wilkerson, GT George, JL Schei, NS Adams, and DW Rondorf. 2007. *Survival and Migration Behavior of Juvenile Salmonids at Lower Granite Dam, 2005*. Report to the U.S Army Corps of Engineers, Final Report of Research, Contract W68SBV50498133, Walla Walla, Washington.

Plumb, JM, AC Braatz, JN Lucchesi, SD Fielding, JM Sprando, GT George, NS Adams, and DW Rondorf. 2003. *Behavior of Radio-Tagged Juvenile Chinook Salmon and Steelhead and Performance of a Removable Spillway Weir at Lower Granite Dam, Washington, 2002.* Report to the U.S. Army Corps of Engineers, Final Report of Research, Contract W68SBV00104592, Walla Walla, Washington.

Plumb, JM, AC Braatz, JN Lucchesi, SD Fielding, AD Cochran, TK Nation, JM Sprando, JL Schei, RW Perry, NS Adams, and DW Rondorf. 2004. *Behavior and Survival of Radio-Tagged Juvenile Chinook Salmon and Steelhead and Performance of a Removable Spillway Weir at Lower Granite Dam, Washington, 2003*. Report to the U.S. Army Corps of Engineers, Final Report of Research, Contract W68SBV00104592, Walla Walla, Washington.

Puls, AL, TD Counihan, CE Walker, JM Hardiman, and IN Duran. 2008. *Survival and Migration Behavior of Subyearling Chinook Salmon at Lower Granite Dam, 2007*. Report of Research by the U.S. Geological Survey to the U.S. Army Corps of Engineers, Walla Walla District, Contract W68SBV70198655, Walla Walla, Washington.

Sall, J. 2002. *Monte Carlo Calibration of Distributions of Partition Statistics* [online]. SAS Institute. Available from http://www.jmp.com/software/whitepapers/pdfs/montecarlocal.pdf [accessed November 2013].

Seber GAF. 1982. *The Estimation of Animal Abundance*. MacMillan, New York.

Skalski JR, RL Townsend, TW Steig, and S Hemstrom. 2010. “Comparison of two alternative approaches for estimating dam passage survival of salmon smolts.” *North American Journal of Fisheries Management* 30:831–839.

Skalski JR and 9 coauthors. 2013a. *BiOp Performance Testing: Passage and Survival of Yearling and Subyearling Chinook Salmon and Juvenile Steelhead at Little Goose Dam, 2012*. PNNL-22140 prepared for the U.S. Army Corps of Engineers, Walla Walla District by PNNL-Pacific Northwest Division, Richland, Washington.

Skalski JR and 9 coauthors. 2013b. *BiOp Performance Testing: Passage and Survival of Yearling and Subyearling Chinook Salmon and Juvenile Steelhead at Lower Monumental Dam, 2012*. PNNL-22100 prepared for the U.S. Army Corps of Engineers, Walla Walla District by PNNL-Pacific Northwest Division, Richland, Washington.

Skalski JR and 12 coauthors. 2014. *BiOp Performance Testing: Passage and Survival of Subyearling Chinook Salmon at Little Goose and Lower Monumental Dams, 2013*. PNNL-22706 prepared for the U.S. Army Corps of Engineers, Walla Walla District by PNNL-Pacific Northwest Division, Richland, Washington.

Skalski, JR, MA Weiland, KD Ham, GR Ploskey, GA McMichael, AH Colotelo, TJ Carlson, CM Woodley, MB Eppard, and EE Hockersmith. 2016. "Status after 5 years of survival compliance testing in the Federal Columbia River Power System (FCRPS)." *North American Journal of Fisheries Management* 36(4):720-730.

Skalski JR, RL Townsend, KD Ham, RA Harnish, T Fu, X Li, AH Colotelo, KA Deters, and JM Lady. 2018. *Passage and Survival of Yearling and Subyearling Chinook Salmon and Steelhead Smolts at Lower Granite Dam, 2018*. Draft Report. PNNL-28211. Pacific Northwest National Laboratory, Richland, WA.

Titzler PS, GA McMichael, and JA Carter. 2010. "Autonomous acoustic receiver deployment and mooring techniques for use in larger rivers and estuaries." *North American Journal of Fisheries Management* 30:853−859.

USACE (U.S. Army Corps of Engineers). 2011. *Surgical Protocols for Implanting JSATS Transmitters into Juvenile Salmonids for Studies Conducted for the U.S. Army Corps of Engineers*. Version 1.0, Portland District, Portland, Oregon.

Walker RW, LM Markillie, AH Colotelo, DR Geist, ME Gay, CM Woodley, MB Eppard, and RS Brown. 2013. "Ultraviolet radiation as disinfection for fish surgical tools." *Animal Biotelemetry 1*. PNNL-SA-86919. doi:10.1186/2050-3385-1-4

Watkins WA and WE Schevill. 1972. "Sound source location by arrival-times on a non-rigid three- dimensional hydrophone array." *Deep-Sea Research* 19:691−706.

Appendix A

Assessment of Survival Model Assumptions

Survival model assumptions are assessed here to ensure that assumptions of the virtual/paired-release (VIPRE) survival model design are not violated. The assumption assessment covered in this section includes surgeon effects/handling mortality and tag shedding, fish size distribution, tag-life corrections, arrival distributions, and downstream mixing.

A.1 Tests of Hypotheses

A.1.1 Tagger Effects

Any tagger effects can be minimized if the distribution of tagging efforts is homogeneous among release groups. Homogeneous mixing is not necessary but can be beneficial if slight differences in survival of fish tagged by different staff occur and go undetected. Chi-square tests of homogeneity found tagger effect to be homogeneous ($P > 0.05$) within the R_1 and R_2 releases, but not the R_3 release (Table A.1).

Reach survival of R_1 fish to rkm 133 (or rkm 140 in the case of the subyearling Chinook [CH0]) tagged by the different taggers were found to be homogeneous ($P > 0.05$) for all three fish stocks, allowing pooling of detection data across taggers (Table A.2).

Table A.1. Numbers of Yearling Chinook (CH1), b) Steelhead (STH), and c) Subyearling Chinook (CH0) Tagged by Individual Staff for Release Groups R_1, R_2, and R_3 during the Dam Passage Survival Study at Lower Granite Dam, 2018

CH1				
Tagger ID		**Numbers Tagged**		
	$\boldsymbol{R_1}$	$\boldsymbol{R_2}$	$\boldsymbol{R_3}$	
A	117	73	75	
B	113	62	68	
C	130	87	81	
D	106	77	74	$P(\chi^2 \geq 1.983) = .921$
STH				
Tagger ID		**Numbers Tagged**		
	$\boldsymbol{R_1}$	$\boldsymbol{R_2}$	$\boldsymbol{R_3}$	
A	170	127	133	
B	167	98	112	
C	189	152	138	
D	154	124	127	$P(\chi^2 \geq 5.160) = .524$
CH0				
Tagger ID		**Numbers Tagged**		
	$\boldsymbol{R_1}$	$\boldsymbol{R_2}$	$\boldsymbol{R_3}$	
A	356	176	193	
B	357	178	152	
C	373	156	157	
D	307	180	188	$P(\chi^2 \geq 14.97) = 0.021$

Table A.2. Reach Survival Estimates of R_1 Releases to rkm 133 (CH1 and STH) or to rkm 140 (CH0) by Tagger Staff. Standard errors in parentheses. *P*-values associated with *F*-tests of homogeneous survival.

Tagger ID	CH1	STH	CH0
A	0.9569 (0.0189)	0.9821 (0.0102)	0.6905 (0.0247)
B	0.9732 (0.0153)	0.9880 (0.0084)	0.7192 (0.0241)
C	0.9536 (0.0185)	0.9947 (0.0053)	0.7772 (0.0217)
D	0.9609 (0.0192)	0.9673 (0.0144)	0.7608 (0.0246)
F-test	0.1693	0.9973	2.0570
P-value	0.9172	0.3929	0.1036

A.1.2 Downstream Mixing

Downstream mixing of arrival release groups V_1, R_2, and R_3 to the hydrophone array at rkm 113 show very good timing of the V_1, R_2, and R_3 releases, as expected (Figure A.1). The arrival modes are nearly identical with the V_1 fish having a slightly more spread-out distribution.

A.1.3 Tag Life

Tag life was monitored separately for spring and summer releases. Tag-life data was fit to the vitality model of Li and Anderson (2009). The spring- and summer-run tags had significantly different survivorship curves ($P = 0.001$), so were not pooled. For the spring releases, average tag life was estimated to be $\bar{t} = 61.11$ days ($\widehat{\mathrm{SE}}(\bar{t}) = 1.22$). For the summer releases, average tag life was estimated to be $\bar{t} = 56.94$ days ($\widehat{\mathrm{SE}}(\bar{t}) = 0.91$). Comparison of the cumulative arrival distributions of spring and summer stocks to the downstream detection array at rkm 68 to the tag-life curves indicate the tag life was adequate for all fish to pass through the study area before tag failure became an issue (Figure A.2).

A.1.4 Representative Fish Size

The VIPRE model assumes the release groups R_1, R_2, and R_3 come from the same fish source and share common baseline survival processes. We tested these assumptions by comparing the length distribution of the fish across release groups (Figure A.3, Figure A.4, and Figure A.5). In the case of all these fish stocks, the release groups were comparable in size.

Another model assumption is that fish used in the survival study are representative of run-of-river (ROR) fish passing LGR. To this end, we compared the length distribution of the release groups R_1, R_2 and, R_3 to the fish sampled at LGR by the Smolt Monitoring Program (SMP) during the respective study periods (Figure A.3, Figure A.4, and Figure A.5). For CH1 and STH, the size distributions of tagged and ROR fish were comparable (Figure A.3 and Figure A.4). For CH0, the size distribution of the tagged fish was slightly truncated at the lower end, as ROR fish in the 60 mm–95 mm range were not tagged (Figure A.5).

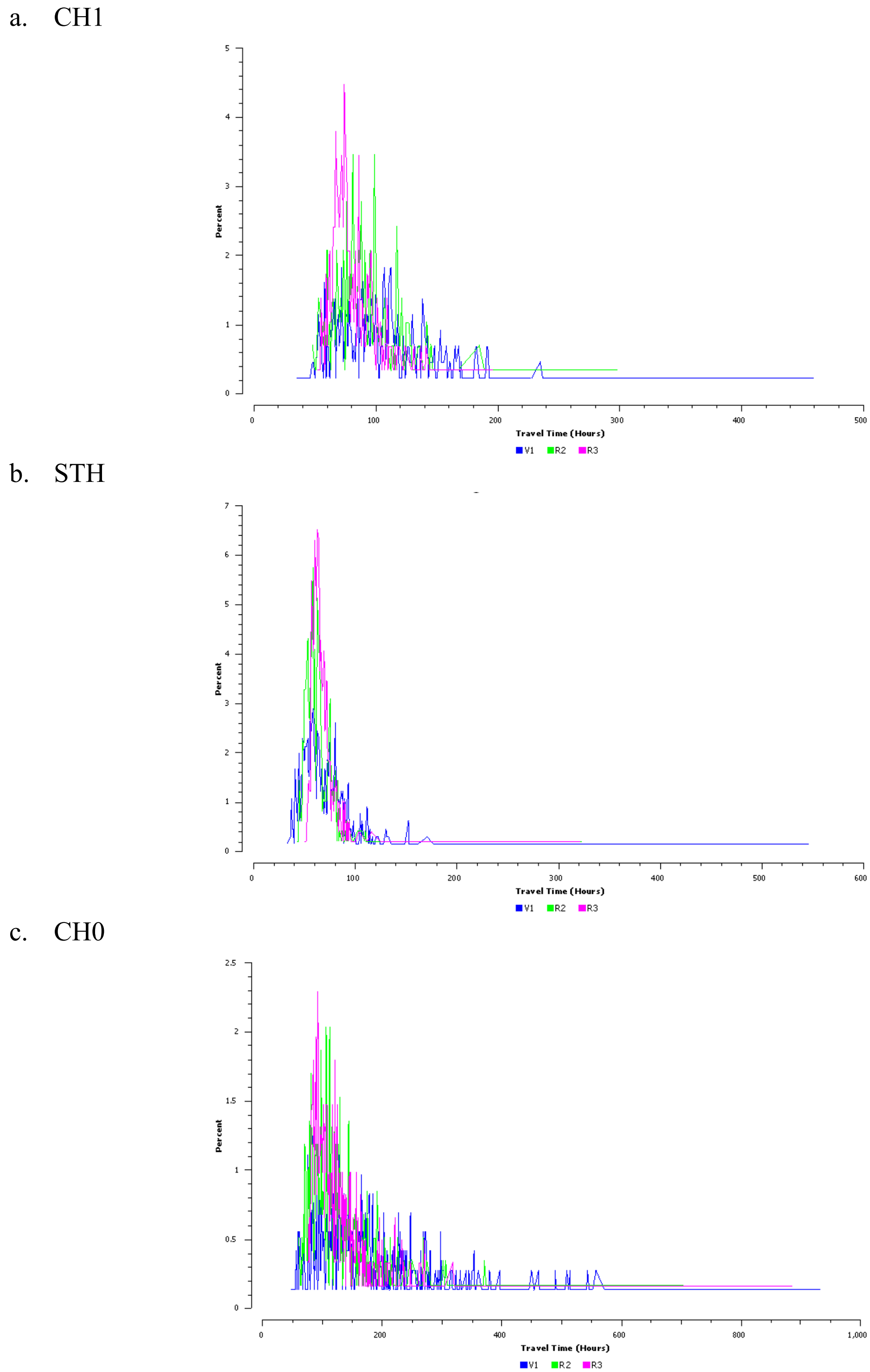

Figure A.1. Frequency Distribution Arrival Plots to Detection Array at rkm 113 for Releases V1, R2, and R3 Used in the VIPRE Model Analysis of Dam Passage Survival

a. CH1

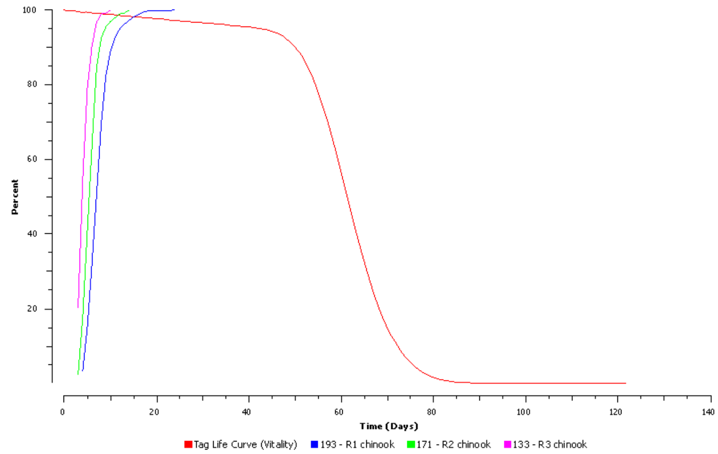

b. STH

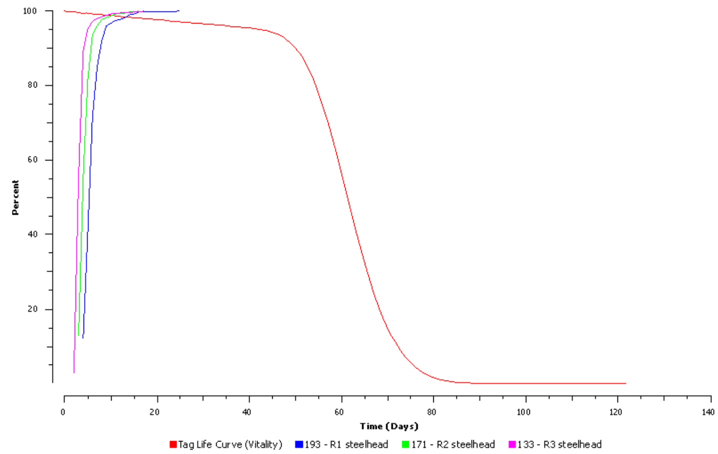

c. CH0

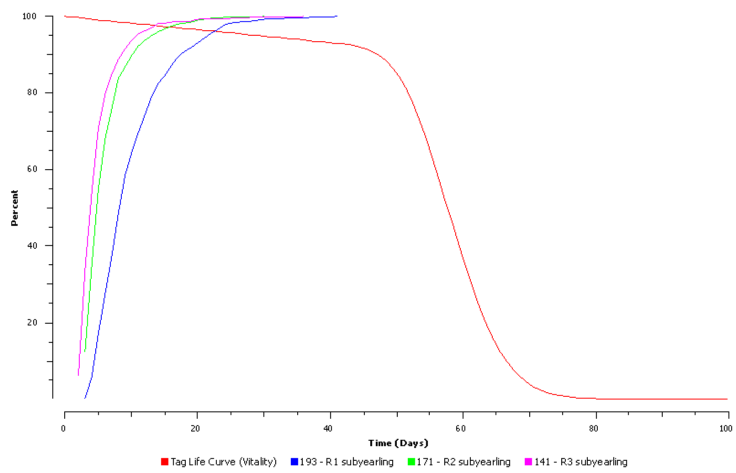

Figure A.2. Comparison of Cumulative Distributions for Tag Life and Travel Times of all Released Fish to the Downstream Detection Array at rkm 68

a. LGR (Release V_1)

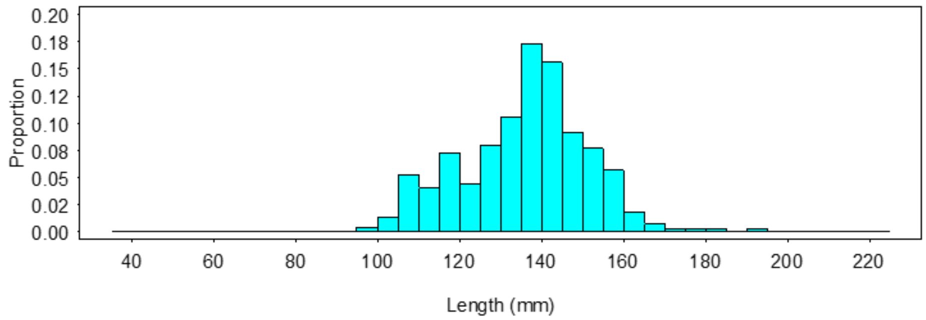

b. LGR Tailrace (Release R_2)

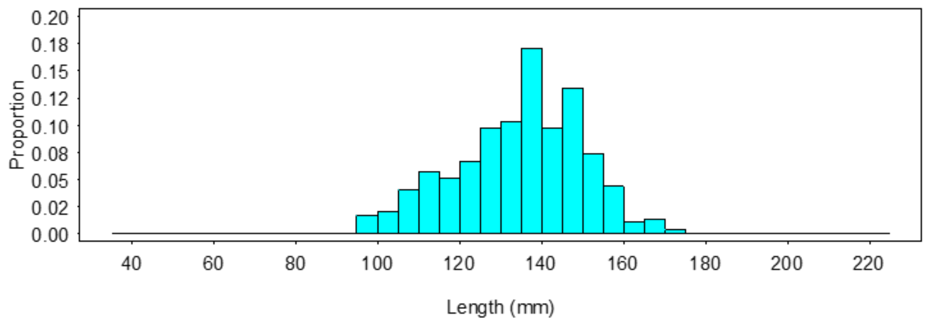

c. Mid-Reservoir (Release R_3)

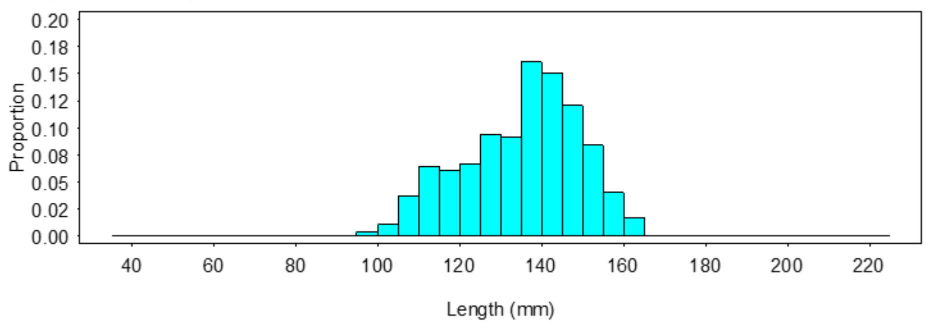

d. ROR

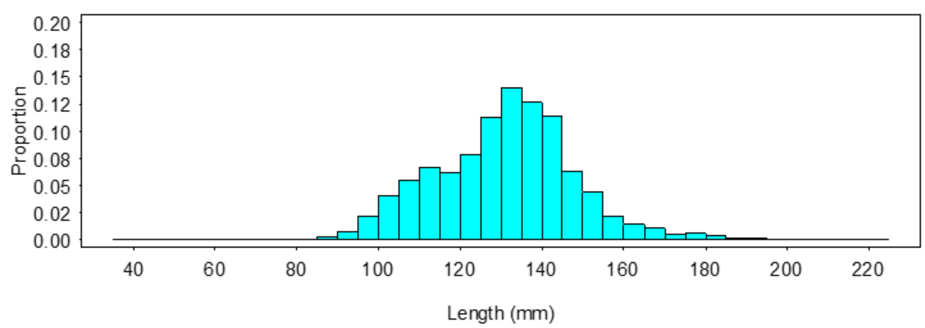

Figure A.3. Relative Frequency Distributions for Fish Lengths (mm) of CH1 Used in a) Release V_1, b) Release R_2, c) Release R_3, and d) ROR Fish Sampled at LGR by the SMP in 2018

a. LGR (Release V_1)

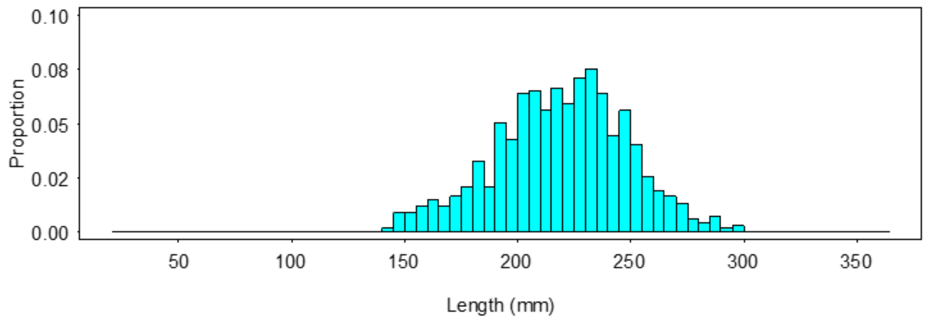

b. LGR Tailrace (Release R_2)

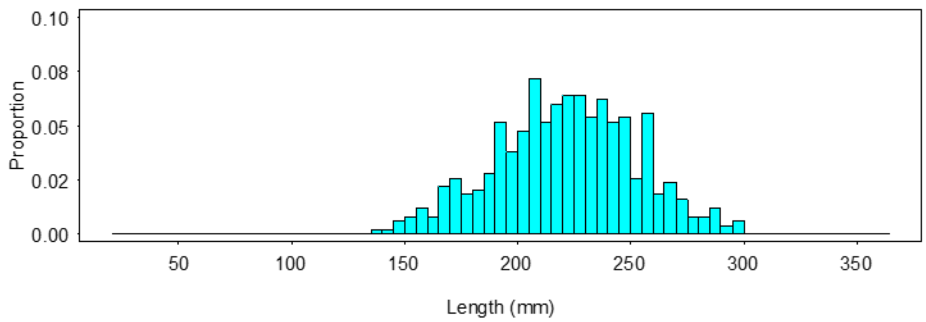

c. Mid-Reservoir (Release R_3)

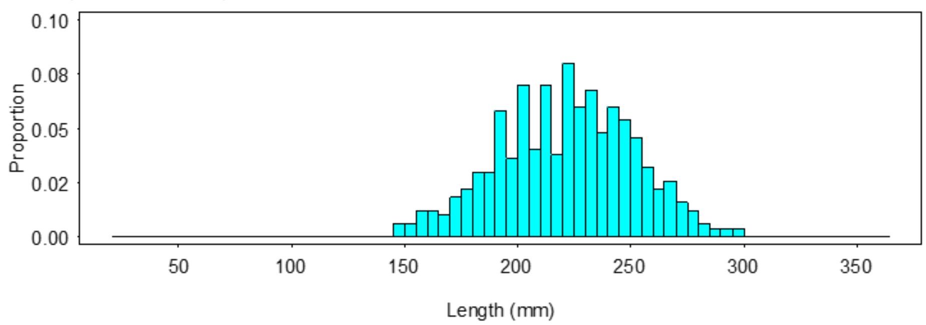

d. ROR

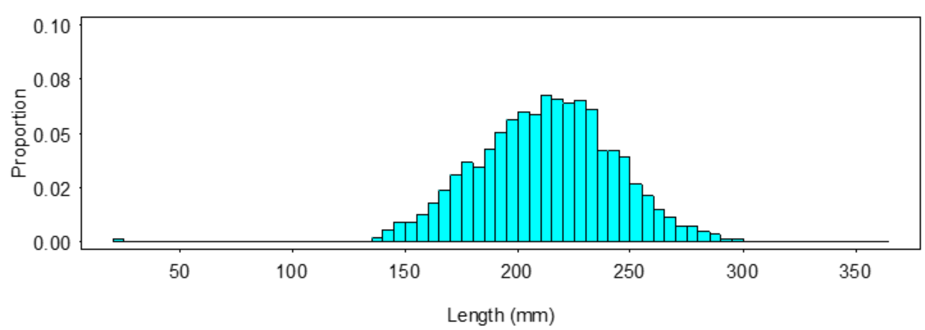

Figure A.4. Relative Frequency Distributions for Fish Lengths (mm) of STH Used in a) Release V_1, b) Release R_2, c) Release R_3, and d) ROR Fish Sampled at LGR by the SMP in 2018

a. LGR (Release V_1)

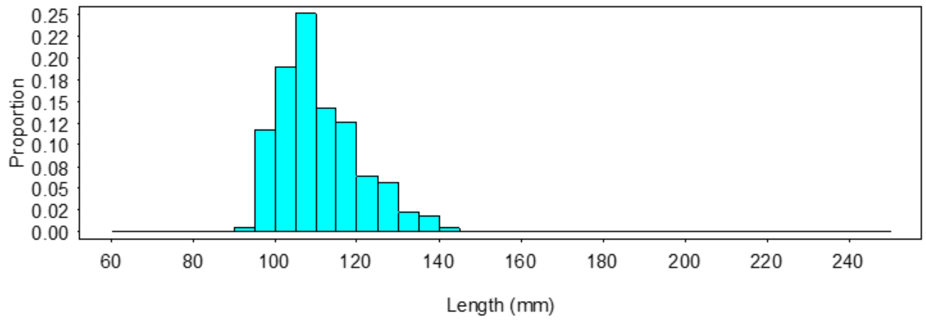

b. LGR Tailrace (Release R_2)

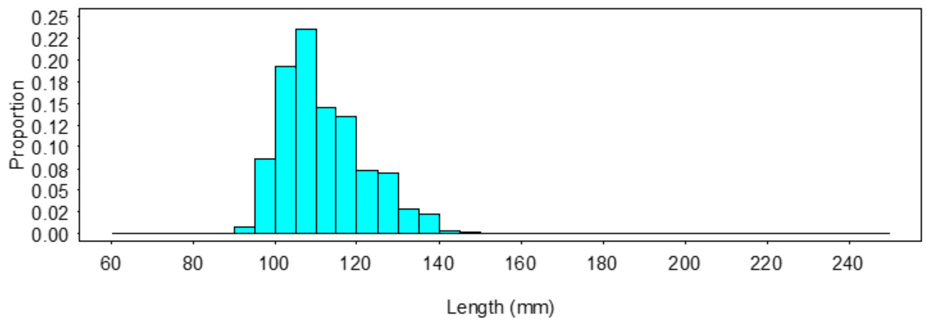

c. Mid-Reservoir (Release R_3)

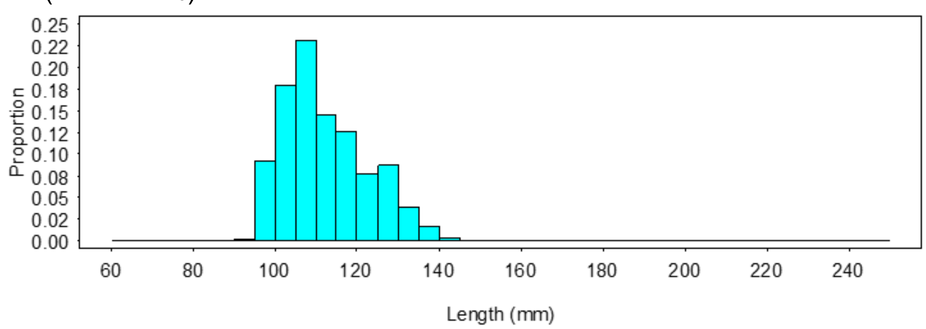

d. ROR

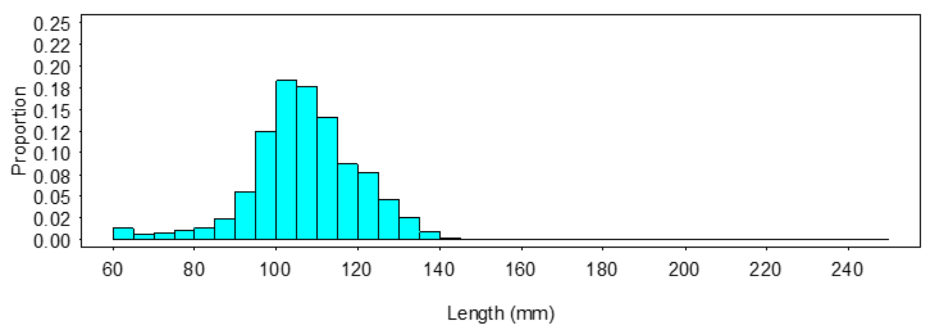

Figure A.5. Relative Frequency Distributions for Fish Lengths (mm) of CH0 used in a) Release V_1, b) Release R_2, c) Release R_3, and d) ROR Fish Sampled at LGR by the Smolt Monitoring Program in 2018

Appendix B

Fish Tagging and Release

Table B.1, Table B.2, and Table B.3 list tagging and release data for CH1, STH, and CH0, respectively.

Table B.1. CH1 Tagged at LGR and Released Live at Three Sites

Tag Date	Release Date	R1_SR193	R2_SR171	R3_SR133	Total
4/16/18	4/17/18	23			23
4/17/18	4/18/18	23	15		38
4/18/18	4/19/18		15	15	30
4/19/18	4/20/18			14	14
4/20/18	4/21/18	23			23
4/21/18	4/22/18	24	15		39
4/22/18	4/23/18		15	15	30
4/23/18	4/24/18			15	15
4/24/18	4/25/18	23			23
4/25/18	4/26/18	23	15		38
4/26/18	4/27/18		14	15	29
4/27/18	4/28/18			15	15
4/28/18	4/29/18	24			24
4/29/18	4/30/18	24	15		39
4/30/18	5/1/18		15	15	30
5/1/18	5/2/18			15	15
5/2/18	5/3/18	24			24
5/3/18	5/4/18	24	15		39
5/4/18	5/5/18		15	15	30
5/5/18	5/6/18			15	15
5/6/18	5/7/18	23			23
5/7/18	5/8/18	23	15		38
5/8/18	5/9/18		15	15	30
5/9/18	5/10/18			15	15
5/10/18	5/11/18	23			23
5/11/18	5/12/18	23	15		38
5/12/18	5/13/18		15	15	30
5/13/18	5/14/18			15	15
5/14/18	5/15/18	24			24
5/15/18	5/16/18	23	15		38
5/16/18	5/17/18		15	15	30
5/17/18	5/18/18			12	12
5/18/18	5/19/18	23			23
5/19/18	5/20/18	23	15		38
5/20/18	5/21/18		15	15	30
5/21/18	5/22/18			15	15
5/22/18	5/23/18	23			23
5/23/18	5/24/18	23	15		38
5/24/18	5/25/18		15	15	30
5/25/18	5/26/18			17	17
Total		466	299	298	1063

Table B.2. STH Tagged at LGR and Released Live at Three Sites

Tag Date	Release Date	R1_SR193	R2_SR171	R3_SR133	Total
4/16/18	4/17/18	34			34
4/17/18	4/18/18	33	25		58
4/18/18	4/19/18		25	25	50
4/19/18	4/20/18			25	25
4/20/18	4/21/18	34			34
4/21/18	4/22/18	34	25		59
4/22/18	4/23/18		25	25	50
4/23/18	4/24/18			25	25
4/24/18	4/25/18	34			34
4/25/18	4/26/18	34	25		59
4/26/18	4/27/18		25	25	50
4/27/18	4/28/18			25	25
4/28/18	4/29/18	34			34
4/29/18	4/30/18	35	25		60
4/30/18	5/1/18		25	25	50
5/1/18	5/2/18			25	25
5/2/18	5/3/18	34			34
5/3/18	5/4/18	34	25		59
5/4/18	5/5/18		25	25	50
5/5/18	5/6/18			25	25
5/6/18	5/7/18	34			34
5/7/18	5/8/18	34	25		59
5/8/18	5/9/18		25	25	50
5/9/18	5/10/18			25	25
5/10/18	5/11/18	34			34
5/11/18	5/12/18	34	25		59
5/12/18	5/13/18		25	25	50
5/13/18	5/14/18			25	25
5/14/18	5/15/18	34			34
5/15/18	5/16/18	34	25		59
5/16/18	5/17/18		25	25	50
5/17/18	5/18/18			22	22
5/18/18	5/19/18	34			34
5/19/18	5/20/18	34	25		59
5/20/18	5/21/18		25	25	50
5/21/18	5/22/18			25	25
5/22/18	5/23/18	34			34
5/23/18	5/24/18	34	26		60
5/24/18	5/25/18		25	25	50
5/25/18	5/26/18			28	28
Total		680	501	500	1681

Table B.3. CH0 Tagged at LGR and Released Live at Three Sites

Tag Date	Release Date	R1_SR193	R2_SR171	R3_SR141	Total
5/30/18	5/31/18	69			69
5/31/18	6/1/18	26	11		37
6/1/18	6/2/18			35	35
6/2/18	6/3/18		34		34
6/3/18	6/4/18	70		34	104
6/4/18	6/5/18	57	28		85
6/5/18	6/6/18			34	34
6/6/18	6/7/18		34		34
6/7/18	6/8/18	70		35	105
6/8/18	6/9/18	77	39		116
6/9/18	6/10/18			34	34
6/10/18	6/11/18		34		34
6/11/18	6/12/18	69		35	104
6/12/18	6/13/18	77	38		115
6/13/18	6/14/18			35	35
6/14/18	6/15/18		35		35
6/15/18	6/16/18	56		25	81
6/16/18	6/17/18	75	38		113
6/17/18	6/18/18			35	35
6/18/18	6/19/18		35		35
6/19/18	6/20/18	70		34	104
6/20/18	6/21/18	78	38		116
6/21/18	6/22/18			34	34
6/22/18	6/23/18		34		34
6/23/18	6/24/18	77		38	115
6/24/18	6/25/18	78	38		116
6/25/18	6/26/18			34	34
6/26/18	6/27/18		34		34
6/27/18	6/28/18	70		35	105
6/28/18	6/29/18	76	38		114
6/29/18	6/30/18			33	33
6/30/18	7/1/18		35		35
7/1/18	7/2/18	75		37	112
7/2/18	7/3/18	77	38		115
7/3/18	7/4/18			35	35
7/4/18	7/5/18		35		35
7/5/18	7/6/18	69		34	103
7/6/18	7/7/18	77	38		115
7/7/18	7/8/18			36	36
7/8/18	7/9/18		36		36
7/9/18	7/10/18			38	38
Total		1393	690	690	2773

Appendix C

Hydrophone and Autonomous Node Deployment Tables

Table C.1. Hydrophone Locations at the LGR Dam-Face Array (rkm 173) in 2018

Node_code	Latitude	Longitude
LGR_P00_01D	46.65746	-117.4311
LGR_P00_01S	46.65746	-117.4311
LGR_P01_02D	46.65767	-117.4309
LGR_P01_02S	46.65767	-117.4309
LGR_P02_03D	46.65787	-117.4307
LGR_P02_03S	46.65787	-117.4307
LGR_P03_04D	46.65808	-117.4305
LGR_P03_04S	46.65808	-117.4305
LGR_P04_05D	46.65828	-117.4303
LGR_P04_05S	46.65828	-117.4303
LGR_P05_06D	46.65849	-117.43
LGR_P05_06S	46.65849	-117.43
LGR_P06D	46.65869	-117.4298
LGR_P06S	46.65869	-117.4298
LGR_RSW_S_01	46.65878	-117.4297
LGR_RSW_S_02	46.65878	-117.4297
LGR_RSW_S_03	46.65878	-117.4297
LGR_RSW_S_04	46.65878	-117.4297
LGR_RSW_N_01	46.65893	-117.4296
LGR_RSW_N_02	46.65893	-117.4296
LGR_RSW_N_03	46.65893	-117.4296
LGR_RSW_N_04	46.65893	-117.4296
LGR_S02_03D	46.65911	-117.4295
LGR_S02_03S	46.65911	-117.4295
LGR_S03_04D	46.65926	-117.4294
LGR_S03_04S	46.65926	-117.4294
LGR_S04_05D	46.6594	-117.4292
LGR_S04_05S	46.6594	-117.4292
LGR_S05_06D	46.65955	-117.4291
LGR_S05_06S	46.65955	-117.4291
LGR_S06_07D	46.65969	-117.4289
LGR_S06_07S	46.65969	-117.4289
LGR_S07_08D	46.65984	-117.4288
LGR_S07_08S	46.65984	-117.4288
LGR_S08D	46.65999	-117.4287
LGR_S08S	46.65999	-117.4287

Table C.2. Hydrophone Locations at the LGS Dam-Face Array (rkm 133) in 2018

Node_code	Latitude	Longitude
LGS_FLS	46.58292	-118.0263
LGS_P00_01D	46.58321	-118.0265
LGS_P00_01S	46.58321	-118.0265
LGS_P01_02D	46.58345	-118.0265
LGS_P01_02S	46.58345	-118.0265
LGS_P04_05D	46.58418	-118.0267
LGS_P04_05S	46.58418	-118.0267
LGS_P06D	46.58464	-118.0268
LGS_P06S	46.58464	-118.0268
LGS_S01D	46.58476	-118.027
LGS_S01S	46.58476	-118.027
LGS_S01_02D	46.58492	-118.027
LGS_S01_02S	46.58492	-118.027
LGS_S04_05D	46.58544	-118.0272
LGS_S04_05S	46.58544	-118.0272
LGS_S07_08D	46.58596	-118.0273
LGS_S07_08S	46.58596	-118.0273
LGS_S08D	46.586126	-118.0274

Table C.3. Approximate Coordinates of Autonomous Nodes Deployed in Arrays Just Above and Below LGR in 2018. Location is a concatenation of an array name and an autonomous node position number. The array name is a concatenation of "SR" for Snake River, with a three-digit number corresponding to river kilometer upstream of the confluence with the Columbia River. Nodes within an array are numbered from river right to river left.

Snake River_kilometer	Array Function	Location	Latitude	Longitude
174	Forebay Entrance	SR174.0_01	46.658397	-117.4133109
		SR174.0_02	46.6568641	-117.4143567
		SR174.0_03	46.655543	-117.415437
		SR174.0_04	46.6540152	-117.4166507
171.5	Tailrace Exit	SR171.5_01	46.6704039	-117.4439107
		SR171.5_02	46.6701126	-117.4444988
		SR171.5_03	46.6698575	-117.4453061
		SR171.5_04	46.6697264	-117.4461967
140	Primary Survival Array (Summer)	SR140.0_01	46.6729429	-117.7632869
		SR140.0_02	46.6725621	-117.761984
		SR140.0_03	46.6723403	-117.760373
133	Primary Survival Array (Spring)	SR133.0_01	46.6252011	-117.8071704
		SR133.0_02	46.624162	-117.8069881
		SR133.0_03	46.6229913	-117.80665
111.5	Secondary Survival Array	SR111.5_01	46.5816996	-118.0457283
		SR111.5_02	46.5813112	-118.04509
		SR111.5_03	46.5808266	-118.0445063
		SR111.5_04	46.5803817	-118.0439392
68	Tertiary Survival Array	SR068.0_01	46.5681028	-118.5300676
		SR068.0_02	46.5671489	-118.5286311
		SR068.0_03	46.5662302	-118.5270331

Appendix D

Capture Histories Used in Survival Analyses

Table D.1. Capture History Data for V_1, R_2, and R_3 Used in Estimated Dam Passage Survival Based on the VIPRE Model

	CH1	STH	CH0
V_1			
1 1 1	411	637	565
0 1 1	1	0	0
1 0 1	0	0	8
0 0 1	0	0	0
1 2 0	4	3	5
0 2 0	0	0	0
1 1 0	20	17	153
0 1 0	1	0	0
2 0 0	0	0	0
1 0 0	4	7	71
0 0 0	14	11	79
R_2			
1 1	270	471	481
0 1	0	1	3
2 0	1	2	6
1 0	18	15	103
0 0	9	12	97
R_3			
1 1	274	473	467
0 1	0	2	2
2 0	2	4	2
1 0	14	15	142
0 0	8	6	77

Table D.2. Dam Survival Estimates—ViRDCt Model

	Live yearling (V_1)	Dead yearling (D_1)	Live STH (V_1)	Dead STH (D_1)	Live subyearling (V_1)	Dead subyearling (D_1)
1 1	439	2	664	3	801	1
0 1	0	0	0	0	1	0
1 0	12	59	8	52	21	37
0 0	4	151	3	128	58	251

For CH1 and STH, the capture histories for forebay-to-tailrace survival are the same as for the dam survival estimates because all those detected at the forebay were detected at the dam face, and vice versa. Capture histories for estimating forebay-to-tailrace survival for CH0 are given in Table D.3 and Table D.4.

Table D.3. Capture History Data for V_1, R_2, and R_3 Used in Estimating Forebay-to-Tailrace Survival Based on the VIPRE Model

	CH0
V_1	
1 1 1	671
0 1 1	0
1 0 1	10
0 0 1	0
1 2 0	5
0 2 0	0
1 1 0	235
0 1 0	0
2 0 0	0
1 0 0	85
0 0 0	175
R_2	
1 1	481
0 1	3
2 0	6
1 0	103
0 0	97
R_3	
1 1	467
0 1	2
2 0	2
1 0	142
0 0	77

Table D.4. ViRDCt Model—Forebay to Tailrace

	Live subyearling (V_1)	Dead subyearling (D_1)
1 1	800	1
0 1	1	0
1 0	21	37
0 0	70	251

Appendix E

Comparing 2018 Results with Past Studies of LGR Passage and Survival

It is worthwhile to compare 2018 to earlier studies conducted at LGR, despite differences in tag technology and array locations. As mentioned earlier, LGR has been an evaluation site for many passage structures and operational scenarios, so we will restrict comparisons to studies with the RSW operating and without the BGS in place. These conditions were in effect during radiotelemetry (RT) studies as early as 2002, and those studies continued through 2006. The following tables compare similar metrics from those earlier studies to the 2018 study results.

Table E.1. Passage Efficiencies of CH1 at Lower Granite Dam

Year	Spill Operation	FPE	SPE	FGE	Source
2002	RSW+8/16 kcfs	0.931 (0.012)	0.781 (0.020)	0.684 (0.048)	Plumb et al. 2003a
2003	RSW +12 kcfs	0.930 (0.010)	0.660 (0.019)	0.800 (0.027)	Plumb et al. 2004
2005	Involuntary Spill	0.906 (0.015)	0.521	0.828 (0.026)	Perry et al. 2007
2006	RSW +12 kcfs	0.919 (0.016)	0.612	0.793 (0.037)	Beeman et al. 2008
2018	**Court-Ordered Gas Cap Spill**	**0.9286 (0.0120)**	**0.6212 (0.0226)**	**0.9389 (0.0181)**	**This Study**

Table E.2. Passage Efficiencies of STH at Lower Granite Dam

Year	Spill Operation	Stock	FPE	SPE	FGE	Source
2002	RSW+8/16 kcfs	Hatchery	0.972 (0.010)	0.728 (0.028)	0.899 (0.037)	Plumb et al. 2003a
		Wild	0.947 (0.014)	0.781 (0.026)	0.759 (0.059)	
2003	RSW +12 kcfs	Hatchery	0.970 (0.012)	0.740 (0.029)	0.880 (0.043)	Plumb et al. 2004
		Wild	0.990 (0.005)	0.710 (0.031)	0.980 (0.016)	
2005	Involuntary Spill	Hatchery	0.966 (0.012)	0.504	0.929 (0.024)	Perry et al. 2007
		Wild	0.963 (0.013)	0.370	0.917 (0.028)	
2006	RSW +12 kcfs	Hatchery	0.942 (0.012)	0.527	0.877 (0.025)	Beeman et al. 2008
2018	**Court-ordered Gas Cap Spill**	**Run-of-River**	**0.9662 (0.0069)**	**0.5735 (0.0190)**	**0.9567 (0.0119)**	**This Study**

Table E.3. Passage Efficiencies of CH0 at Lower Granite Dam

Year	Spill operation	FPE	SPE	FGE	Source
2005	RSW Spill	0.974 (0.008)	0.559 (0.077)	0.793 (0.059)	Perry et al. 2007
2006	1-Stop	0.951 (0.012)	0.728	0.819 (0.041)	Beeman et al. 2008
	4-Stop	0.901 (0.015)	0.659	0.709 (0.039)	
2007	1-Stop	0.899 (0.017)	0.713	0.649 (0.050)	Puls et al. 2008
	4-Stop	0.912 (0.014)	0.758	0.637 (0.048)	
2018	**Court-Ordered Gas Cap Spill then RSW+20kcfs**	**0.9125 (0.0095)**	**0.7969 (0.0135)**	**0.5995 (0.0364)**	**This Study**

Table E.4. Survival Estimates at Lower Granite Dam During Spill

Species	Year	Spill Operation	Dam Survival	Source
CH1	2005	Involuntary Spill	0.973 (0.021)	Perry et al. 2007
	2006	24-hr Spill RSW+12 kcfs	0.967 (0.012)	Beeman et al. 2008
	2018	**Court-Ordered Gas Cap Spill**	**0.9726 (0.0159)**	**This Study (VIPRE)**
			0.9877 (0.0062)	**This Study (ViRDCt)**
STH	2006	24-hr Spill RSW+12 kcfs	0.958 (0.011)	Beeman et al. 2008
	2018	**Court-Ordered Gas Cap Spill**	**0.9959 (0.0099)**	**This Study (VIPRE)**
			0.9936 (0.0037)	**This Study (ViRDCt)**
CH0	2007	24-hr Spill RSW+12 kcfs	0.887 (0.020)	Puls et al. 2008
	2018	**Court-Ordered Gas Cap Spill then RSW+20kcfs**	**0.9422 (0.0217)**	**This Study (VIPRE)**
			0.9242 (0.0098)	**This Study (ViRDCt)**

Table E.5. Survival Estimates by Route for CH1 at Lower Granite Dam During Spill

Year	Spill Operation	Spillway	RSW	JBS	Turbine	Source
2003	24-hr Spill RSW+12 kcfs	-	0.980 (0.023)	-	-	Plumb et al. 2004
2005	Involuntary Spill	0.905 (0.057)	0.982 (0.016)	0.097 (0.018)	1.011 (0.169)	Perry et al. 2007
2006	24-hr Spill RSW+12 kcfs	0.970 (0.018)	0.985 (0.016)	0.987 (0.014)	0.815 (0.086)	Beeman et al. 2008
2018	**Court-Ordered Gas Cap Spill**	**0.9521 (0.0244)**	**0.9855 (0.0172)**	**0.9961 (0.0158)**	**0.8779 (0.0599)**	**This Study (VIPRE)**
		0.9898 (0.0102)	**1.0016 (0.0360)**	**1.0001 (0.0264)**	**0.8697 (0.0604)**	**This Study (ViRDCt)**

Table E.6. Survival Estimates by Route for STH at Lower Granite Dam During Spill

Year	Spill Operation	Spillway	RSW	JBS	Turbine	Source
2006	24-hr Spill RSW+12 kcfs	0.985 (0.013)	0.952 (0.022)	0.955 (0.017)	0.879 (0.082)	Beeman et al. 2008
2018	**Court-Ordered Gas Cap Spill**	**1.0003 (0.0119)**	**0.9843 (0.0141)**	**1.0111 (0.0087)**	**0.8804 (0.0715)**	**This Study (VIPRE)**
		1.0002 (0.0153)	**0.9937 (0.0063)**	**1.0000 (0.0124)**	**0.9076 (0.0626)**	**This Study (ViRDCt)**

Table E.7. Survival Estimates by Route for CH0 at Lower Granite Dam During Spill

Year	Spill Operation	Spillway	RSW	JBS	Turbine	Source
2007	24-hr Spill RSW+12 kcfs	0.811 (0.044)	0.922 (0.023)	0.853 (0.042)	0.872 (0.067)	Puls et al. 2008
2018	**Court-Ordered Gas Cap Spill**	**0.8456 (0.0321)**	**0.9655 (0.0230)**	**1.0023 (0.0277)**	**0.9949 (0.0306)**	**This Study (VIPRE)**
		0.8450 (0.0323)	**0.9654 (0.0234)**	**1.0022 (0.0280)**	**0.9949 (0.0309)**	**This Study (ViRDCt)**

PNNL-29052

Pacific Northwest National Laboratory

902 Battelle Boulevard
P.O. Box 999
Richland, WA 99354
1-888-375-PNNL (7665)

www.pnnl.gov